$CD8^+$ T Cell Dysfunction in Chronic HCV Infection and its Association with Liver Fibrosis

Felicia Deonarine

Department of Biochemistry, Microbiology and Immunology
Faculty of Medicine
University of Ottawa

Thesis submitted to the Faculty of Graduate and Postdoctoral Studies in partial fulfillment of the requirements for the degree of Masters of Science in Microbiology and Immunology

Abstract

Infection with hepatitis C virus (HCV) can cause liver damage known as fibrosis, which often leads to liver disease and hepatocellular carcinoma. The impairment of circulating, bulk (non-specific and specific) $CD8^+$ T cells within HCV-infection, characterized by an altered phenotype and the increased expression of pro-apoptotic genes, is observed when compared to uninfected controls. The relationship between bulk $CD8^+$ T cell function and the extent of liver damage has not been demonstrated. In this study, widespread immune alterations were observed in untreated HCV infection with advanced liver fibrosis. Untreated HCV-infected individuals with advanced fibrosis possessed a significantly decreased proportion of naïve $CD8^+$ T cells and an increased proportion of late effector memory $CD8^+$ T cells compared to uninfected controls. Upon T cell receptor (TCR) stimulation, these individuals also had an increased intracellular IFN-γ expression for four $CD8^+$ T cell subsets, a decreased CD107a expression for central memory $CD8^+$ T cells, and a decreased perforin induction for naïve and central memory $CD8^+$ T cells. These immune alterations did not reverse 24 weeks after viral cure. This study indicates there is a relationship between the differentiation and function of bulk $CD8^+$ T cells and the extent of liver damage within HCV infection.

Acknowledgements

Firstly, I would like to thank my supervisor Dr. Jonathan Angel for his scientific advice, encouragement, and support. As a graduate student, I was provided several chances to develop extensive communication and presentation skills through research presentations at scientific meetings. I would also like to thank Dr. Angela Crawley's research group for the opportunity to study for my master's degree. The overall guidance and feedback I received from peers and prominent immunologists promoted my professional growth and desire to learn.

I would like to thank my thesis advisory committee members, Dr. Subash Sad and Dr. Seung-Hwan Lee for their supervision regarding project design and execution. Dr. Lee also kindly provided the anti-CD3 used in this thesis. I would also like to thank Dr. Jonathan Angel's lab technician and post-doctoral fellows, Stephanie Burke-Schinkel, Dr. Sandra Côté, and Dr. Tamara Berthoud, for their technical assistance, excellent training, and scientific advice. Stephanie Burke-Schinkel kindly completed the Luminex Magpix experiments in this thesis.

In addition, I would like to thank the HIV-Work-in-Progress group at The Ottawa Hospital (TOH) - General Campus and the Biochemistry, Microbiology and Immunology Work-in-Progress group at the University of Ottawa for their constant guidance concerning project implementation and execution.

Lastly, I would like to thank Dr. Curtis Cooper for providing me with the opportunity to witness the clinical aspects of viral hepatitis. This thesis would not have been possible without the numerous samples that were generously provided by Dr. Curtis Cooper. I would like to thank the volunteers and patients who charitably donated blood. I would also like to thank the nurses, doctors, and research coordinators at the Clinical Investigation Unit and the Viral Hepatitis Clinic at TOH - General Campus who kindly collected samples for use in my project.

Table of Contents

List of Abbreviations

AICD – activation-induced cell death
APCs – antigen-presenting cells
Bcl-2 – B cell lymphoma 2
Blimp-1 – B lymphocyte induced maturation protein 1
cDCs – conventional DCs
CIU – clinical investigative unit
CLDN1 – claudin-1
DAAs – direct acting antivirals
DAMPs – damage-associated molecular patterns
DCs – dendritic cells
ds – double stranded
ECM – extracellular matrix
EGFR – epidermal growth factor receptor
EOMES – eomesodermin
ER – endoplasmic reticulum
ESLD – end-stage liver disease
FMO – fluorescence minus one
HBV – hepatitis B virus
HCC – hepatocellular carcinoma
HCV – hepatitis C virus
HIV – human immunodeficiency virus
HSCs – hepatic stellate cells
IPS-1 – IFN promoter-stimulator 1
IRES – internal ribosome entry site
IRF-3 – IFN regulatory factor-3
iVDU – intravenous drug users
LAMPs – lysosome-associated membrane glycoproteins
LCMV – lymphocytic choriomeningitis virus
LN – lymph nodes
MAVS – mitochondrial antiviral signalling protein
MFB – myofibroblasts
MHC – major histocompatibility complex
MTOC – microtubule-organizing centre
nABs – neutralizing antibodies
NASH – non-alcoholic steatohepatitis
NFAT – nuclear factor of activated T cells
NGF-R – nerve growth factor receptor
NK – natural killer cells
NLRs – NOD-like receptors
NOD – nucleotide oligomerization domain
OCLN – occludin
PAMPs – pathogen-associated molecular patterns
PBMCs – peripheral blood mononuclear cells
pDCs – plasmacytoid DCs

peg-IFN – pegylated interferon
PFA – paraformaldehyde
PMA – phorbol 12-myristate 13-acetate
PRRs – pattern recognition receptors
RBV – ribavirin
RLRs – RIG- I-like receptors
RNA – ribonucleic acid
RT – room temperature
SEB – staphylococcal enterotoxin B
SECs – sinusoidal endothelial cells
SR-BI – scavenger receptor class B type I
src – sarcoma
SVR – sustained virological response
T-bet – T-box transcriptional factor
TCR – T cell receptor
Th – T helper
TIM-3 – T cell immunoglobulin and mucin domain-containing molecule 3
TLRs – toll-like receptors
TNF – tumour necrosis factor
TOH – The Ottawa Hospital
TREC – T cell receptor excision circle
TRIF – TIR-domain-containing adapter-inducing interferon- β
UTR – untranslated region

List of Figures

LIST OF TABLES

Chapter 1: Introduction

1.1 Hepatitis C Virus Infection

Globally, the number of hepatitis C virus (HCV) infections has been estimated to be over 185 million with the highest prevalence in Central and East Asia and North Africa/the Middle East (1). HCV is a blood-borne virus which can lead to end-stage liver disease (ESLD), portal hypertension, and hepatocellular carcinoma (HCC) (2). An HCV infection is characterized as acute or chronic within the 6-month period following the point of infection (3). Symptoms may appear within this time, including jaundice, fatigue, joint pain, itchy skin, and dark urine (4). Although spontaneous clearance occurs in 25% of individuals infected, the majority develop a chronic infection (3). Approximately 25% of individuals living with chronic HCV develop liver cirrhosis within decades after initial infection (5). Recent advances in HCV medication have revolutionized treatment success with an achievement of over 90% sustained virological response (SVR) rates (6). SVR is defined as an absence of detectable HCV RNA determined 24 weeks after the end of treatment (7). Despite effective treatments, liver damage is not always reversed once a cure has been achieved (8, 9) and access to treatment varies both globally and nationally. Furthermore, many are unaware of their HCV status and transmission rates remain high among at-risk intravenous drug users (iVDU). Thus, continued research in the field of HCV pathogenesis is needed to permanently arrest the spread of infection around the world.

1.2 Hepatitis C Virology

HCV is a small hepatotropic virus, belonging to the family *Flaviviridae* and genus *hepacivirus*, with a circular and positive single-stranded RNA genome (10). It has a non-lytic life cycle that results in the production of progeny without host cell damage or death. HCV has six

main genotypes with 67 subtypes (4, 11). During the viral life cycle, the HCV genome polyprotein is processed to produce three structural proteins (core, envelope glycoprotein E1, and envelope glycoprotein E2) and seven non-structural proteins (core protein p7, protease NS2–3, serine protease NS3, protease co-factor NS4A, replication regulators NS4B and NS5A, and RNA-dependent RNA polymerase NS5B) (12). The life cycle of HCV can be divided into four steps: (i) viral entry, (ii) genome translation and polyprotein processing, (iii) genome replication, and (iv) viral particle assembly and release from the host cell (13).

Viral entry of HCV into hepatocytes is a highly regulated process involving several host and viral factors and lipoproteins. There are four HCV entry factors required for infection, including tetraspanin CD81, scavenger receptor class B type I (SR-BI), and tight junction proteins claudin-1 (CLDN1) and occludin (OCLN) (14). Binding of envelope glycoprotein E2 to CD81 and SR-BI has been demonstrated during viral entry (13). CLDN1 and OCLN are necessary for the post-binding step of HCV entry, but the mechanism has yet to be determined (14). The role of envelope glycoprotein E1 is less understood, but has been hypothesized to be important in the fusion process (15). Additional host molecules support HCV entry, including receptor tyrosine kinases EGFR (epidermal growth factor receptor) and ephrin receptor A2, cholesterol transporter Niemann–Pick C1-like 1, transferrin receptor 1, and calcium-regulated adhesion molecule E-cadherin (14). After the HCV particle has bound to cells via viral receptors, internalization occurs through clathrin-mediated endocytosis followed by a fusion step from within a low pH endosomal compartment (16). Fusion results in the release of the viral RNA genome into the liver cell.

Within the hepatocyte cytoplasm, HCV polyprotein is translated using the positive-stranded RNA genome as a template to produce a polyprotein precursor bound to the endoplasmic reticulum (ER) (17). Following translation, the polyprotein is processed by cellular (e.g. signal peptidases) and viral proteases (NS2, NS3/4A) to generate ten structural and non-structural HCV proteins (17). Translation machinery is directly recruited to HCV RNA for the production of viral proteins, because capping prior to translation initiation is unnecessary as a result of the internal ribosome entry site (IRES) in the 5'- untranslated region (5'-UTR) (18). Once produced, structural proteins E1 and E2 form dimers and localize to the ER network (19). The NS5B protein, essential for viral replication, produces numerous copies of the viral genome using an intermediate minus strand (20). Viral RNA synthesis occurs in an ER-derived cytosolic compartment, called the membranous web or HCV replication complex, composed of HCV non-structural proteins, viral genomes, and host factors (21).

Viral assembly occurs after the RNA genome, and structural proteins E1, E2, and core, have been synthesized. After replication, the HCV genome is packaged within core protein to produce a capsid (13). Mature core protein resides on the surface of storage organelles called lipid droplets, which are located within the host cytoplasm (22). The non-structural HCV protein p7 is essential for proper capsid formation as non-functional variants are unable to completely incorporate viral RNA (22). The capsid is transported into the ER lumen where it obtains a host-derived envelope embedded with E1-E2 dimers (23). Afterwards, the progeny follow the secretory pathway resulting in migration to the host cell surface and release from the infected cell (24). HCV virions complex with host lipoprotein in bloodstream circulation due to the close association of their secretory pathways (13).

1.3 Hepatitis C Virus Treatment

HCV therapy is used to prevent hepatic and extra-hepatic complications as well as to improve overall survival (25). However, previous treatments involving pegylated interferon (peg-IFN) and the addition of ribavirin (RBV) were ineffective in curing more than 40% of treated individuals and unsuccessful in preventing relapse in those who responded (26-28). IFN-based treatments also resulted in side effects, including bone marrow suppression, flu-like symptoms, neuropsychiatric disorders, and autoimmune syndromes (29). Recent advances in HCV treatment have improved SVR achievement rates to over 90% (6, 30). These new treatments, called direct-acting antivirals (DAAs), prevent replication of HCV by inhibiting different parts of the viral machinery. DAA-based treatments are also highly tolerable and require less time for viral cure to be achieved compared to IFN-based therapies (31).

Two well-known and effective DAAs for treatment of HCV include Holkira Pak and Harvoni. Holkira Pak is composed of ritonavir (an HIV protease inhibitor), paritaprevir (an HCV protease inhibitor), ombitasvir (NS5A inhibitor), and dasabuvir (nonnucleoside polymerase inhibitor) (32). Harvoni is composed of two DAAs, sofosbuvir (nucleotide analogue) and ledipasvir (NS5A inhibitor) (33). Both medications are approved to treat genotype 1, the predominant HCV genotype present in Canada, and are associated with SVR achievement rates of over 90% (34).

Although effective HCV medications exist, current treatment rates are unable to eliminate HCV transmission (35). There are several factors resulting in unsatisfactory treatment rates, including high treatment costs (36, 37) and HCV recurrence in patients with ongoing high-risk

behaviours (38). In addition, liver damage is not always reversed once a cure has been achieved (8, 9).

1.4 Hepatitis C Infection and the Liver

1.4.1 Histology of the Liver

The liver has many roles, including the synthesis, metabolism, storage, and localization of amino acids, proteins, carbohydrates, fats, and vitamins. Additionally, the liver is responsible for the detoxification of approximately one-third of the body's total blood volume every minute, allowing various cell types within the circulation to encounter the internal hepatic environment (39). This vital organ receives blood through both the portal vein and the hepatic artery.

The liver can be divided into hexagonal-shaped functional units called lobuli, which are surrounded by portal triads (branches of bile duct, hepatic artery, and portal vein). A liver lobule is defined by the presence of hepatocyte layers (parenchymal cell of the liver) and sinusoids surrounding a central vein. Sinusoids are the capillary branches of the portal vein and hepatic artery which travel through the lobule from the portal triads towards the central vein (40). Exchange of proteins and other components between the blood and hepatocytes occurs within the space of Disse, which contains plasma (41). The space of Disse is an area between the layer of hepatocytes and the sinusoids within a liver lobule.

The liver is composed of several different cell types with various functions. Representing 80% of the liver's cell composition, hepatocytes perform most functions of the liver, including regulation of carbohydrate and lipid metabolism, clearance of cellular toxins, and synthesis of plasma proteins (41). The remaining 20% of cells in the liver are non-parenchymal and include Kupffer cells, hepatic stellate cells (HSCs), sinusoidal endothelial cells (SECs), biliary epithelial

cells, lymphocytes, and oval cells. Kupffer cells are a type of macrophage predominantly located within sinusoids that function in the removal of senescent and damaged erythrocytes from the liver vasculature and mediation of the inflammatory immune response. HSCs are fat-storing fibroblasts located in the space of Disse that represent 5-8% of liver cells and function in the storage of vitamin A, turnover of extracellular matrix, and regulation of sinusoid contractility. Located in the wall of sinusoids, SECs filter the blood received by hepatocytes and generate T cell tolerance through antigen presentation. In the bile ducts of portal triads, biliary epithelial cells transport water, secrete mediators of cell development and differentiation, and express molecules for effector leukocyte adhesion to promote clearance of infected cells (42). Finally, oval cells are liver progenitors capable of differentiating into both hepatocytes and bile duct cells (43).

1.4.2 Fibrogenesis and Cirrhosis

Chronic HCV infection is characterized by a slow progression of liver scarring known as fibrosis. Importantly, progression of fibrosis does not occur identically between HCV-infected individuals (44). A number of factors that increase the rate of fibrosis progression have been identified: male gender, longer infection duration, individual's age at time of infection (over 40 years), large alcohol consumption, long term immunosuppression (Human immunodeficiency virus (HIV), organ transplantation), Hepatitis B virus (HBV) co-infection, and unsuccessful antiviral therapy (44).

The repair of liver damage involves two possibilities: (i) the regenerative phase in which damaged cells are replaced by the same type of cells and (ii) fibrosis, in which connective tissue is replaced by parenchymal tissue (45). Activation of HSCs due to liver insult and hepatocyte

death is the main mechanism leading to liver fibrosis (46). Following activation, HSCs undergo an inflammatory phase leading to myofibroblasts (MFB) differentiation. Many other cell types can also become MFB, including resident mesenchymal cells, epithelial and endothelial cells, and circulating fibroblast-like cells called fibrocytes (45).

MFB within the liver serve to repair, regenerate, and restore the liver following tissue injury by secreting collagen, a component of the extracellular matrix (ECM), and stimulating cytokines (47). The cytokines released create a positive feedback loop with the HSCs and MFBs to facilitate the fibrogenic process. Growth factors, proteolytic enzymes, angiogenic factors, and fibrogenic cytokines sustain the production of ECM by MFB (45). Uncontrolled accumulation of ECM due to repeated liver injury, as in chronic HCV disease, replaces normal tissue with permanent scar tissue, leading to the inability of the liver to perform vital functions.

Significant accumulation of scar tissue in the liver can lead to cirrhosis. Degeneration and necrosis of hepatocytes, presence of regenerative nodules, loss of liver function, defenestration of sinusoidal endothelium, presence of a subendothelial basement membrane, and formation of fibrotic septa commonly characterize liver cirrhosis regardless of etiology (48).

In the past, liver biopsies were used to determine the fibrosis stage of an individual. Currently, it is more common to use a non-invasive method of identifying an individual's degree of liver fibrosis (46). This technology, termed the Fibroscan, uses transient elastography to measure the stiffness of the liver. The amount of fibrotic tissue is proportional to the level of stiffness observed within the liver. The METAVIR score system provides a means to classify the reported stiffness (Table 1).

Table 1. METAVIR Score System

METAVIR Score	Liver Stiffness (kPa)	Liver Anatomy
F0-F1	1-7.3	No fibrosis
F1-F2	7.3-9	Portal fibrosis without septa
F2	9-9.8	Portal fibrosis with rare septa
F3	9.8-13	Numerous septa without cirrhosis
F3-F4	13-15	
F4	>15	Cirrhosis

1.5 Immune Response to HCV

1.5.1 Innate Immune Response

In HCV infection, innate immunity plays a significant role in the control of viral replication and signalling of the adaptive immune system. The innate immune response is activated when conserved motifs of microbial origin, known as pathogen-associated molecular patterns (PAMPs), are recognized by cell pattern recognition receptors (PRRs) on or within different types of innate immune cells (49). A number of innate immune cells, including monocytes, neutrophils, and dendritic cells (DCs), are activated upon recognition of PAMPs (50).

There are three major classes of PRRs, including RIG-I-like receptors (RLRs), Toll-like receptors (TLRs), and nucleotide oligomerization domain (NOD)-like receptors (NLRs) (51). RLRs are cytosolic PRRs that sense RNA viruses. RIG-I and its adaptor protein, IFN promoter-stimulator 1 (IPS-1), recognize HCV within hours of infection, leading to the activation of IFN regulatory factor-3 (IRF-3) and the host IFN-α/ β response which control viral dissemination

through death of infected cells (52). NS3/4A has been shown to block RIG-I signalling through cleavage of a downstream protein called mitochondrial antiviral signalling protein (MAVS) from intracellular membranes (53). MAVS must be attached to membranes for IFN induction to occur through downstream signalling. One TLR that plays a significant role in HCV is TLR-3 (54). The TLR-3 ligand is a dsRNA replication intermediate that accumulates during HCV after uptake of cell components from dead infected cells. It has been shown that HCV NS3/4A protease targets the TLR-3 signalling-adaptor protein known as TIR-domain-containing adapter-inducing interferon- β (TRIF) to inhibit host detection of HCV (55). Finally, NLRs are thought to be activated by intracellular stress signals and drive inflammatory responses following recognition of cytosolic viral products or metabolites. Damage-associated molecular patterns (DAMPs), a type of intracellular stress signal, can notify NLRs in the context of HCV to facilitate the inflammatory response due to hepatocyte infection (56).

The early phase of HCV infection is characterized by an increasing plasma viral load and the production of type I interferons (IFN-α, IFN-β) by HCV-infected hepatocytes and DCs, which lead to control of viral replication (57, 58). DCs are a key component of innate immunity due to their ability to present antigen and produce cytokines that prime $CD4^+$ helper T cells and $CD8^+$ T cells (59). A subset of DCs known as plasmacytoid DCs (pDCs) rapidly produce type I interferons upon viral recognition through TLR-7 and TLR-9 (60, 61). In chronic HCV infection, a lower frequency of pDCs in peripheral blood and an impaired capacity to produce IFN-α upon stimulation with short single-stranded synthetic DNA molecules (containing cytosine-phosphodiester-guanine) has been observed (62). Conventional DCs (cDCs) have also been shown to produce IFN-α following TLR-3 recognition of HCV (63). Importantly, cDCs produce high levels of IL-12, which subsequently stimulate IFN-γ production by activated T cells (64).

An increased frequency of cDCs in acute HCV infection is associated with viral clearance, while a decreased frequency may lead to chronic HCV infection (65).

During HCV infection, natural killer (NK) cells eliminate viruses through direct killing of infected hepatocytes and pro-inflammatory cytokine production. However, the action of NK cells in HCV infection can lead to liver damage and high IFN-γ production by cDCs, which facilitates local inflammation (58). Cytokines produced by pDCs, liver-resident macrophages, and HCV-infected hepatocytes alter the frequency of NK cells, T cells, and myeloid cells in the liver during HCV infection. HCV has been shown to regulate pro-inflammatory TNF-α responses to prevent control of the infection by the immune system (66).

1.5.2 Adaptive Immune Response

Adaptive immune responses are usually observed 1-2 months following initial HCV infection, although HCV RNA can be detected as early as 1-3 weeks post infection (67). Neutralizing antibodies (nABs), which block viral access to host cells, have been discovered for structural and non-structural HCV proteins with the majority mapped to E1 and E2 (68). Several nABs have been identified that target the CD81-binding region of E2 (69-71). This process is highly effective because CD81 is an indispensable HCV entry factor (72). The generation of nABs against non-structural proteins is thought to occur in response to debris from damaged cells (73).

The contribution of nABs to HCV progression is unclear. However, increasing research has indicated an important role for nABs in spontaneous viral clearance (74-76). During chronic infection, individuals with hypogammaglobulinemia, defined as a reduction in nABs, experience increased and more rapid HCV progression (77). Despite the role of nABs in HCV clearance,

chronic infection often sets in due to viral escape mechanisms. Some examples of the mechanisms used by HCV include sequence changes due to error-prone HCV polymerase (78), decoy epitopes (79), epitope masking by heavy glycosylation of envelope proteins (80), lipid shielding (81), interfering antibodies that block nABs (73), and cell-to-cell transmission of the virus in a neutralization-resistant fashion (82).

HCV viral infection is also controlled through multi-specific and long-lasting T cell responses (83). Both $CD4^+$ and $CD8^+$ T cells are primed by antigen-presenting cells (APCs) in the lymph nodes (LN) and migrate to the site of infection once activated (84). $CD4^+$ and $CD8^+$ T cells are activated through interaction between their T cell receptor (TCR) and the Major Histocompatibility Complex (MHC) on the surface of APC as well as through their co-stimulatory molecules and the associated ligands (e.g. CD28/B7 and CD27/ CD70) in the presence of a stimulating cytokine environment (85). Activated $CD4^+$ T cells produce T helper (Th) - 1 cytokines such as IFN-γ and IL-2, which aide in expansion of $CD8^+$ T cells (86). $CD8^+$ T cells clear viruses through direct destruction of infected cells and production of type-1 cytokines capable of viral eradication through an organized and specific immune response (84). Once activated, virus-specific $CD8^+$ T cells exhibit effector functions. When the pathogen has been eliminated, negative co-stimulatory molecules such as PD-1 and CTLA-4 are expressed, and the cells become inactive and decline in frequency. A small number of antigen-specific $CD8^+$ T cells develop into a memory population, able to rapidly induce a cytotoxic response if the pathogen is ever re-encountered (87).

Chronic HCV infection occurs despite the presence of HCV-specific $CD4^+$ and $CD8^+$ T cell responses. HCV uses multiple mechanisms to avoid recognition from these cell types,

including HCV escape mutations at the TCR (88), regulatory T cell (Tregs) induction (89), and exhaustion (90).

1.6 $CD8^+$ T Cell Subsets

Once MHC molecules have been loaded with peptide at the site of infection, APC migrate to the draining LN to activate naïve $CD8^+$ T cells (T_N) (91, 92). Recognition of its peptide through the TCR results in the initiation of a signaling cascade (93), which allows for the production of cytokines and cytotoxic molecules (94). Co-stimulatory receptors, such as CD28, positively modulate TCR signaling (95).

The duration, quantity, and class of antigenic stimulation determine the non-linear pathway of $CD8^+$ T cell differentiation into effector (T_E), effector memory (T_{EM}), or central memory (T_{CM}) cells (96). This process involves gradual changes in surface marker expression and cytolytic activity, defining numerous subsets. Antigen inexperienced T_N cells are characterized *in vivo* by the lack of expressed effector mediators, including IFN-γ, granzyme B, perforin and Fas/CD95, and a low proliferative capacity (e.g., long telomeres, high levels of T cell receptor excision circle (TREC) copies) (97). T_N cells are the largest subset of $CD8^+$ T cells and the frequencies are inversely correlated with the age of the individual (98). On the other hand, T_E is a subset of antigen-experienced $CD8^+$ T cells characterized as short-lived with the ability to migrate to the site of infection and produce substantial levels of cytolytic effector molecules that kill infected cells. Furthermore, the two antigen-experienced memory subsets, T_{EM} and T_{CM}, have a long life-span and are capable of proliferating. More specifically, T_{EM} are characterized by the ability to migrate to infected and inflamed tissue and display immediate effector function upon antigen recognition (99). In contrast, T_{CM} cells express lymph-node

homing receptors such as CCR7 and do not possess immediate effector function. Furthermore, T_{CM} are capable of differentiation into T_{EM} cells upon secondary antigenic stimulation.

Three surface markers including CD27, CD45, and CCR7 are commonly used to distinguish between $CD8^+$ T cell subsets (97). CD27, a member of the TNF/ NGF-R (Tumour Necrosis Factor/Nerve Growth Factor Receptor) family, is highly induced upon $CD8^+$ T cell activation and is gradually diminished after prolonged stimulation (97, 100). CD27 has been shown to play a role in antigen-specific expansion of the T_N subset (101). CCR7 is a chemokine receptor that controls lymphocyte migration, which is highly expressed on T_{CM} and T_N, which recirculate from peripheral blood to secondary lymphoid tissues in search of peptide (102). CD45 is a protein tyrosine phosphatase regulating src-family kinases with two isoforms including CD45RA and CD45RO (99). Upon antigen experience, memory $CD8^+$ T cell subsets lose CD45RA and gain CD45RO expression. CCR7, CD45RA, and CD27 can be used to distinguish eight different $CD8^+$ T cell subsets: T_N, $T_{N\ CD27}{}^{NEG}$, T_{CM}, $T_{CM\ CD27}{}^{NEG}$, T_{EEM} (early effector memory), T_{LEM} (late effector memory), $T_{E,}$ and T_{pE} (pre-effector). These subsets are phenotypically defined in Table 3 as follows: T_N ($CCR7^+CD45RA^+CD27^+$), $T_{N\ CD27}{}^{NEG}$ ($CCR7^+CD45RA^+CD27^-$), T_E ($CCR7^-CD45RA^+CD27^-$), T_{pE} ($CCR7^-CD45RA^+CD27^+$), T_{EEM} ($CCR7^-CD45RA^-CD27^+$), T_{LEM} ($CCR7^-CD45RA^-CD27^-$), T_{CM} ($CCR7^+CD45RA^-CD27^+$), and $T_{CM\ CD27}{}^{NEG}$ ($CCR7^+CD45RA^-CD27^-$) (97, 103).

Studies have proposed several differentiation models for these subsets. One model is based on telomere lengths, whereby the longest are found in the least differentiated subsets that have experienced the smallest number of cell divisions: $T_N \rightarrow T_{CM} \rightarrow T_{EEM} \rightarrow T_{pE} \rightarrow T_{LEM} \rightarrow T_E$ (96, 98). The loss of CD27 is associated with increased differentiation towards T_E cells, thus T_{CM}

$_{CD27}^{NEG}$ cells are expected to have arisen from T_{CM} cells positive for CD27 (103). The T_{pE} cells, so named by Romero *et al*, are defined by long telomeres, reduced TRECs compared to T_N cells, and intermediate effector functions including expression of granzyme B, perforin, IFN-γ, and TNF-α (96).

The effector memory $CD8^+$ T cell subset including T_{EEM} and T_{LEM} can be further differentiated based on expression of CD28 (97). T_{EEM} cells include T_{EM1} ($CD27^+CD28^+$) and T_{EM2} ($CD27^+CD28^-$), and T_{LEM} cells include T_{EM3} ($CD27^-CD28^-$) and T_{EM4} ($CD27^-CD28^+$). T_{EM1} and T_{EM4} cells possess low levels of granzyme B and perforin, express high levels of CD127/ IL-7Rα, and have a replicative history like T_{CM}. T_{EM2} and T_{EM3} cells express cytolytic molecules characteristic of effector cells. Finally, T_{EM3} experience strong *ex vivo* cytolytic activity and many cell divisions, thus resembling T_E cells.

Once differentiated, T_E migrate to the site of infection to destroy infected cells in an antigen-specific manner, releasing perforin to create pores in the target membrane and granzymes to induce programmed cell death of the target (104). Koch *et al* described a proportional relationship between percentage of T_E cells and the age of the individual. Other important $CD8^+$ T cell responses to infection include production of cytokines, including IL-2, IL-10, and IFN-γ, which promotes the survival of immune cells and modulates the adaptive immune response (105, 106).When the pathogen is cleared in acute infection, the frequency of T_E declines and a small number of antigen-specific cells may develop into a memory population, which rapidly respond to a previously encountered pathogen (87).

1.7 Activation of $CD8^+$ T cells

$CD8^+$ T cells produce and express several cytokines and cytolytic molecules in response to recognition of their cognate antigen, including IFN-γ (107), CD107a (90), and perforin (108), in order to effectively resolve infection. $CD8^+$ T cells also respond to IFN-γ through the heterodimeric cell surface receptor called IFN-γR (109). IFN-γ activates macrophages, augments antigen presentation, induces MHC-peptide complexes, facilitates lymphocyte-endothelial interactions, regulates T cell polarization and proliferation, and stimulates apoptosis to control viral replication (110). Thus, IFN-γ production is often targeted by pathogens as an immune evasion strategy (111).

$CD8^+$ T cells use two major mechanisms to initiate killing of target cells: the granule-dependent pathway and the independent (FasL/Fas) pathway (112). The granule-dependent pathway uses pre-formed molecules housed in secretory lysosomes to mediate direct killing of the target cell. The proteins contained in the lysosomes are known as granules and include perforin, which forms a pore in the target cell (113), and granzymes, which initiate apoptosis of the target cell (114). The membranes of the secretory lysosomes are composed of glycoproteins (LAMPs) not normally found on the cell surface, including CD107a (LAMP-1), CD107b (LAMP-2), and CD63 (LAMP-3) (115). The process of degranulation involves the organized movement of the granule-containing lysosome to the cell exterior followed by membrane fusion and content release into the immunological synapse (115). Thus, degranulation leads to the presence of LAMPs on the cell surface, which are later removed through the process of endocytosis (116). Measurement of intracellular cytolytic molecule expression in combination with LAMP expression is used to provide a more accurate indication of degranulation occurrence (117).

Upon TCR stimulation, $CD8^+$ T cells develop effector functions through changes in gene expression (118). T-bet and eomesodermin (EOMES) are the main transcription factors stimulated by TCR and IFN-γR triggering that regulate production of IFN-γ and perforin (119). Additional transcription factors bind a proximal promoter in the IFN-γ gene to promote expression in a calcineurin-dependent manner with the aid of NFAT (nuclear factor of activated T cells) (120). TCR triggering also leads to a cytosolic increase in calcium concentration, which allows the microtubule-organizing center (MTOC) and secretory lysosomes to rapidly move towards the target cell (121).

1.8 Impaired $CD8^+$ T Cells in Chronic HCV Infection

1.8.1 HCV-specific $CD8^+$ T Cell Impairment

The mean frequency of HCV-specific $CD8^+$ T cells isolated from the blood of patients with chronic hepatitis C is 0.05-2% (122, 123). During persistent antigenic stimulation as in chronic infection, virus-specific $CD8^+$ T cells may experience functional impairment termed exhaustion (124). This impairment can be characterized by a loss of effector functions in a hierarchical manner (125) associated with low degranulation efficiency and a reduced production of various cytokines (90). The process of exhaustion has been investigated in the context of HCV-specific $CD8^+$ T cells in chronic HCV infection (126-128). During chronic HCV infection, additional properties are weakened, including IL-2 production, survival, and proliferation (129). TNF-α production persists longer during chronic disease with loss of IFN-γ production occurring afterwards.

Exhausted $CD8^+$ T cells up-regulate inhibitory receptors, including PD-1, LAG-3, CD244, CD160, CTLA-4, and Tim-3 (130). Ultimately, the balance between co-stimulatory and

co-inhibitory signals regulates T cell responses. The reasons for virus-specific $CD8^+$ T cell impairment during chronic HCV infection have not been completely elucidated. However, evidence indicates lack of $CD4^+$ T cell help, facilitation by regulatory T cells, and expression of immunomodulatory cytokines could contribute (e.g. IL-10).

1.8.2 Intrahepatic $CD8^+$ T Cell Impairment

HCV pathogenesis and disease outcome are dependent on $CD8^+$ T cell responses in the liver (131). Intrahepatic leukocytes, including $CD8^+$ T cells, remain in the liver through adherence with sinusoids (132). During chronic HCV infection, $CD4^+$ and $CD8^+$ T cells are the largest lymphocyte subsets present within the liver (133). NK T cells, NK cells, and B cells can also be found within the liver. The most abundant subset of $CD8^+$ T cells in the liver are T_E (134). In addition, the frequency of intrahepatic $CD4^+$ and $CD8^+$ T cells increases with disease progression with the level of liver inflammation directly proportional to the expression of chemokine homing receptors and activation markers. Thus, it is rational to expect the function of $CD8^+$ T cells to be important in the immune response to HCV.

During chronic HCV infection, intrahepatic $CD8^+$ T cells have been shown to produce significantly less IFN-γ compared to circulating counterparts in response to the superantigen staphylococcal enterotoxin B (SEB) (135) and anti-CD3 stimulation (136). Additionally, intrahepatic HCV-specific $CD8^+$ T cells have been shown to secrete less IFN-γ in response to HCV-derived peptides previously shown to be HLA-A2-restricted epitopes (137). Intrahepatic $CD8^+$ T cells also possess lower intracellular perforin and express higher levels of FasL compared to their peripheral blood counterparts (135). This finding could be a result of immunotolerant liver signals causing chronic degranulation of intrahepatic $CD8^+$ T cells (138).

The study performed by Wang *et al* suggests a prominent role for the granule-independent pathway of $CD8^+$ T cell mediated killing. Furthermore, the apoptotic potential of intrahepatic $CD8^+$ T cells is significantly greater compared to those within the circulation (139, 140). Finally, intrahepatic $CD8^+$ T cells are less proliferative compared to their circulating counterparts after stimulation with anti-CD3 and rIL-2 reagents (135).

1.8.3 Bulk $CD8^+$ T Cell Impairment

The phenotype and functions of HCV-specific $CD8^+$ T cells have been extensively studied in the context of chronic HCV infection. In contrast, bulk $CD8^+$ T cells comprised of both non-specific and virus-specific $CD8^+$ T cells have been less well studied. However, evidence indicates a pervasive effect of HCV on the global population of $CD8^+$ T cells in terms of phenotype and function. Although more highly expressed on HCV-specific $CD8^+$ T cells, up-regulation of an inhibitory receptor called *T-cell immunoglobulin and mucin domain-containing molecule 3* (TIM-3) has also been observed on bulk $CD8^+$ T cells in chronic HCV infection (141). TIM-3 is a membrane protein implicated in the exhaustion process of chronic viral infections. Furthermore, an analysis of CMV-specific $CD8^+$ T cells in the context of chronic HCV infection discovered a reduction in the expression of markers related to maturity, an increased expression of CCR7, and a reduced expression of Fas and perforin upon peptide stimulation compared to uninfected controls (142).

Some studies have identified a unique expression of apoptosis-related genes (143) and a reduced production of anti-apoptotic molecule *B-cell lymphoma 2* (Bcl-2) in response to IL-7 for circulating bulk $CD8^+$ T cells within chronic HCV infection (144). Importantly, Bcl-2 expression was inversely correlated with liver damage. In addition, $CD8^+$ T cells with DNA damage in the

form of double stranded breaks are more abundant in the liver and are associated with increasing liver fibrosis (145).

Additional studies have identified reduced cytokine signaling in bulk $CD8^+$ T cells during chronic HCV infection. For example, phosphorylation of STAT5 upon IL-7 stimulation was reduced in circulating bulk $CD8^+$ T cells from chronic HCV infection compared to uninfected controls (144). STAT5 is a signal transducer for IL-7 and IL-15 that is necessary for proper effector $CD8^+$ T cell responses (146). Another study showed reduced IFN-γ, perforin, TNF-α, and CD107a expression upon anti-CD3 stimulation for intrahepatic bulk $CD8^+$ T cells during chronic HCV infection compared to uninfected controls (136). Nisii *et al* also found a decreasing frequency of intrahepatic bulk IFN-γ^+CD8^+ T cells with increasing degree of liver damage (measured using the METAVIR scoring system). Thus, there is previously established evidence indicating a global effect of HCV infection on bulk $CD8^+$ T cells.

1.8.4 Reversal of $CD8^+$T Cell Impairment

Previous studies have demonstrated a reversal of $CD8^+$ T cell dysfunction. The presence of highly expressed inhibitory receptors on $CD8^+$ T cells during chronic HCV infection led to the evaluation of receptor blockade to reverse the effects of exhaustion (147, 148). In a study evaluating the effects of PD-1/CTLA-4 blockage on $CD8^+$ T cell exhaustion in the liver, HCV-specific effector function was restored (149). However, exhaustion reversal did not occur when PD-1 or CTLA-4 were used to block separately. In contrast, another study showed PD-1 blockage alone to be effective in restoring proliferation of blood-derived $CD8^+$ T cells (150). The difference between these two studies could be due to the overexpression of CTLA-4 on intrahepatic $CD8^+$ T cells during chronic HCV infection compared to those in the circulation.

Additional studies have evaluated markers of exhaustion before and after viral cure. In a study evaluating the effects of peg-IFN and ribavirin on peripheral blood $CD8^+$ T cell exhaustion, it was determined that SVR did not result in full restoration of memory $CD8^+$ T cell response (151). Other studies did not observe a restoration of $CD8^+$ T cell properties during chronic HCV infection after viral cure was achieved using peg-IFN therapies (152-154). Few studies have investigated the relationship between DAA-based therapies and $CD8^+$ T cell exhaustion. One such study showed restoration of HCV-specific $CD8^+$ T cell proliferation after stimulation with HCV-specific peptides and anti-CD28 in the majority of patients approximately four weeks after SVR achievement (155). The patients used in this study were treated with faldaprevir (a protease inhibitor) and deleobuvir (a non-nucleoside polymerase inhibitor) with or without ribavirin.

1.9 Rationale and Hypothesis

Effective virus-specific $CD8^+$ T cell responses have been associated with spontaneous clearance of virus during acute HCV infection (156-159). During chronic HCV infection, virus-specific $CD8^+$ T cells have been shown to display abnormal characteristics that can affect their ability to survive, proliferate, and perform effector functions (160). This phenomenon, often seen in chronic viral infections including HBV (161) and HCV, is referred to as T cell exhaustion. Although less studied, T cell exhaustion in chronic HCV infection has been observed in bulk $CD8^+$ T cells (both virus-specific and non-specific) within the liver and peripheral blood (136, 144). Previous studies indicate a global effect of chronic HCV infection on bulk $CD8^+$ T cells. However, whether functional impairment of bulk $CD8^+$ T cells during chronic HCV infection is associated with the extent of liver damage has yet to be addressed. Understanding the relationship between bulk $CD8^+$ T cells and liver damage is of great interest because it could

reveal unknown aspects of HCV pathogenesis that could eventually provide prognostic indicators of liver disease. Therefore, the hypothesis of this thesis is that the extent of liver damage in chronic HCV is correlated with dysfunction of bulk $CD8^+$ T cells in the circulation.

1.10 Statement of Objectives

To determine if a relationship exists between HCV-induced liver damage and bulk $CD8^+$ T cell function during chronic HCV infection, there were two main objectives. Objective 1: to characterize the functionality of $CD8^+$ T cells from chronically HCV-infected patients in the context of the degree of liver damage. Objective 2: to determine if effective HCV therapy changes the functionality of $CD8^+$ T cells.

Chapter 2: Materials and Methods

2.1 Study Subjects

The groups of subjects used in this study were HCV^- donors, chronically infected (> six months HCV RNA-positive) HCV^+ TX^- (treatment naïve) individuals, and chronically infected HCV^+ TX^+ individuals (12-week regimen of ABT450r, ombitasvir, dasabuvir ± ribavirin). The treatment timeline for HCV^+TX^+ individuals is illustrated in Figure 1 below. Exclusion criteria for all HCV^+ individuals included HBV infection, HIV infection, and alcohol consumption > 50 g/day. Exclusion criteria for HCV^+ TX^+ individuals also included HCV infection with genotypes 2-4. Age, gender, ethnicity, characteristics of HCV infection, and fibrosis stage are indicated in Table 2.

The Ottawa Health Science Network Research Ethics Board approved intravenous blood collection from fully consenting human subjects. Nurses in the Clinical Investigative Unit (CIU) and the Viral Hepatitis Clinic performed the phlebotomies. Fibrotic scores were measured using the METAVIR score system and acquired using a non-invasive transient elastrography technique called a FibroScan®. HCV^+TX^- individuals were divided into two groups based on degree of liver damage (F0-F2 or F3-F4) after the Viral Hepatitis Clinic performed the fibrotic assessment.

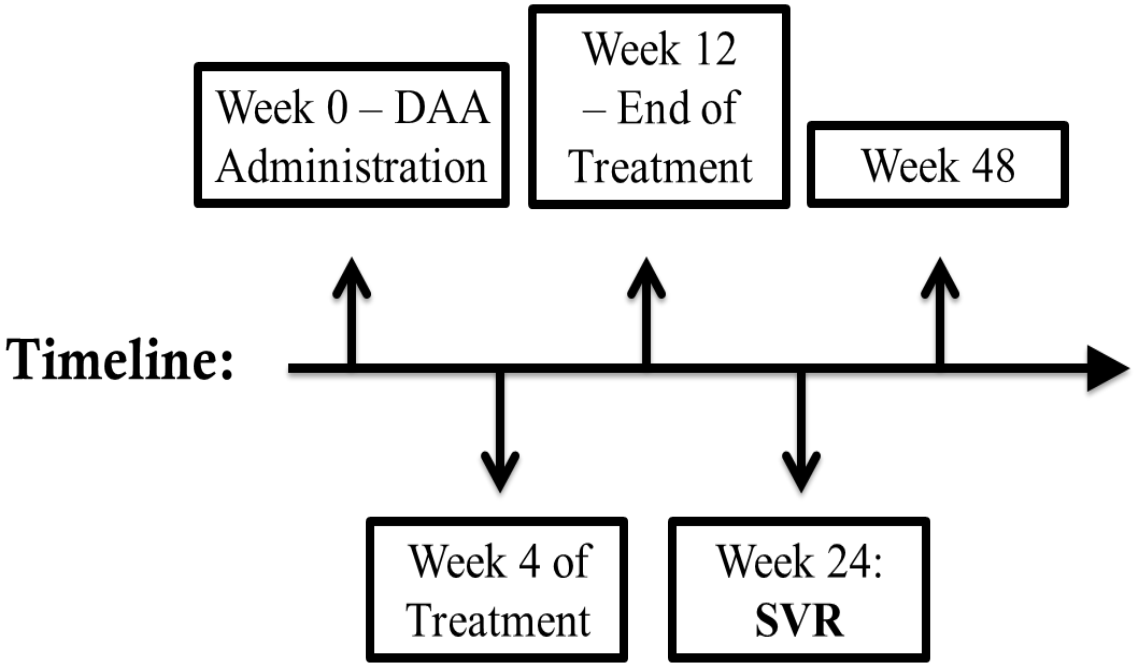

Figure 1: Treatment timeline for HCV^{+}TX^{+} individuals. This clinical study was led by Dr. Curtis Cooper at TOH-General Campus. DAA – Direct Acting Antivirals; SVR – Sustained Virological Response

Table 2. Characteristics of Study Subjects

		HCV^- Controls	HCV^+TX^- Individuals Minimal Fibrotic Stage	HCV^+TX^- Individuals Advanced Fibrotic Stage	HCV^+TX^+ Harvoni ± Ribavirin	
					Week 0 (Treatment Initiation)	24 Weeks Post SVR
Gender	Male	8	9	8	4	
	Female	7	3	1	3	
Total n		15	12	9	7	
Mean Age ± SD		41.83 ± 11.32	55.92 ± 9.94	52.11 ± 5.71	60.00 ± 9.76	
Ethnicity (% Caucasian)		80%	92%	89%	86%	
HCV Genotype						
	1		9	7	7	
	2		2*	1		
	3		1	1		
Ribavirin Treatment					6/9	
Fibrosis Stage [a]						
	0-2		12		5	6
	3-4			9	2	1
HCV RNA (IU/mL) Mean±SD			$2.6x10^6$ ± $3.6x10^6$	$2.8x10^6$ ± $4.4x10^6$	$3.5x10^6$ ± $2.86x10^6$	
ALT (U/L) Mean±SD			56.08 ± 15.31	107.67 ± 70.84	87.86 ± 60.43	24.71 ± 13.03

[a] Measured by fibroscan (Metavir system)
*One participant with genotype 2a and 4 co-infection

2.2 Isolation and Freezing of Peripheral Blood Mononuclear Cells

Human blood received from the CIU or the Viral Hepatitis Clinic was processed by Ficoll density gradient centrifugation to isolate peripheral blood mononuclear cells (PBMCs). Heparinized blood (30mL) was slowly layered on 15mL of lymphoprep (Stemcell Technologies, Vancouver, British Columbia, Canada) and centrifuged for 30 minutes at 470xg with the break off (Heraeus Instuments Megafuge 1.0). After centrifugation, the PBMC-containing buffy coat was collected using a Pasteur pipette and washed with PBS twice for 10 minutes at 470xg with the brake on. PBMCs were counted using the trypan blue (Sigma-Aldrich, Oakville, Ontario, Canada) exclusion method and washed with PBS one last time.

PBMCs were frozen for later use following a previously published protocol (162). Briefly, PBMCs were suspended at 1-2 x10^7 cells/mL in 90% FBS (Gibco, Life Technologies, Burlington, Ontario, Canada) and 10% DMSO (Sigma-Aldrich). Next, the cells were frozen in cryovials (Nalgene, Thermo Fisher Scientific) at -80^{o}C using a slow temperature-lowering polyethylene vial holder (Nalgene, Thermo Fisher Scientific, Waltham, MA, USA). Cryovials were transferred to liquid nitrogen (~ -200^{o}C) within a week.

2.3 Thawing of Peripheral Blood Mononuclear Cells

Cells were stored in liquid nitrogen for ≥ 1 week before thawing. Cryovials destined to be thawed were removed from liquid nitrogen and added to a bead bath at 37^{o}C for approximately 5 minutes or until the ice crystals had almost completely disappeared. Warmed R10 media, composed of RPMI (Gibco, Life Technologies) with 10% FBS, was added drop wise to each vial until the volumes were doubled. Cryovials belonging to the same individual were pooled and washed twice with warmed complete RPMI media at 470xg for 7 minutes. Finally, cells were re-

suspended in R20 media (RPMI supplemented with 20% FBS) and incubated overnight at 37°C and 5% CO_2.

2.4 Isolation of $CD8^+$ T Cells

Isolation of $CD8^+$ T cells from thawed PBMCs rested overnight was completed as described for the EasySep™ Human CD8 Positive Selection Kit II (STEMCELL Technologies, Vancouver, British Columbia, Canada). Briefly, PBMCs were counted, washed, and suspended at $1x10^8$ cells/mL in sort buffer (0.5% BSA, 2mM EDTA, PBS). If the volume exceeded 250µl of sort buffer, the "The Big Easy" EasySep™ magnet and a 14mL polystyrene round-bottom tube were used along with the associated protocol. If the volume was less than 250µl, the EasySep™ magnet and a 5mL polystyrene round-bottom tube were used instead. All tubes were incubated for 3 minutes with the selection cocktail (100µl/1mL PBMC) and then with rapidspheres (50µl/1mL PBMC). The tubes were topped up to 5mL or 2.5mL with sort buffer for The Big Easy and the EasySep™ magnets, respectively. Next, the tubes were placed in their respective magnets for 3 minutes and flipped into a waste beaker to remove any unbound cells. The process of sort buffer addition, magnet placement, and decanting was repeated two additional times before the cells were suspended in warmed R20 media for overnight rest at 37°C and 5% CO_2. Purity of isolated $CD8^+$ T-cells was checked regularly by flow cytometry, with a mean of 85.7% ± 5.7.

2.5 Cell Surface Phenotyping of $CD8^+$ T Cells

Isolated $CD8^+$ T cells from thawed PBMCs were surface stained and analyzed by flow cytometry on an FC500 machine (Beckman Coulter, Marseille, France) to identify the proportion of cells within eight subsets. $CD8^+$ T cells ($2x10^5$ per sample condition) were incubated in 100µl of 1% BSA-PBS with 10µl of CD27-PC5 (clone 1A4CD27, Beckman Coulter) and 5µl of CCR7-

APC/CY7 (Clone G043H7, Biolegend, San Diego, CA, USA) for 20 minutes in the dark at room temperature (RT). After washing with 1% BSA-PBS, cells were fixed with 200µl paraformaldehyde (PFA) for 20 minutes in the dark at RT. Cells were washed again and incubated in 100µl of 1% BSA-PBS with 10µl of CD45RA-ECD (clone 2H4LDH11LDB9, Beckman Coulter) for 20 minutes in the dark at RT. Finally, cells were washed twice with 1% BSA-PBS and assessed using flow cytometry.

CCR7, CD45RA, and CD27 identified eight $CD8^+$ T cell subsets: Naïve (T_N), naïve $CD27^{NEG}$ ($T_{N\ CD27^-}$), effector (T_E), pre-effector (T_{pE}), early effector memory (T_{EEM}), late effector memory (T_{LEM}), central memory (T_{CM}), and central memory $CD27^{NEG}$ ($T_{CM\ CD27^-}$). These subsets are defined as follows in this thesis: T_N ($CCR7^+CD45RA^+CD27^+$), $T_{N\ CD27^-}$ ($CCR7^+CD45RA^+CD27^-$), T_E ($CCR7^-CD45RA^+CD27^-$), T_{pE} (CCR7-CD45RA+$CD27^+$), T_{EEM} ($CCR7^-CD45RA^-CD27^+$), T_{LEM} ($CCR7^-CD45RA^-CD27^-$), T_{CM} ($CCR7^+CD45RA^-CD27^+$), and $T_{CM\ CD27^-}$ ($CCR7^+CD45RA^-CD27^-$) (96, 97, 103). Fluorescence minus one (FMO) controls (containing all antibodies apart from one) were used for gating within the preliminary lymphocyte gate by determining the location of the negative population. The preliminary lymphocyte gate was identified through the size and granularity range of the cells. Approximately 8000 to 50 000 events were collected in the lymphocyte gate and 3000 events were collected within the T_E gate (subset with lowest proportion of cells) where possible.

2.6 T-cell Receptor Stimulation using Anti-CD3 and Anti-CD28

A 96-well flat-bottom ELISA plate (Sarstedt, Nümbrecht, Germany) was UV-sterilized for 300 seconds. Wells were coated with 200µL of anti-CD3 (kindly provided by Dr. Seung-Hwan Lee at the University of Ottawa) at 10µg/mL or 200µL of PBS. The plates were incubated overnight at 4°C.

Following 24 hours of incubation, the isolated $CD8^+$ T cells were counted and re-suspended in warmed R20 media at $4x10^6$ cells/mL. Immediately after the ELISA plate was washed three times with PBS, $2x10^5$ $CD8^+$ T cells (50µL per well) were added to each well. Soluble anti-CD28 (50µL at 10µg/mL; Biolegend) was added to the wells previously coated with anti-CD3, and warmed R20 media (50µL) was added to the wells previously coated with PBS. Finally, the ELISA plate was incubated at 37°C and 5% CO_2 for 48 hours, after which the cells were stained to identify $CD8^+$ T cell subsets (see chapter 2.5), intracellular IFN-γ and perforin expression (see chapters 2.7 and 2.8), and surface expression of CD107a (see chapter 2.9).

2.7 Measurement of IFN-γ Expression

Six hours before the end of the 48-hour anti-CD3 and anti-CD28 stimulation, 50µl of a golgi inhibitor (Brefeldin A) was added at 15µg/mL to all wells destined to be stained for intracellular IFN-γ expression. At the end of the 48-hour incubation period, the $CD8^+$ T cells were surface stained with CD45RA-ECD, CD27-PC5, and CCR7-APC/CY7 to identify $CD8^+$ T cell subsets. After the surface staining, the plate was washed twice and incubated in 100µl saponin (Sigma-Aldrich) in 10% Human AB serum (Vally Biomedical Inc., Winchester, VA, USA). Next, 10µl of IFN-γ FITC (clone 4S.B3, Biolegend) was added to the IFN-γ wells before the plate was incubated for 30 minutes in the dark at 4°C. Additionally, IgG1κ - FITC isotype (clone MOPC-21, Biolegend) stained and stimulated wells were performed to evaluate non-specific binding. After intracellular staining, cells were washed twice with PBS and analyzed using flow cytometry.

2.8 Measurement of Perforin Expression

Stimulation was performed as described in chapter 2.6. A golgi inhibitor was not added for the measurement of intracellular perforin expression. Staining was performed following the

protocol mentioned above in chapter 2.7. The perforin and isotype wells were stained with 10µl of perforin- FITC (clone δG9, BD Pharmingen, BD Bioscience, San Jose, CA, USA) and IgG2b-FITC (clone 27-35, BD Pharmingen, BD Bioscience), respectively. The staining protocol was adjusted to minimize non-specific binding through the addition of human AB serum (10%) during staining (Figure S1).

2.9 Measurement of CD107a Expression

Stimulation was performed as described in chapter 2.6. In contrast to intracellular perforin and IFN-γ expression, 8µM of the golgi inhibitor monensin (BD Pharmingen, BD Bioscience) was added 6 hours before the end of the 48-hour anti-CD3 and anti-CD28 stimulation. Staining was performed following the protocol mentioned above in chapter 2.7. CD107a and isotype wells were stained with 10µl of CD107a- FITC (clone H4A3, BD Bioscience) and IgG1κ - FITC (clone MOPC-21, BD Bioscience), respectively. The staining protocol was adjusted to minimize non-specific binding through the addition of human AB serum (10%) during staining (Figure S2).

2.10 Collection of Supernatants

Following stimulation with anti-CD3 and anti-CD28 as described in chapter 2.6, plates were centrifuged at 470xg for 5 minutes. Approximately 100ul of supernatants were collected from the unstimulated and stimulated wells not treated with a golgi inhibitor. Supernatants were inactivated (potentially infected cells were lysed) for 1 hour at 37^{o}C and 5% $C0_2$ using 10% of a solution containing 1% triton X-100 (Sigma-Aldrich) and 3% tributyl phosphate (Sigma-Aldrich). Vials of supernatants were placed in -20^{o}C for long-term storage and future Luminex MAGPIX® experiments.

2.11 Measurement of IFN-γ and Perforin in Supernatants

Measurement of released IFN-γ and perforin in supernatants after 48 hours of anti-CD3 and anti-CD28 stimulation was performed as described for an immunology multiplex assay (Millipore Sigma, St. Louis, Missouri, USA) analysed with a MAGPIX® reader (Millipore Sigma). Briefly, thawed and inactivated supernatants were incubated at 4°C on a plate shaker overnight with beads conjugated to a capture antibody specific for a particular analyte, in this case perforin or IFN-γ. The next day, biotinylated detection antibodies and Streptavidin-PE conjugate were incubated with the supernatants before reading on the MAGPIX® reader. Biotin and Streptavidin bind tightly together, allowing identification of captured analyte through expression of the PE fluorochrome. Each individual capture bead was identified based on size and the amount of analyte after bioassay completion was quantified through fluorescent reporter signals.

2.12 Analysis and Statistics

The analysis of flow cytometry and MAGPIX® data was conducted using FCS Express Research Edition 4.0 (De Novo Software, Los Angeles, California, USA) and MILLIPLEX® Analyst 4.0 (xPONENT Software, Toronto, Ontario, Canada), respectively. Graphs and statistics were performed using GraphPad Prism 5.0 and 6.0 software (San Diego, California, USA). Statistical analysis included paired and unpaired (depending on the compared sample groups) two-tailed Student's *t*-test for $CD8^+$ T cell subset distribution experiments and one-tailed Student's *t*-test for cytokine and functional marker expression experiments (significance when $p \leq 0.05$). In this thesis, data values are communicated as means ± standard deviation.

Chapter 3: Results

3.1 Phenotype of Blood-derived $CD8^+$ T Cells during Untreated Chronic HCV Infection

The subset distribution of $CD8^+$ T cells in uninfected controls and chronic HCV infection was assessed as shown in Table 3. $CD8^+$ T cells, isolated from thawed PBMCs, were analysed by surface expression of CD45RA and CCR7, referred to in this thesis as the *two-marker* gating strategy. Four subsets of $CD8^+$ T cells were identified, including naïve (T_N), effector (T_E), effector memory (T_{EM}), and central memory (T_{CM}). The purity of isolated $CD8^+$ T cells is depicted in Figure S3. The gating strategy and data collected for the *two-marker* strategy are illustrated in Figures 2A and 2B. These $CD8^+$ T cell subsets are defined as follows: T_N ($CCR7^+CD45RA^+$), T_E ($CCR7^-CD45RA^+$), T_{EM} ($CCR7^-CD45RA^-$), and T_{CM} ($CCR7^+CD45RA^-$). In uninfected controls, the $CD8^+$ T cell subset distribution was similar to previous reports (144, 163) which identified the largest population as T_N. In the present study, the observed results were (mean ± SD): T_N (40.1% ± 18.0), T_E (9.4% ± 5.1), T_{EM} (25.3% ± 12.3), and T_{CM} (25.3% ± 11.4) (Figure 2B). $CD8^+$ T cell subset distribution for untreated $HCV^{+\ Min.\ Fibrosis}$ individuals (fibrotic score F0-F2) was not significantly different compared to the uninfected controls: T_N (30.6% ± 15.3), T_E (13.5% ± 8.2), T_{EM} (30.3% ± 14.0), and T_{CM} (25.7% ± 7.2) (Figure 2B). Finally, $CD8^+$ T cell subset distribution for untreated $HCV^{+\ Adv.\ Fibrosis}$ individuals (fibrotic score F3-F4) was significantly different (unpaired Student's *t*-test) compared to uninfected controls in each category except T_{CM}: T_N (21.2% ± 9.8), T_E (16.5% ± 6.8), T_{EM} (39.9% ± 14.2), and T_{CM} (22.4% ± 11.5) (Figure 2B). To summarize, the proportion of T_N was significantly lower ($P = 0.02$ by unpaired Student's *t*-test) and the proportion of T_E and T_{EM} were significantly higher ($P = 0.02$ and $P = 0.03$, respectively) in $HCV^{+\ Adv.\ Fibrosis}$ compared to controls. However, no significant differences were observed between $HCV^{+\ Adv.\ Fibrosis}$ and $HCV^{+\ Min.\ Fibrosis}$.

$CD8^+$ T cell subset distribution was also analyzed using the expression of an additional surface marker known as CD27, commonly used to identify $CD8^+$ T cell subsets (101, 164, 165). CD27 is a TNF-family receptor that diminishes during maturation and differentiation of $CD8^+$ T cells (103). The use of CD27 in combination with CD45RA and CCR7 surface expression to identify $CD8^+$ T cell subsets is referred to in this thesis as the *three-marker* gating strategy. The gating strategy and the data collected for this strategy are illustrated in Figures 2C and 2D. This method resulted in the assessment of a larger number of $CD8^+$ T cell subsets, including T_N, $T_{N\ CD27^-}$ (naïve $CD27^{NEG}$), T_E, T_{pE} (pre-effector), T_{EEM} (early effector memory), T_{LEM} (late effector memory), T_{CM}, and $T_{CM\ CD27^-}$ (central memory $CD27^{NEG}$). These eight subsets are defined as follows: T_N ($CCR7^+CD45RA^+CD27^+$), $T_{N\ CD27^-}$ ($CCR7^+CD45RA^+CD27^-$), T_E ($CCR7^-CD45RA^+CD27^-$), T_{pE} ($CCR7^-CD45RA^+CD27^+$), T_{EEM} ($CCR7^-CD45RA^-CD27^+$), T_{LEM} ($CCR7^-CD45RA^-CD27^-$), T_{CM} ($CCR7^+CD45RA^-CD27^+$), and $T_{CM\ CD27^-}$ ($CCR7^+CD45RA^-CD27^-$). The $CD8^+$ T cell subset distribution of uninfected controls was as follows: T_N (36.7% ± 17.1), $T_{N\ CD27^-}$ (3.4% ± 1.8), T_E (7.9% ± 4.7), T_{pE} (1.4% ± 0.7), T_{EEM} (6.8% ± 2.8), T_{LEM} (18.5% ± 12.6), T_{CM} (17.2% ± 8.0), and $T_{CM\ CD27^-}$ (8.1% ± 3.9) (Figure 2D). $CD8^+$ T cell subset distribution for untreated $HCV^{+\ Min.\ Fibrosis}$ individuals was not significantly different compared to uninfected controls. However, a lower percentage of T_N and a higher percentage of T_{LEM} was observed for $HCV^{+\ Min.\ Fibrosis}$ compared to controls: T_N (24.8% ± 14.5), $T_{N\ CD27^-}$ (5.8% ± 2.6), T_E (12.1% ± 7.5), T_{pE} (1.3% ± 1.2), T_{EEM} (7.9% ± 10.1), T_{LEM} (22.4% ± 9.1), T_{CM} (14.0% ± 3.7), and $T_{CM\ CD27^-}$ (11.7% ± 4.4) (Figure 2D). Importantly, the proportion of T_N for untreated $HCV^{+\ Adv.\ Fibrosis}$ individuals was significantly lower ($P = 0.009$ by unpaired Student's *t*-test) compared to uninfected controls and the proportion of T_{LEM} was significantly higher ($P = 0.02$ by unpaired Student's *t*-test): T_N (15.8% ± 8.3), $T_{N\ CD27^-}$ (5.4% ± 2.6), T_E (13.5% ± 7.0), T_{pE} (3.0% ± 4.6),

T_{EEM} (4.8% ± 3.5), T_{LEM} (35.1% ± 15.5), T_{CM} (10.2% ± 8.6), and $T_{CM\ CD27^-}$ (12.5% ± 6.2) (Figure 2D). The finding of a significantly decreased proportion of T_N in $HCV^{+\ Adv.\ Fibrosis}$ compared to controls supported results from the *two-marker* strategy. However, the *three-marker* strategy did not show a significant increase in the proportion of T_E measured for $HCV^{+\ Adv.\ Fibrosis}$. Furthermore, T_{LEM} was identified as the larger subset contributing to effector memory $CD8^+$ T cells. The proportion of T_{LEM} was significantly increased in $HCV^{+\ Adv.\ Fibrosis}$ compared to both uninfected controls and $HCV^{+\ Min.\ Fibrosis}$ (P = 0.02 and P = 0.05 by unpaired Student's *t*-test, respectively).

Two-marker $CD8^+$ T Cell Subset (CD45RA & CCR7)	CCR7	CD45RA	Three-Marker $CD8^+$ T Cell Subset (CD45RA, CD27 & CCR7)	CD27
Naïve	+	+	Naïve (T_N)	+
			Naïve $CD27^-$ ($T_{N\ CD27}^{NEG}$)	-
Effector	-	+	Effector (T_E)	-
			Pre-effector (T_{pE})	+
Effector Memory	-	-	Early Effector Memory (T_{EEM})	+
			Late Effector Memory (T_{LEM})	-
Central Memory	+	-	Central Memory (T_{CM})	+
			Central Memory $CD27^-$ ($T_{CM\ CD27}^{NEG}$)	-

Table 3: Phenotypic descriptions of $CD8^+$ T cell subsets. Table to describe the two-*marker* and *three-marker* strategies to define cell subsets. The *two-marker* strategy uses the surface marker expression of CD45RA and CCR7 and the *three-marker* strategy uses the surface marker expression of CD45RA, CCR7, and CD27.

A

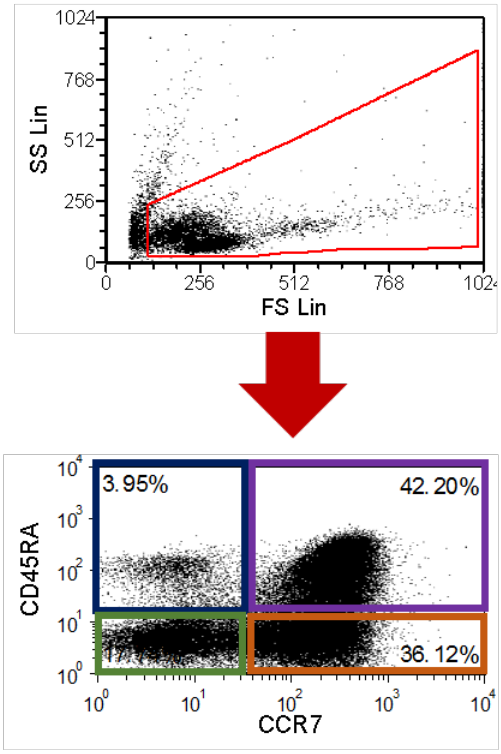
1024
768
512
256
0
SS Lin
0
256
512
768
1024
FS Lin
Naïve
Effector
Effector Memory
Central Memory
3.95%
42.20%
36.12%
CD45RA
CCR7

B

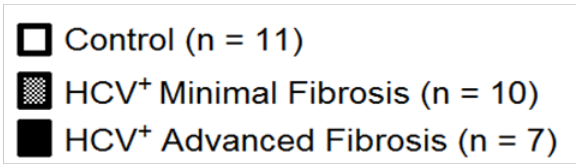
Control (n = 11)
HCV+ Minimal Fibrosis (n = 10)
HCV+ Advanced Fibrosis (n = 7)

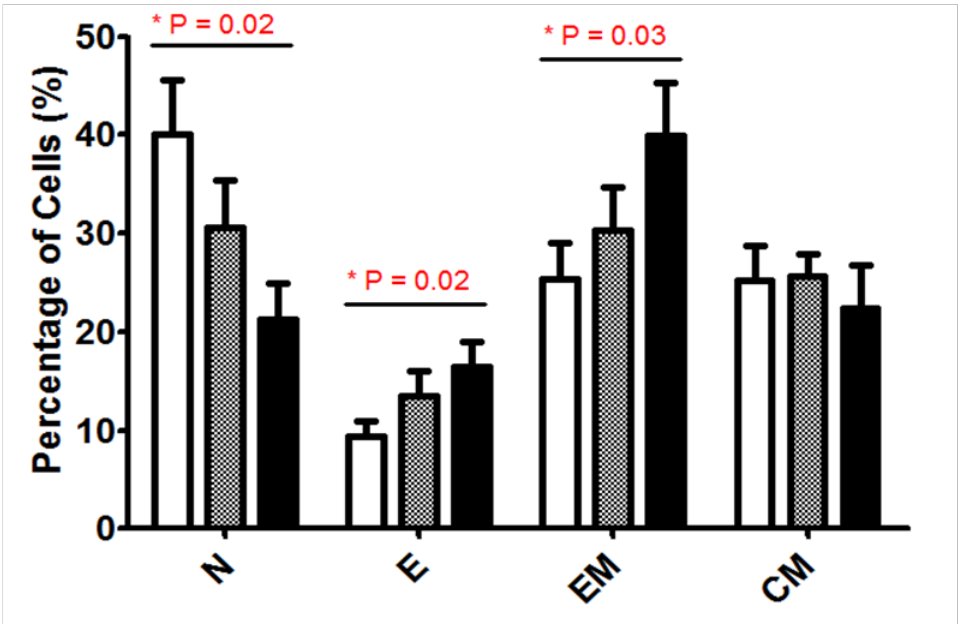
* P = 0.02
* P = 0.03
* P = 0.02
Percentage of Cells (%)
50
40
30
20
10
0
N
E
EM
CM

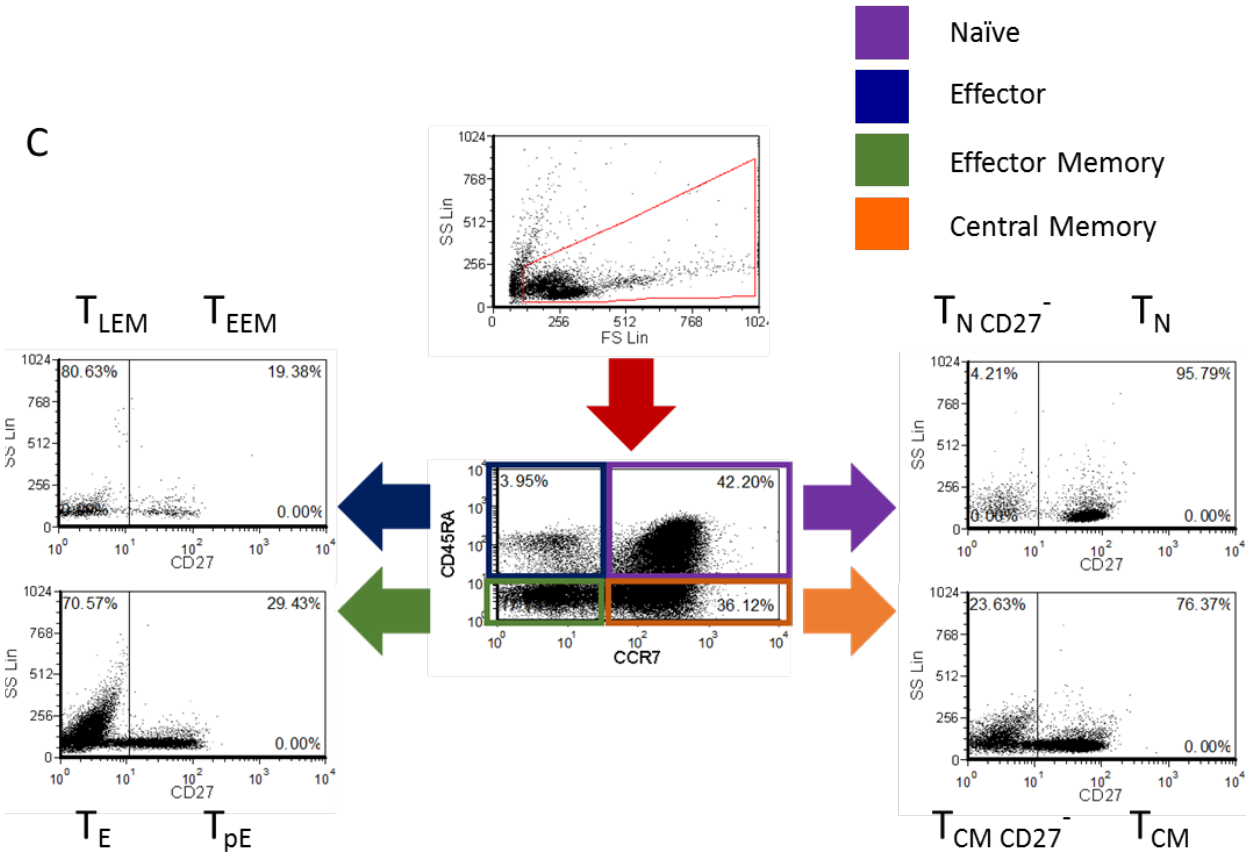
C
Naïve
Effector
Effector Memory
Central Memory
SS Lin
FS Lin
CD45RA
CCR7
CD27
3.95%
42.20%
36.12%
T_{LEM}
T_{EEM}
80.63%
19.38%
0.00%
0.00%
T_E
T_{pE}
70.57%
29.43%
0.00%
0.00%
$T_{N\ CD27^-}$
T_N
4.21%
95.79%
0.00%
0.00%
$T_{CM\ CD27^-}$
T_{CM}
23.63%
76.37%
0.00%
0.00%

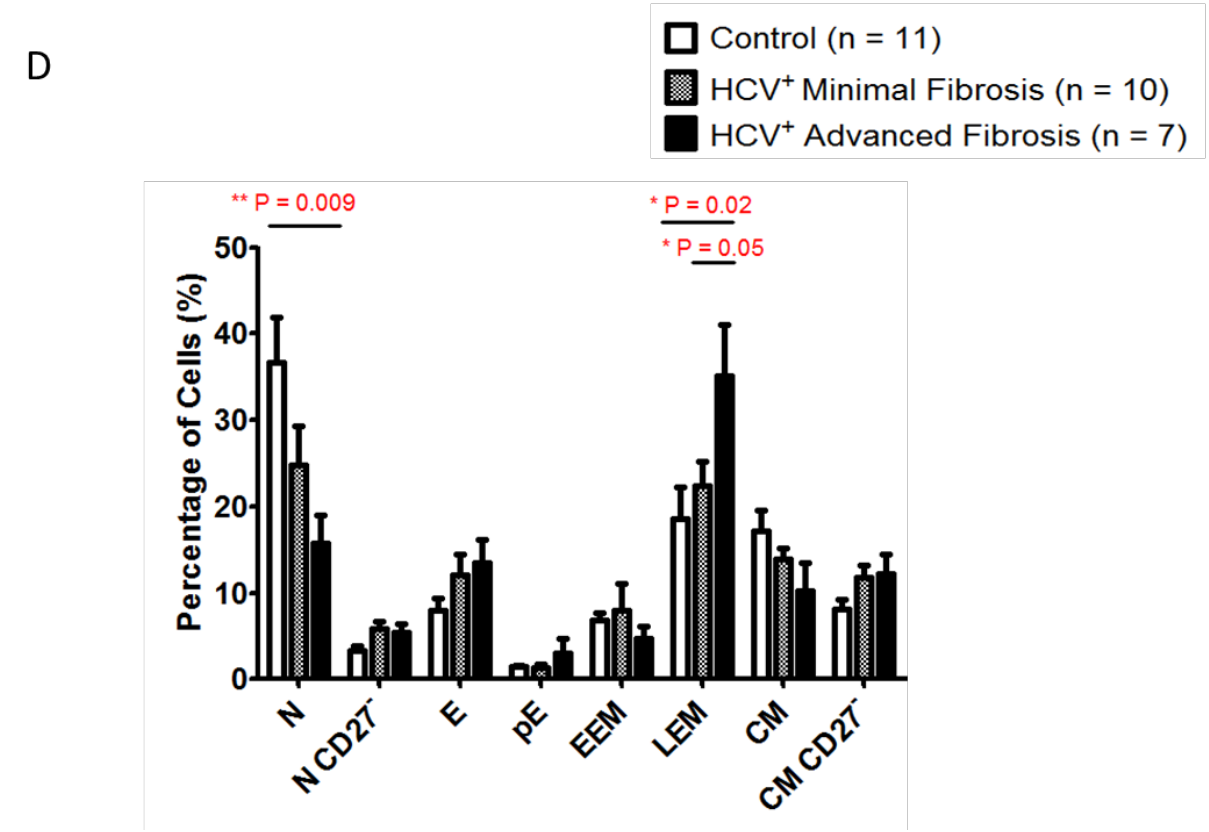
D
Control (n = 11)
HCV+ Minimal Fibrosis (n = 10)
HCV+ Advanced Fibrosis (n = 7)
** P = 0.009
* P = 0.02
* P = 0.05
Percentage of Cells (%)
0
10
20
30
40
50
N
N CD27-
E
pE
EEM
LEM
CM
CM CD27-

Figure 2: Isolated $CD8^+$ T cells were stained for surface markers to identify the percentage of cells within a subset. A) *Two-marker* gating strategy using expression of surface markers CD45RA and CCR7 to identify the percentage of cells within each of four subsets, defined as follows: naïve ($CCR7^+CD45RA^+$), effector ($CCR7^-CD45RA^+$), effector memory ($CCR7^-CD45RA^-$), and central memory ($CCR7^+CD45RA^-$). **B)** $CD8^+$ T cell subset distribution for controls (n = 11), untreated $HCV^{+\ \text{Min. Fibrosis}}$ (n = 10), and untreated $HCV^{+\ \text{Adv. Fibrosis}}$ (n = 7) using the *two-marker* gating strategy. **C)** *Three-marker* gating strategy using expression of surface markers CD45RA, CCR7, and CD27 to identify the percentage of cells within each of eight subsets, defined as follows: naïve ($CCR7^+CD45RA^+CD27^+$), naïve $CD27^{NEG}$ ($CCR7^+CD45RA^+CD27^-$), effector ($CCR7^-CD45RA^+CD27^-$), pre-effector ($CCR7^-CD45RA^+CD27^+$), early effector memory ($CCR7^-CD45RA^-CD27^+$), late effector memory ($CCR7^-CD45RA^-CD27^-$), central memory ($CCR7^+CD45RA^-CD27^+$), and central memory $CD27^{NEG}$ ($CCR7^+CD45RA^-CD27^-$). **D)** $CD8^+$ T cell subset distribution for controls (n = 11), untreated $HCV^{+\ \text{Min. Fibrosis}}$ (n = 10) and untreated $HCV^{+\ \text{Adv. Fibrosis}}$ (n = 7) using the *three-marker* gating strategy.

3.2 IFN-γ Expression of Blood-derived $CD8^+$ T Cells during Untreated HCV Chronic Infection

IFN-γ expression was measured in uninfected and HCV-infected $CD8^+$ T cells (cells derived from individuals infected chronically with HCV) to assess the relationship between liver fibrosis and the inflammatory response. Flow cytometry was used to measure the stimulation-induced intracellular expression of IFN-γ for the entire population of $CD8^+$ T cells, referred to as the bulk in this thesis (Figure 3A and B). More specifically, bulk $CD8^+$ T cells include both non-specific and specific $CD8^+$ T cells. The optimization of anti-CD3/CD28 stimulation was determined using a time course and dose response (Figure S4). The expression of intracellular IFN-γ in $CD8^+$ T cells following 48 hours of anti-CD3/CD28 stimulation for each TX^- donor/patient group (uninfected controls, $HCV^{+\text{ Min. Fibrosis}}$, and $HCV^{+\text{ Adv. Fibrosis}}$) is depicted in Figure 3B. Induction of IFN-γ is defined by the significance between the numbers of IFN-γ^+ cells in unstimulated cultures compared to the number in stimulated cultures. Anti-CD3/CD28 induced IFN-γ expression in $CD8^+$ T cells from all donor/patient groups (controls: $P = 0.0002$; $HCV^{+\text{ Min. Fibrosis}}$: $P = 0.0001$; $HCV^{+\text{ Adv. Fibrosis}}$: $P = 0.004$; by paired Student's *t*-test). Notably, there was a significantly lower percentage of IFN-γ^+ $CD8^+$ T cells in $HCV^{+\text{ Min. Fibrosis}}$ upon stimulation compared to uninfected controls ($P = 0.03$ by unpaired Student's *t*-test).

Luminex MAGPIX® was used to measure the concentration of IFN-γ in culture supernatants collected from unstimulated and anti-CD3/CD28 stimulated $CD8^+$ T cells. The measured concentrations for each donor/patient group are depicted in Figure 3C. IFN-γ expression in culture supernatants was significantly induced by anti-CD3/CD28 for each donor/patient group (controls: $P = 0.01$; $HCV^{+\text{ Min. Fibrosis}}$: $P = 0.01$; $HCV^{+\text{ Adv. Fibrosis}}$: $P = 0.005$; by paired Student's *t*-test). Interestingly, there was a significantly higher concentration of IFN-γ

in $HCV^{+\ Adv.\ Fibrosis}$ upon stimulation compared to $HCV^{+\ Min.\ Fibrosis}$ ($P = 0.02$ by unpaired Student's *t*-test). Contrary to intracellular IFN-γ expression, the amount released upon stimulation for $HCV^{+\ Min.\ Fibrosis}$ was not significantly lower compared to uninfected controls.

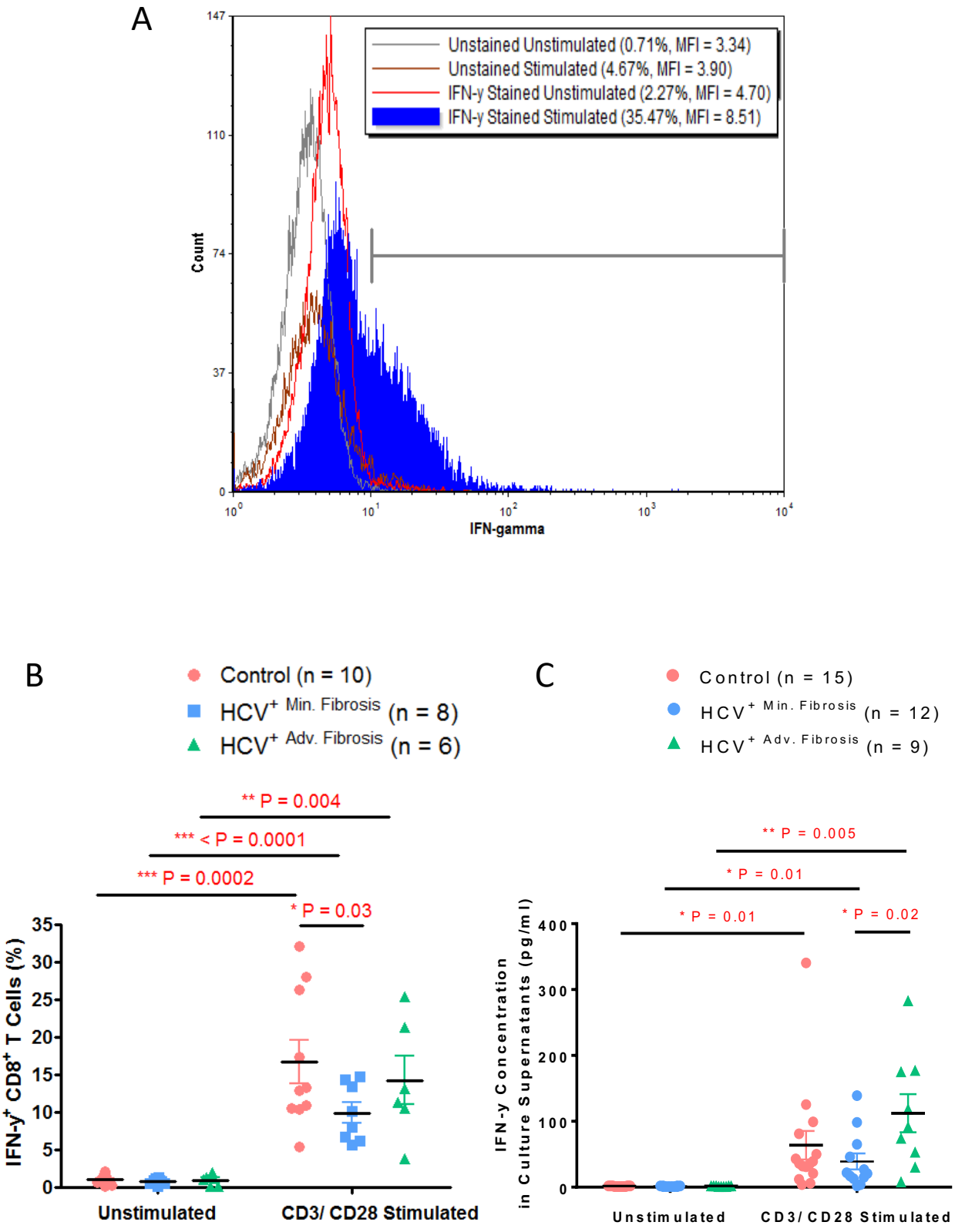
A
Unstained Unstimulated (0.71%, MFI = 3.34)
Unstained Stimulated (4.67%, MFI = 3.90)
IFN-γ Stained Unstimulated (2.27%, MFI = 4.70)
IFN-γ Stained Stimulated (35.47%, MFI = 8.51)
Count
IFN-gamma
B
Control (n = 10)
HCV+ Min. Fibrosis (n = 8)
HCV+ Adv. Fibrosis (n = 6)
** P = 0.004
*** < P = 0.0001
*** P = 0.0002
* P = 0.03
IFN-γ+ CD8+ T Cells (%)
Unstimulated
CD3/ CD28 Stimulated
C
Control (n = 15)
HCV+ Min. Fibrosis (n = 12)
HCV+ Adv. Fibrosis (n = 9)
** P = 0.005
* P = 0.01
* P = 0.01
* P = 0.02
IFN-γ Concentration in Culture Supernatants (pg/ml)
Unstimulated
CD3/ CD28 Stimulated

Figure 3: IFN-γ expression without stimulation and after 48 hours of anti-CD3/CD28 stimulation. A) Representative histogram of intracellular IFN-γ expression measured by flow cytometry for bulk $CD8^+$ T cells in four conditions: unstained unstimulated, unstained CD3/CD28 stimulated, IFN-γ stained unstimulated, and IFN-γ stained CD3/CD28 stimulated. **B)** Intracellular IFN-γ expression of bulk $CD8^+$ T cells measured by flow cytometry for controls (n = 10), untreated $HCV^{+\ \text{Min. Fibrosis}}$ (n = 8), and untreated $HCV^{+\ \text{Adv. Fibrosis}}$ (n = 6). **C)** IFN-γ concentration within culture supernatants of $CD8^+$ T cells measured using MAGPIX for controls (n = 15), untreated $HCV^{+\ \text{Min. Fibrosis}}$ (n = 12), and untreated $HCV^{+\ \text{Adv. Fibrosis}}$ (n = 9).

3.3 IFN-γ Expression of Eight $CD8^+$ T Cell Subsets during Untreated HCV Chronic Infection

The *three-marker* gating strategy depicted in Figure 2C was used to distinguish between eight subsets previously described in Table 3 based on IFN-γ expression. The representative dot plots in Figure 4A show the intracellular IFN-γ expression of T_{CM} (upper quadrants) and $T_{CM\ CD27^-}$ (lower quadrants) from uninfected controls in the absence (left dot plot) and presence (right dot plot) of anti-CD3/CD28 stimulation.

The intracellular IFN-γ expressions within T_N, T_E, $T_{EEM,}$ and T_{CM} subsets are shown in Figure 4B. Of note, there was a significantly higher percentage of T_E (unpaired Student's *t*-test) expressing IFN-γ upon stimulation in $HCV^{+\ Adv.\ Fibrosis}$ compared to both $HCV^{+\ Min.\ Fibrosis}$ ($P = 0.02$) and uninfected controls ($P = 0.03$). No significant differences were observed between the donor/patient groups in the remaining $CD8^+$ T cell subsets (Figure 4B).

The intracellular IFN-γ expressions within $T_{N\ CD27^-}$, T_{pE}, $T_{LEM,}$ and $T_{CM\ CD27^-}$ subsets are shown in Figure 4C. Both $T_{N\ CD27^-}$ and $T_{CM\ CD27^-}$ subsets had a significantly higher percentage of cells in $HCV^{+\ Adv.\ Fibrosis}$ (unpaired Student's *t*-test) expressing IFN-γ after stimulation compared to $HCV^{+\ Min.\ Fibrosis}$ ($T_{N\ CD27^-}$: $P = 0.02$; $T_{CM\ CD27^-}$: $P = 0.01$) and uninfected controls ($T_{N\ CD27^-}$: $P = 0.008$; $T_{CM\ CD27^-}$: $P = 0.02$). Similarly, T_{LEM} had a significantly larger percentage of IFN-γ^+ cells after stimulation in $HCV^{+\ Adv.\ Fibrosis}$ compared to $HCV^{+\ Min.\ Fibrosis}$ ($P = 0.03$ by Student's *t*-test). No significant differences were observed between donor/patient groups in T_{pE}, the remaining $CD8^+$ T cell subset in Figure 4C.

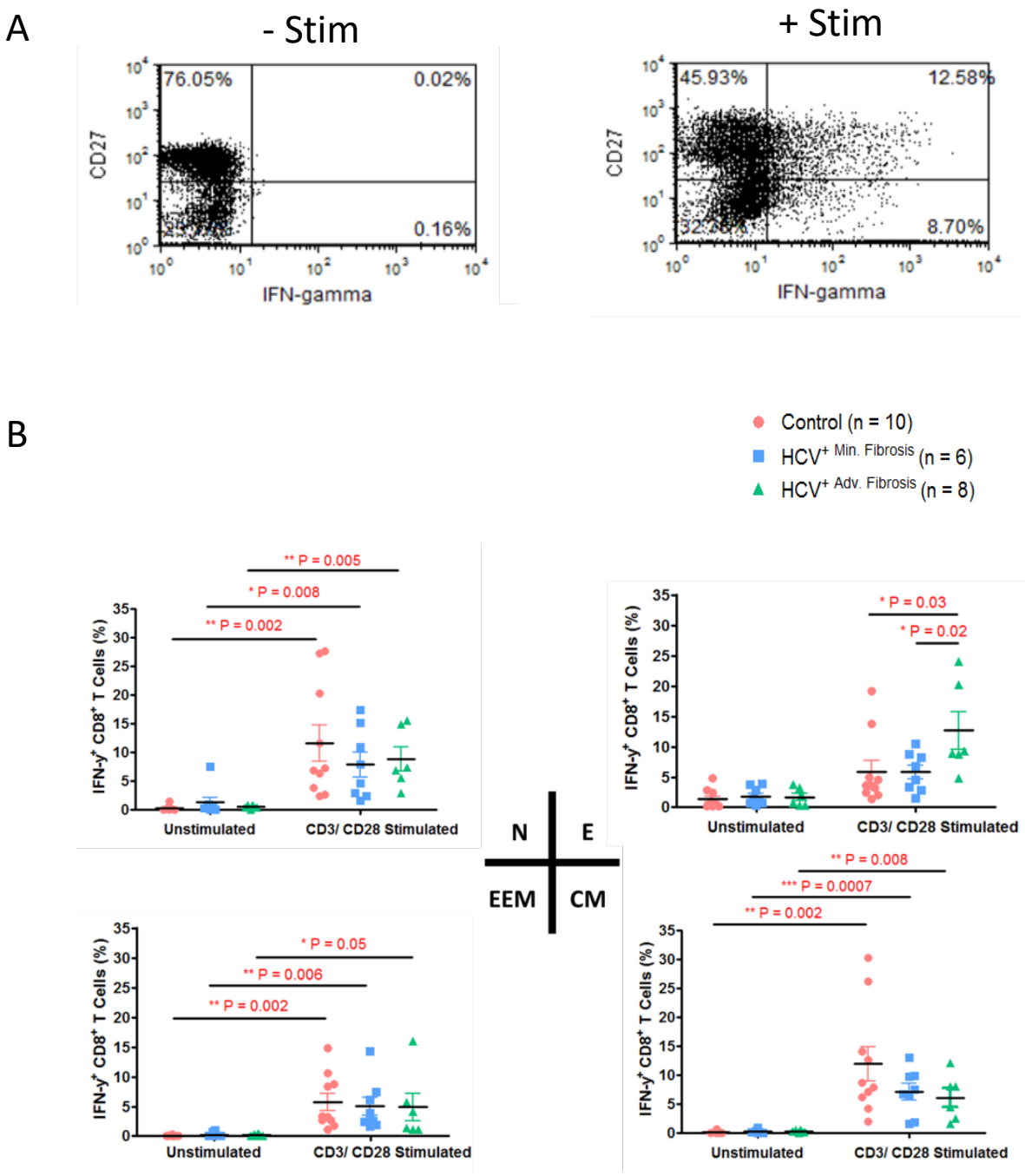
A
- Stim
+ Stim
76.05%
0.02%
0.16%
45.93%
12.58%
8.70%
CD27
IFN-gamma
B
Control (n = 10)
HCV+ Min. Fibrosis (n = 6)
HCV+ Adv. Fibrosis (n = 8)
IFN-γ+ CD8+ T Cells (%)
Unstimulated
CD3/ CD28 Stimulated
** P = 0.005
* P = 0.008
** P = 0.002
* P = 0.03
* P = 0.02
* P = 0.05
** P = 0.006
** P = 0.002
** P = 0.008
*** P = 0.0007
** P = 0.002
N
E
EEM
CM

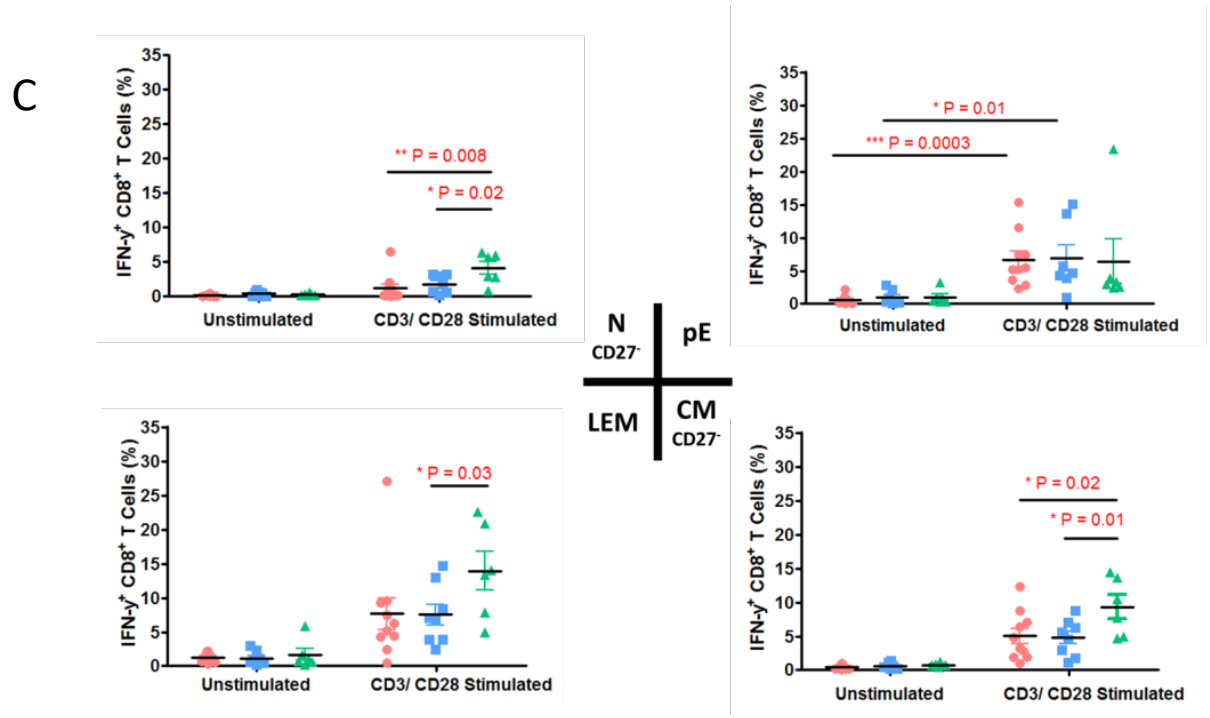

Figure 4: Intracellular IFN-γ expression of $CD8^+$ T cells measured by flow cytometry for controls (n = 10), $HCV^{+\ Min.\ Fibrosis}$ (n = 6), and $HCV^{+\ Adv.\ Fibrosis}$ (n = 8) after 48 hours of anti-CD3/CD28 stimulation. A) Representative intracellular IFN-γ dot plots using the *three-marker* gating strategy for T_{CM} (top quadrants) and $T_{CM\ CD27^-}$ (bottom quadrants) in uninfected controls without stimulation (left) and after anti-CD3/CD28 stimulation (right). **B)** IFN-γ expression in naïve (top left), effector (top right), early effector memory (bottom left), and central memory (bottom right) thawed $CD8^+$ T cells upon anti-CD3/CD28 stimulation. **C)** IFN-γ expression in naïve $CD27^-$ (top left), pre-effector (top right), late effector memory (bottom left), and central memory $CD27^-$ (bottom right) thawed $CD8^+$ T cells upon anti-CD3/ CD28 stimulation.

3.4 CD107a Expression of Blood-derived $CD8^+$ T Cells during Untreated Chronic HCV Infection

CD107a expression was measured in $CD8^+$ T cells from uninfected and HCV-infected individuals to assess the possible effects of liver fibrosis on activation and degranulation, important components of the adaptive immune response. CD107a is present on the inside of endosome membranes which house perforin and granzymes. The parameters of anti-CD3/CD28 stimulation were determined using a time course and dose response (Figure S5). The expression of CD107a upon 48 hours of anti-CD3/CD28 stimulation was analyzed in bulk $CD8^+$ T cells and subsets for each TX^- donor/patient group (Figure 5A - E). The induction of CD107a expression due to anti-CD3/CD28 stimulation in bulk $CD8^+$ T cells for each donor/patient group is shown in Figure 5A (controls: $P = 0.0001$; $HCV^{+\text{ Min. Fibrosis}}$: $P = 0.0001$; $HCV^{+\text{ Adv. Fibrosis}}$: $P = 0.02$; by paired Student's *t*-test). A representative histogram of CD107a expression for $CD8^+$ T cells isolated from an uninfected control is shown in Figure 5B. Similar to intracellular IFN-γ expression in bulk $CD8^+$ T cells, a significantly lower percentage of $CD107a^+$ $CD8^+$ T cells was observed in $HCV^{+\text{ Min. Fibrosis}}$ after stimulation ($P = 0.002$ by unpaired Student's *t*-test) compared to uninfected controls.

The representative dot plot for unstimulated (top) and anti-CD3/CD28 stimulated (bottom) conditions is illustrated in Figure 5C for T_{CM} (top quadrants) and $T_{CM\ CD27^-}$ (bottom quadrants). The *three-marker* gating strategy (Figure 2C) was used to identify the eight $CD8^+$ T cell subsets described in Table 3.

The CD107a expressions within the T_N, T_E, T_{EEM}, and T_{CM} subsets are illustrated in Figure 5D. The expression of CD107a was significantly lower (unpaired Student's *t*-test) following anti-CD3/CD28 stimulation in T_N ($P = 0.05$) and T_{CM} ($P = 0.004$) for $HCV^{+\text{ Min. Fibrosis}}$

compared to uninfected controls. Interestingly, the percentage of CD107a^{+} T_{CM} for HCV$^{+\text{ Adv. Fibrosis}}$ after stimulation was also significantly lower compared to uninfected controls ($P = 0.03$ by unpaired Student's *t*-test). No significant differences between donor/patient groups were observed for the remaining CD8^{+} T cell subsets in Figure 5D, including T_{EEM} and T_{E}.

The CD107a expressions within $T_{N\ CD27^{-}}$, T_{pE}, $T_{LEM,}$ and $T_{CM\ CD27^{-}}$ subsets are depicted in Figure 5E. Significant differences in CD107a expression for each subset were not observed between the donor/patient groups upon stimulation (Figure 5E). Interestingly, induction of CD107a expression following anti-CD3/CD28 stimulation did not occur for HCV$^{+\text{ Min. Fibrosis}}$ or HCV$^{+\text{ Adv. Fibrosis}}$ in T_{pE} but was significantly induced for uninfected controls ($P < 0.0001$ by paired Student's *t*-test). Additionally, a significantly higher percentage of CD107a^{+} T_{pE} cells were detected in the unstimulated condition for infected donors compared to the uninfected controls ($P = 0.04$ for HCV$^{+\text{ Min. Fibrosis}}$ and $P = 0.05$ for HCV$^{+\text{ Adv. Fibrosis}}$ by unpaired Student's *t*-test).

A

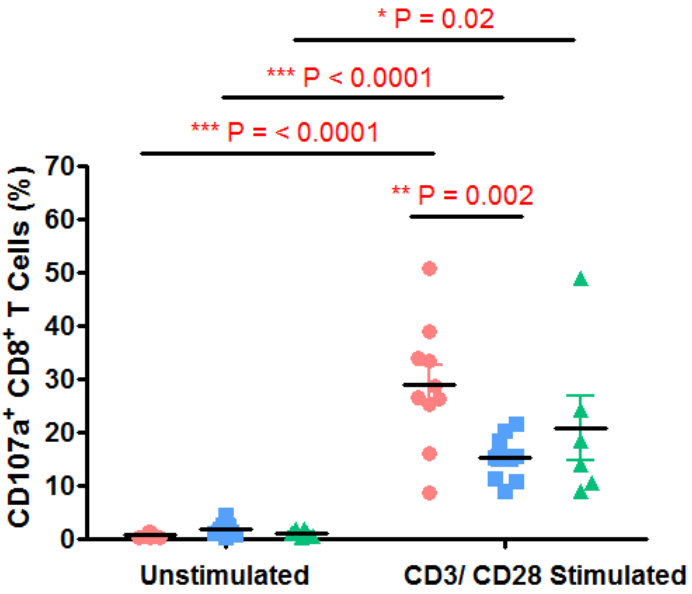
* P = 0.02
*** P < 0.0001
*** P = < 0.0001
** P = 0.002
CD107a+ CD8+ T Cells (%)
70
60
50
40
30
20
10
0
Unstimulated
CD3/ CD28 Stimulated

B

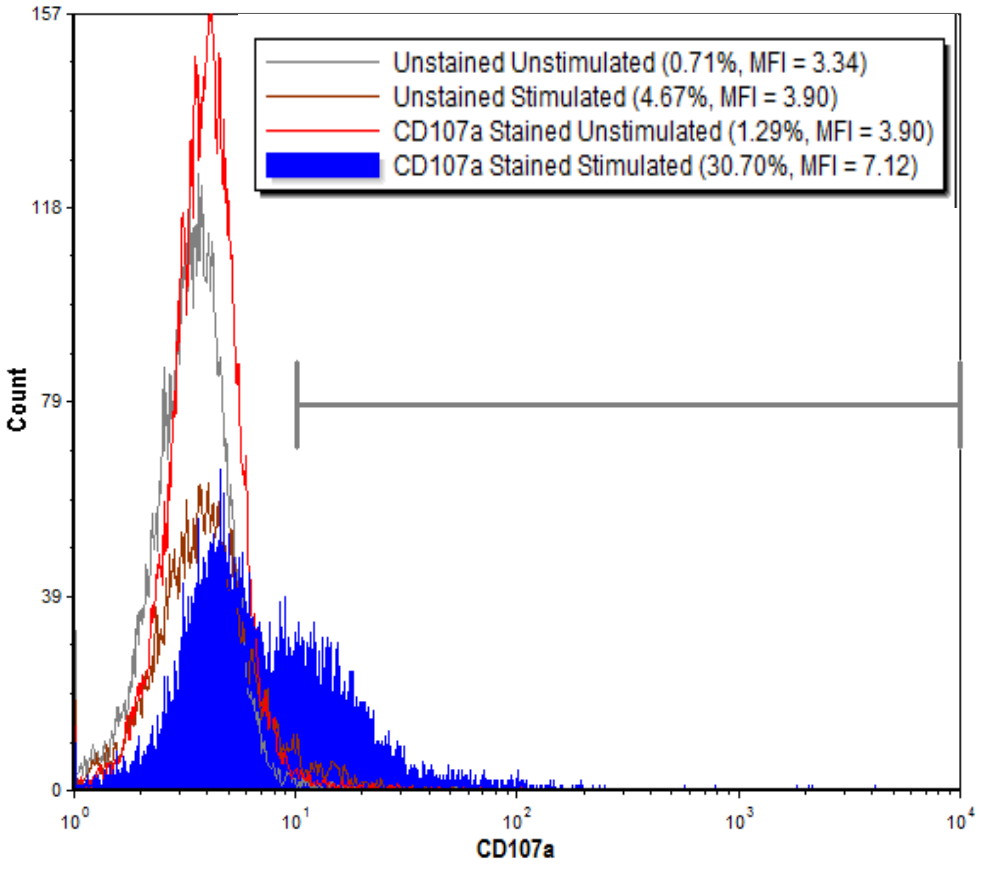
Unstained Unstimulated (0.71%, MFI = 3.34)
Unstained Stimulated (4.67%, MFI = 3.90)
CD107a Stained Unstimulated (1.29%, MFI = 3.90)
CD107a Stained Stimulated (30.70%, MFI = 7.12)
Count
157
118
79
39
0
CD107a

C

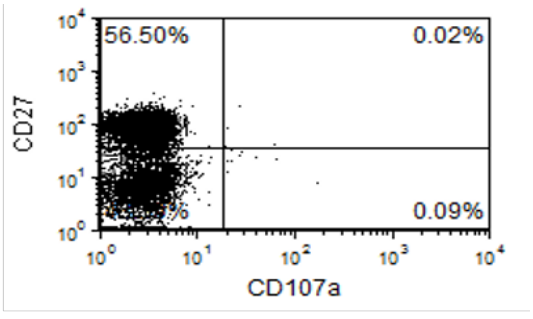
56.50%
0.02%
0.09%
CD27
CD107a

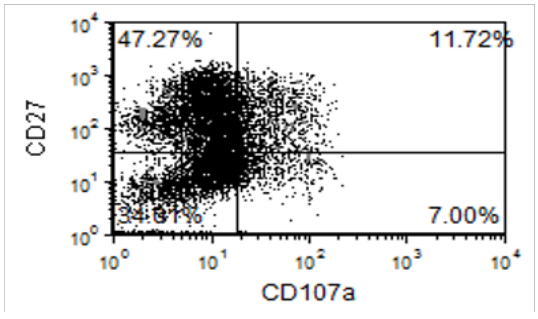
47.27%
11.72%
7.00%
CD27
CD107a

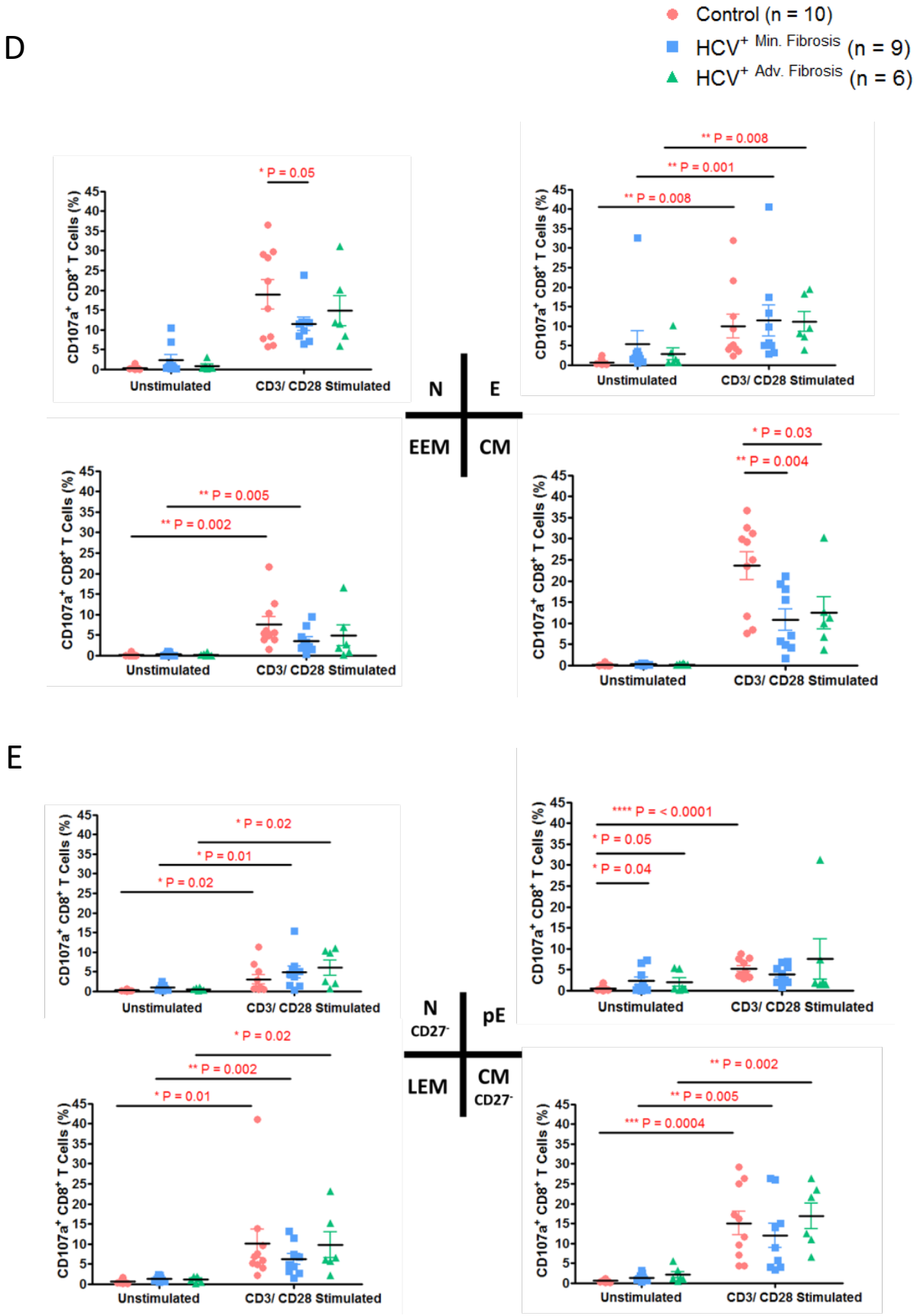
D
Control (n = 10)
HCV+ Min. Fibrosis (n = 9)
HCV+ Adv. Fibrosis (n = 6)
N
E
EEM
CM
CD107a+ CD8+ T Cells (%)
Unstimulated
CD3/ CD28 Stimulated
* P = 0.05
** P = 0.008
** P = 0.001
** P = 0.008
** P = 0.005
** P = 0.002
* P = 0.03
** P = 0.004
E
N
CD27-
pE
LEM
CM
CD27-
* P = 0.02
* P = 0.01
* P = 0.02
**** P = < 0.0001
* P = 0.05
* P = 0.04
* P = 0.02
** P = 0.002
* P = 0.01
** P = 0.002
** P = 0.005
*** P = 0.0004

Figure 5: CD107a expression of $CD8^+$ T cells measured by flow cytometry for controls (n = 10), $HCV^{+\ Min.\ Fibrosis}$ (n = 9), and $HCV^{+\ Adv.\ Fibrosis}$ (n = 6) after anti-CD3/CD28 stimulation. **A)** CD107a expression in bulk $CD8^+$ T cells. **B)** Representative histogram of CD107a expression in an uninfected control measured by flow cytometry for bulk $CD8^+$ T cells in four conditions: unstained unstimulated, unstained CD3/CD28 stimulated, CD107a stained unstimulated, and CD107a stained CD3/CD28 stimulated. **C)** Representative CD107a dot plots for T_{CM} in uninfected controls without stimulation (left) and after anti-CD3/CD28 stimulation (right). **D)** CD107a expression in naïve (top left), effector (top right), early effector memory (bottom left), and central memory (bottom right) thawed $CD8^+$ T cells upon anti-CD3/CD28 stimulation. **E)** CD107a expression in naïve $CD27^-$ (top left), pre-effector (top right), late effector memory (bottom left), and central memory $CD27^-$ (bottom right) thawed $CD8^+$ T cells upon anti-CD3/CD28 stimulation.

3.5 Perforin Expression of Blood-derived Bulk $CD8^+$ T Cells during Untreated Chronic HCV Infection

Perforin expression was measured in $CD8^+$ T cells from uninfected and HCV-infected individuals to assess the effects of liver fibrosis on the adaptive immune response. The parameters of anti-CD3/CD28 stimulation were determined using a time course and dose response (Figure S6). Intracellular perforin expression in bulk $CD8^+$ T cells was measured using flow cytometry (Figure 6A and B). Perforin expression was significantly induced by stimulation (paired Student *t*-test) in each donor/patient group (controls: $P = 0.007$; $HCV^{+\text{ Min. Fibrosis}}$: $P = 0.0001$; $HCV^{+\text{ Adv. Fibrosis}}$: $P = 0.009$). However, no significant differences in $CD8^+$ T cell perforin expression between the HCV^+ and HCV^- donors were detected in either the non-stimulated or the anti-CD3/CD28 stimulated cultures.

Perforin concentrations in $CD8^+$ T cell culture supernatants following stimulation with anti-CD3/CD28 for 48 hours were measured using Luminex MAGPIX® (Figure 6C). Perforin expression was significantly induced by anti-CD3/CD28 (paired Student's *t*-test) in each donor/patient group (controls: $P = 0.0001$; $HCV^{+\text{ Min. Fibrosis}}$: $P = 0.005$; $HCV^{+\text{ Adv. Fibrosis}}$: $P = 0.007$). Contrary to the results obtained for intracellular perforin expression, a significantly lower perforin concentration (unpaired Student's *t*-test) was observed upon stimulation for $HCV^{+\text{ Min. Fibrosis}}$ compared to uninfected controls ($P = 0.002$) and $HCV^{+\text{ Adv. Fibrosis}}$ ($P = 0.01$).

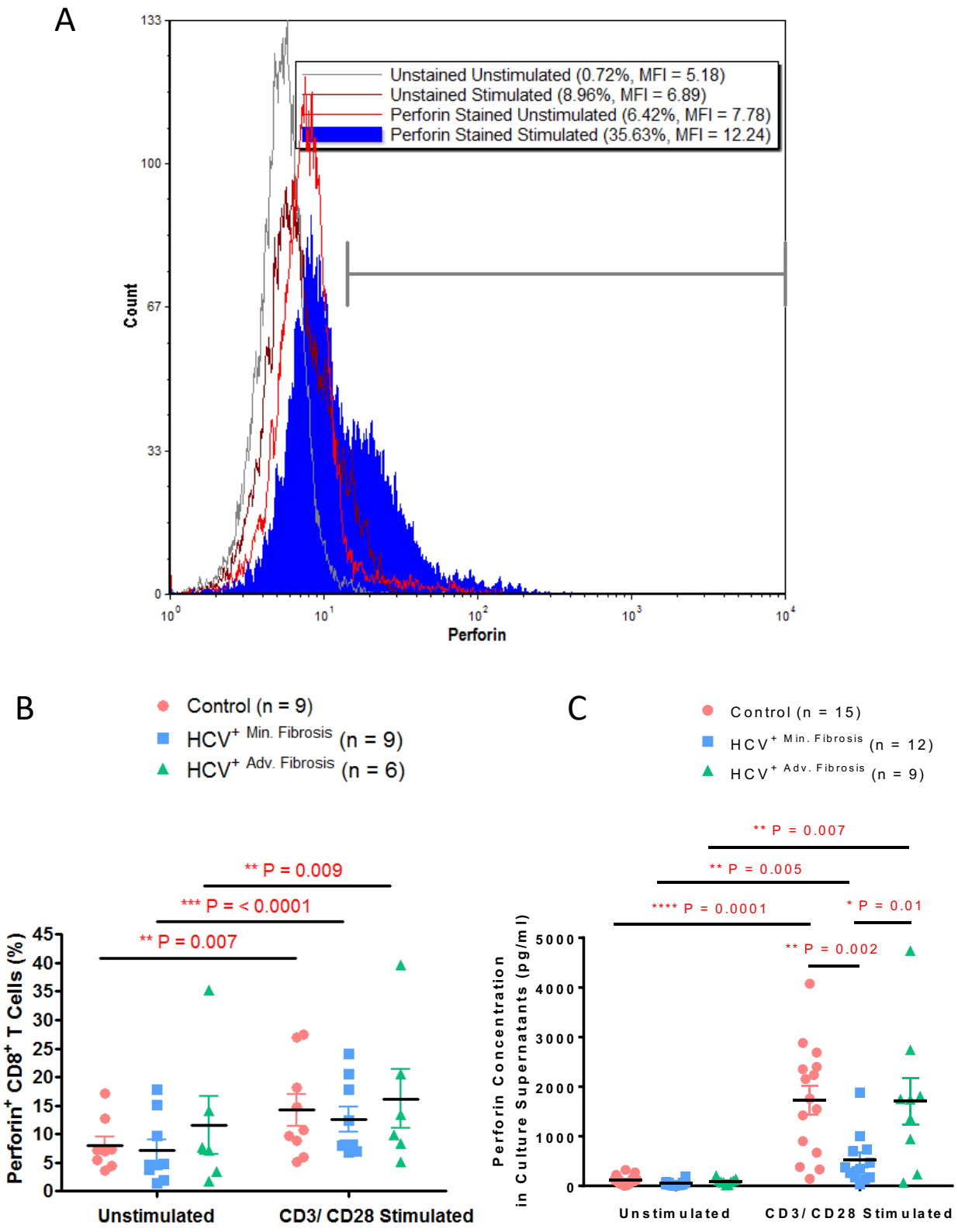
A
Unstained Unstimulated (0.72%, MFI = 5.18)
Unstained Stimulated (8.96%, MFI = 6.89)
Perforin Stained Unstimulated (6.42%, MFI = 7.78)
Perforin Stained Stimulated (35.63%, MFI = 12.24)
Count
Perforin
B
Control (n = 9)
HCV+ Min. Fibrosis (n = 9)
HCV+ Adv. Fibrosis (n = 6)
** P = 0.009
*** P = < 0.0001
** P = 0.007
Perforin+ CD8+ T Cells (%)
Unstimulated
CD3/ CD28 Stimulated
C
Control (n = 15)
HCV+ Min. Fibrosis (n = 12)
HCV+ Adv. Fibrosis (n = 9)
** P = 0.007
** P = 0.005
**** P = 0.0001
* P = 0.01
** P = 0.002
Perforin Concentration in Culture Supernatants (pg/ml)
Unstimulated
CD3/ CD28 Stimulated

Figure 6: Perforin expression without stimulation and after 48 hours of anti-CD3/CD28 stimulation. A) Representative histogram of intracellular perforin expression measured by flow cytometry for bulk $CD8^+$ T cells in four conditions: unstained unstimulated, unstained CD3/CD28 stimulated, perforin stained unstimulated, and perforin stained CD3/CD28 stimulated. **B)** Intracellular perforin expression of bulk $CD8^+$ T cells measured by flow cytometry for controls (n = 9), untreated $HCV^{+\ \text{Min. Fibrosis}}$ (n = 9), and untreated $HCV^{+\ \text{Adv. Fibrosis}}$ (n = 6). **C)** Perforin concentration within culture supernatants of $CD8^+$ T cells measured using MAGPIX for controls (n = 15), untreated $HCV^{+\ \text{Min. Fibrosis}}$ (n = 12), and untreated $HCV^{+\ \text{Adv. Fibrosis}}$ (n = 9).

3.6 Perforin Expression of Eight $CD8^+$ T Cell Subsets During Untreated Chronic HCV Infection

After intracellular perforin expression was measured in bulk $CD8^+$ T cells, the *three-marker* gating strategy depicted in Figure 2C was used to distinguish between eight subsets previously described in Table 3. The representative dot plots in Figure 7A show the intracellular perforin expression of T_{pE} (upper quadrants) and T_E (lower quadrants) from an uninfected control in the absence (left dot plot) and presence (right dot plot) of anti-CD3/CD28 stimulation.

The intracellular perforin expressions for T_N, T_E, $T_{EEM,}$ and T_{CM} subsets are shown in Figure 7B. Perforin expression was significantly induced (paired Student's *t*-test) upon anti-CD3/CD28 stimulation in T_N for uninfected controls ($P = 0.05$) and $HCV^{+\text{ Min. Fibrosis}}$ ($P = 0.02$). Perforin induction was also significant (paired Student's *t*-test) in T_{CM} for uninfected controls ($P = 0.0006$) and $HCV^{+\text{ Min. Fibrosis}}$ ($P = 0.01$). Perforin expression was significantly induced (paired Student's *t*-test) in T_E for both $HCV^{+\text{ Min. Fibrosis}}$ ($P = 0.02$) and $HCV^{+\text{ Adv. Fibrosis}}$ ($P = 0.05$). Finally, perforin induction was only significant in T_{EEM} for uninfected controls ($P = 0.05$ by paired Student's *t*-test). There were no significant differences in perforin expression between donor/patient groups within the non-stimulated nor the anti-CD3/CD28 stimulated cultures.

The intracellular perforin expressions for $T_{N\ CD27^-}$, T_{pE}, $T_{LEM,}$ and $T_{CM\ CD27^-}$ subsets are shown in Figure 7C. The percentage of $perforin^+$ $T_{N\ CD27^-}$ cells induced by anti-CD3/CD28 stimulation in uninfected controls was significantly lower (by unpaired Student's *t*-test) compared to both $HCV^{+\text{ Min. Fibrosis}}$ ($P = 0.05$) and $HCV^{+\text{ Adv. Fibrosis}}$ ($P = 0.03$). There was a significantly higher percentage of $perforin^+$ T_{LEM} in $HCV^{+\text{ Min. Fibrosis}}$ after stimulation compared to uninfected controls ($P = 0.05$ by unpaired Student's *t*-test). Similarly to T_{CM} (Figure 7B), perforin was significantly induced (by paired Student's *t*-test) in $T_{CM\ CD27^-}$ for uninfected controls

($P = 0.0002$) and $HCV^{+\ \text{Min. Fibrosis}}$ ($P = 0.02$). Finally, the T_{pE} subset had no significant differences between donor/patient groups and no significant perforin induction upon stimulation.

A

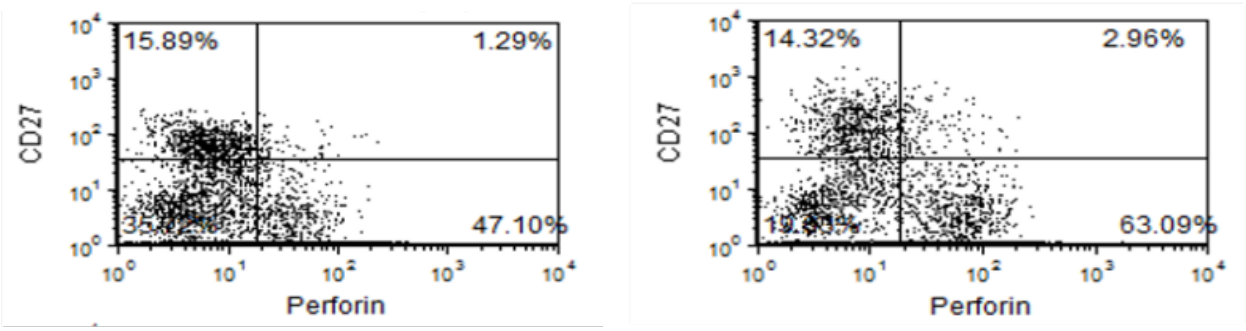
15.89%
1.29%
47.10%
CD27
Perforin
14.32%
2.96%
63.09%
CD27
Perforin

B

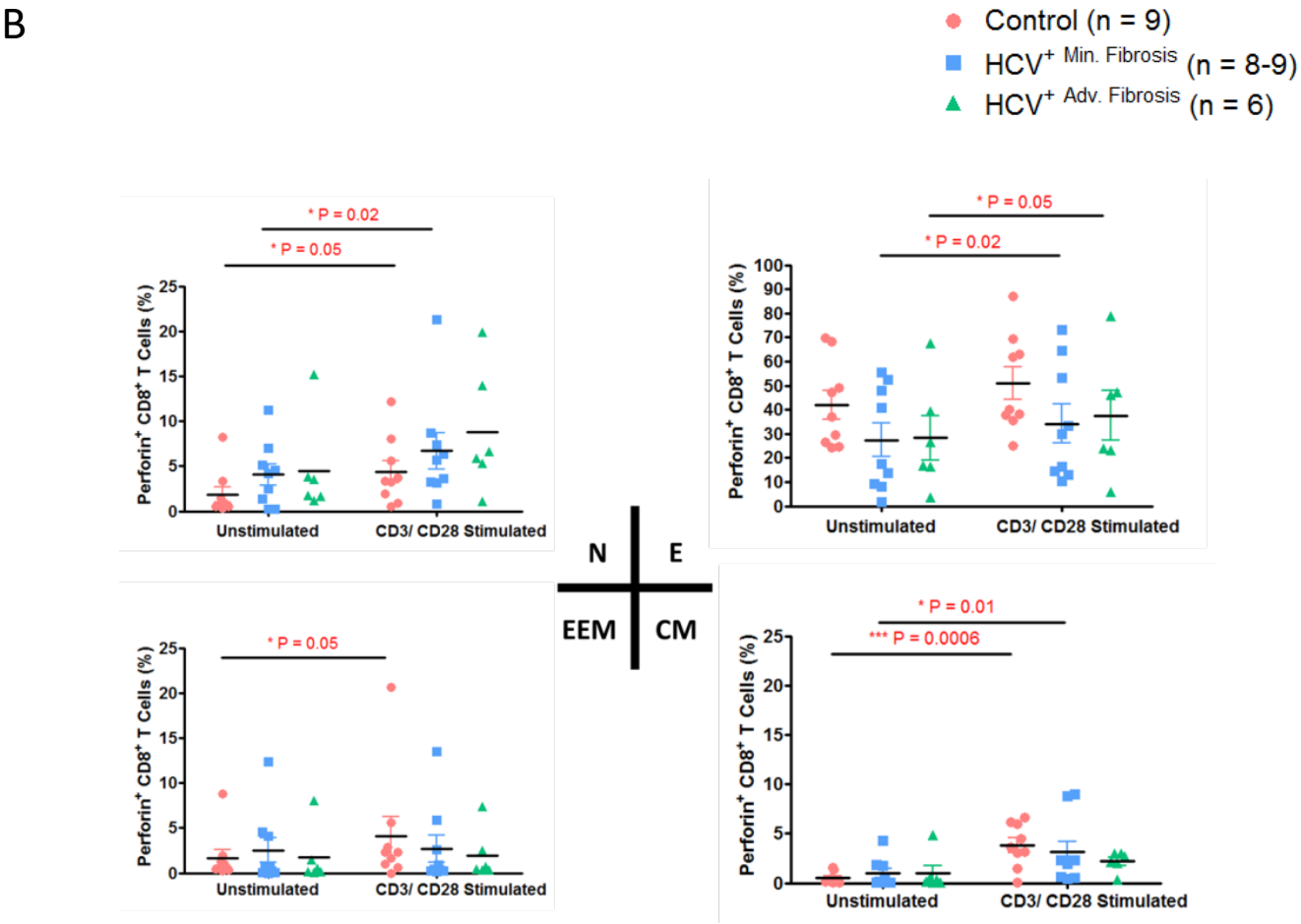
Control (n = 9)
HCV+ Min. Fibrosis (n = 8-9)
HCV+ Adv. Fibrosis (n = 6)
* P = 0.02
* P = 0.05
Perforin+ CD8+ T Cells (%)
Unstimulated
CD3/ CD28 Stimulated
* P = 0.05
* P = 0.02
Perforin+ CD8+ T Cells (%)
Unstimulated
CD3/ CD28 Stimulated
N
E
EEM
CM
* P = 0.05
Perforin+ CD8+ T Cells (%)
Unstimulated
CD3/ CD28 Stimulated
* P = 0.01
*** P = 0.0006
Perforin+ CD8+ T Cells (%)
Unstimulated
CD3/ CD28 Stimulated

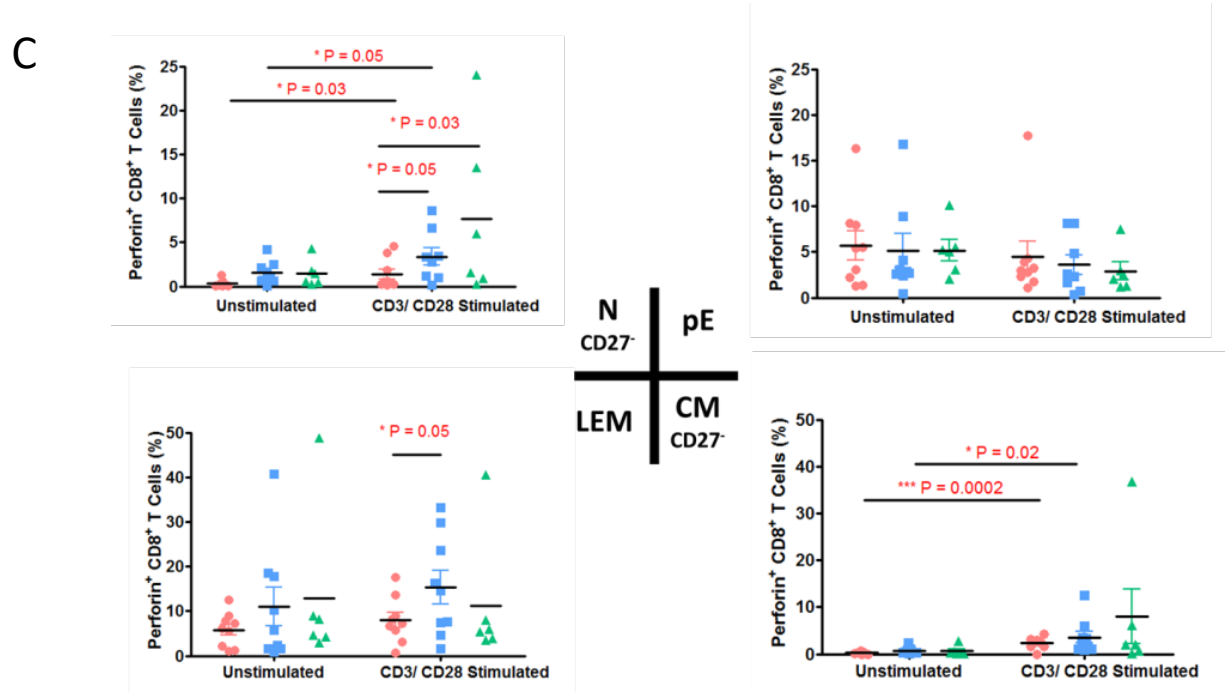

Figure 7: Intracellular perforin expression of CD8$^+$ T cells measured by flow cytometry for controls (n = 9), HCV$^+$ $^{\text{Min. Fibrosis}}$ (n = 8-9), and HCV$^+$ $^{\text{Adv. Fibrosis}}$ (n = 6) after anti-CD3/CD28 stimulation. A) Representative intracellular perforin dot plots using the *three-marker* gating strategy for T_{pE} (top quadrants) and T_E (bottom quadrants) in uninfected controls without stimulation (left) and after anti-CD3/CD28 stimulation (right). **B)** Perforin expression in naïve (top left), effector (top right), early effector memory (bottom left), and central memory (bottom right) thawed CD8$^+$ T cells upon anti-CD3/CD28 stimulation. **C)** Perforin expression in naïve CD27$^-$ (top left), pre-effector (top right), late effector memory (bottom left), and central memory CD27$^-$ (bottom right) thawed CD8$^+$ T cells upon anti-CD3/CD28 stimulation.

3.7 Phenotype of Blood-derived $CD8^+$ T Cells at Week 0 and Week 48 of Treatment During Chronic HCV Infection

The distribution of peripheral $CD8^+$ T cell subsets before and after treatment in HCV^+ individuals was determined to assess the relationship between SVR and the function of $CD8^+$ T cells from patients. The timeline for the treatment study used in these experiments is illustrated in Figure 1. Patients were evaluated at week 0 (treatment initiation) and week 48 (24 weeks after SVR). As described previously in Chapter 3.1, thawed and isolated $CD8^+$ T cells were analysed using the *two-marker* and *three-marker* gating strategies. The *two-marker* gating strategy utilized the surface expression of CD45RA and CCR7 to identify four subsets of $CD8^+$ T cells, including T_N, T_E, T_{EM}, and T_{CM} (Table 3). The $CD8^+$ T cell subset distribution for the HCV^+ individuals at week 0 of treatment was not significantly different from previous findings for untreated HCV^+ individuals in Chapter 3.1: T_N (30.5% ± 20.4), T_E (14.1% ± 13.8), T_{EM} (23.7% ± 15.5), and T_{CM} (31.7% ± 10.8) (Figure 8A). The HCV^+ individuals at week 48 of treatment did not differ significantly (by paired Student's *t*-test) from the distribution for week 0: T_N (22.8% ± 17.3), T_E (17.5% ± 10.3), T_{EM} (28.6% ± 12.0), and T_{CM} (31.0% ± 14.8) (Figure 8A).

The *three-marker* gating strategy utilized the surface expression of CD45RA, CCR7, and CD27 to identify eight $CD8^+$ T cell subsets, including T_N, $T_{N\,CD27^-}$, T_E, T_{pE}, T_{EEM}, T_{LEM}, T_{CM}, and $T_{CM\,CD27^-}$. Similar to the *two-marker* strategy, the $CD8^+$ T cell subset distribution of the HCV^+ individuals at week 0 of treatment was not significantly different (by paired Student's *t*-test) from observed results in Chapter 3.1: T_N (23.0% ± 14.8), $T_{N\,CD27^-}$ (7.5% ± 6.1), T_E (12.7% ± 12.9), T_{pE} (1.4% ± 1.2), T_{EEM} (7.1% ± 4.8), T_{LEM} (16.7% ± 11.1), T_{CM} (16.5% ± 7.1), and $T_{CM\,CD27^-}$ (15.3% ± 6.3) (Figure 8B). Finally, the $CD8^+$ T cell subset distribution for the HCV^+ individuals at week 48 of treatment was not significantly different from week 0 (by paired

Student's *t*-test). The percentages of the eight $CD8^+$ T cell subsets for the HCV^+ individuals at week 48 of treatment are as follows: T_N (16.7% ± 14.6), $T_{N\ CD27^-}$ (6.1% ± 4.4), T_E (16.3% ± 10.0), T_{pE} (1.3% ± 1.1), T_{EEM} (7.2% ± 5.8), T_{LEM} (21.4% ± 10.6), T_{CM} (17.8% ± 9.0), and $T_{CM\ CD27^-}$ (13.3% ± 6.4) (Figure 8B).

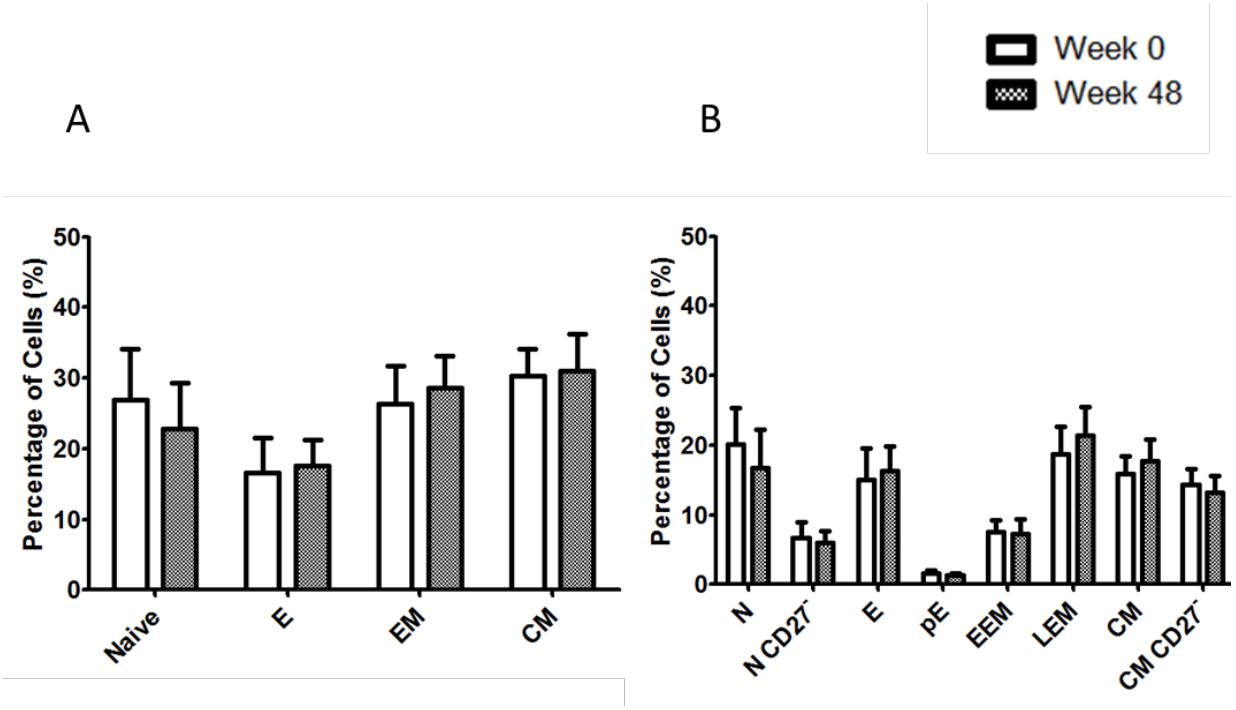

Figure 8: Isolated CD8$^+$ T cells from thawed PBMC samples for treated HCV$^+$ individuals (n = 8) at week 0 (treatment start) and week 48 (9 months after treatment finish/6 months after SVR) were surface stained to identify percentage of cells within a subset. A) The *two-marker* gating strategy was used to identify the percentage of cells within each of four subsets, defined as follows: naïve (CCR7$^+$CD45RA$^+$), effector (CCR7$^-$CD45RA$^+$), effector memory (CCR7$^-$CD45RA$^-$), and central memory (CCR7$^+$CD45RA$^-$). **B)** The *three-marker* gating strategy was used to identify the percentage of cells within each of eight subsets, defined as follows: naïve (CCR7$^+$CD45RA$^+$CD27$^+$), naïve CD27^{NEG} (CCR7$^+$CD45RA$^+$CD27$^-$), effector (CCR7$^-$CD45RA$^+$CD27$^-$), pre-effector (CCR7$^-$CD45RA$^+$CD27$^+$), early effector memory (CCR7$^-$CD45RA$^-$CD27$^+$), late effector memory (CCR7$^-$CD45RA$^-$CD27$^-$), central memory (CCR7$^+$CD45RA$^-$CD27$^+$), and central memory CD27^{NEG} (CCR7$^+$CD45RA$^-$CD27$^-$).

3.8 Intracellular IFN-γ Expression of Blood-derived $CD8^+$ T Cells at Week 0 and Week 48 of Treatment during HCV Chronic Infection

Intracellular IFN-γ expression was measured in bulk $CD8^+$ T cells (Figure 9A). Out of eight individuals undergoing treatment, six had fewer IFN-γ^+ $CD8^+$ T cells upon stimulation at week 48 of treatment when compared to week 0. However, overall there was no statistically significant difference (paired Student's *t*-test) between week 0 and week 48 for either the unstimulated or the anti-CD3/CD28 stimulated $CD8^+$ T cells.

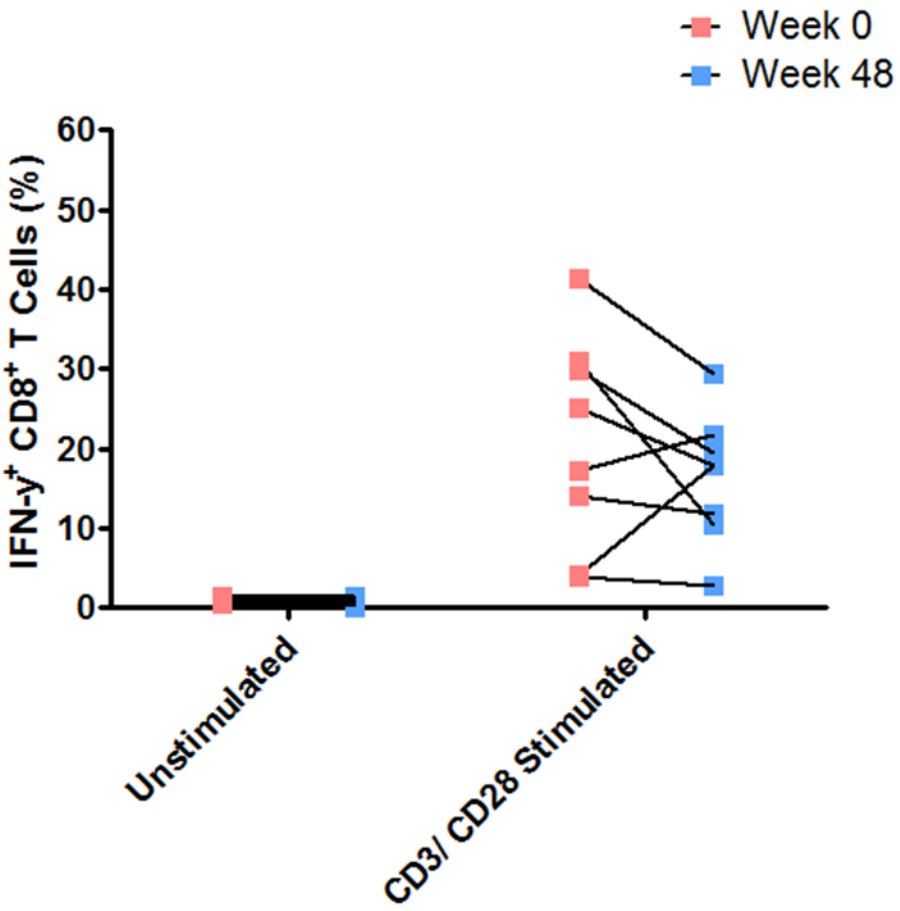

Figure 9: Intracellular IFN-γ expression of bulk $CD8^+$ T cells isolated from HCV^+TX^+ individuals (n = 8) at week 0 and week 48 after 48 hours of anti-CD3/CD28 stimulation measured using flow cytometry.

3.9 CD107a Expression of Blood-derived $CD8^+$ T Cells at Week 0 and Week 48 of Treatment during Chronic HCV Infection

Using flow cytometry, CD107a expression was measured for bulk $CD8^+$ T cells in the presence and absence of a 48-hour anti-CD3/CD28 stimulation (Figure 10). Between week 0 and week 48, four of the eight individuals tested showed an increase in the percentage of $CD107a^+$ $CD8^+$ T cells following anti-CD3/CD28 stimulation, while the other four donors showed a decrease in the percentage of $CD107a^+$ $CD8^+$ T cells. Overall, there were no statistically significant differences observed between the individuals before and after treatment.

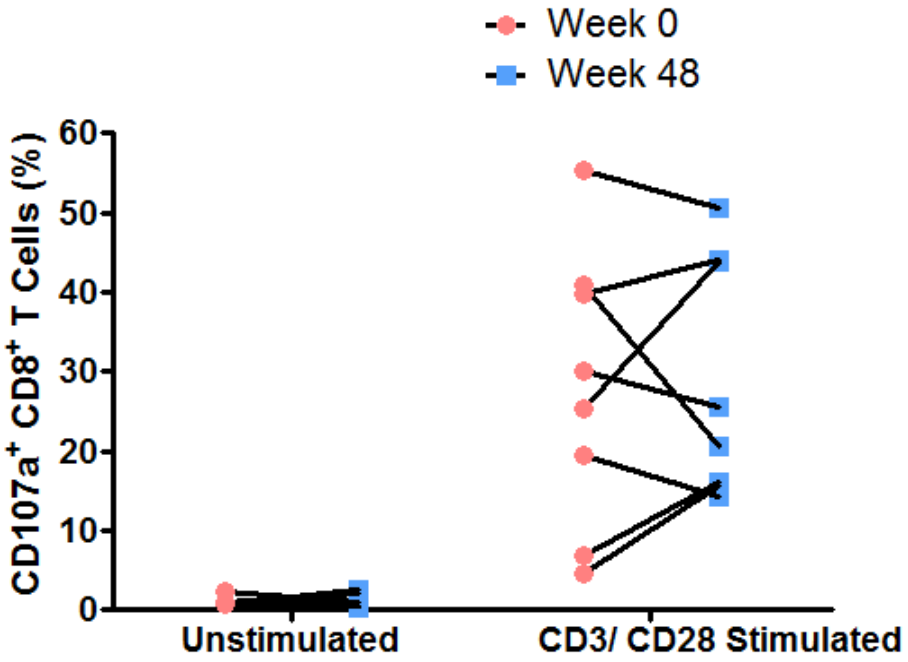

Figure 10: CD107a expression of bulk $CD8^+$ T cells isolated from HCV^+TX^+ individuals (n = 8) at week 0 and week 48 after 48 hours of anti-CD3/CD28 stimulation measured using flow cytometry.

3.10 Perforin Expression of Blood-derived $CD8^+$ T Cells at Week 0 and Week 48 of Treatment during Chronic HCV Infection

Intracellular perforin expression for bulk $CD8^+$ T cells isolated from chronic HCV^+ individuals at week 0 and week 48 of treatment was measured using flow cytometry (Figure 11). Perforin expression in the absence of stimulation was unchanged for all except one individual when comparing weeks 0 and 48. This individual had a four-fold decrease of $perforin^+CD8^+$ T cells at week 48 compared to week 0. Out of the seven individuals used in this experiment, three had a lower percentage, two had a higher percentage and two had a similar percentage of $CD8^+$ T cells capable of producing perforin upon stimulation at week 48 compared to week 0. Overall, statistical significances were not observed between weeks 0 and 48 for both the unstimulated and anti-CD3/CD28 stimulated conditions.

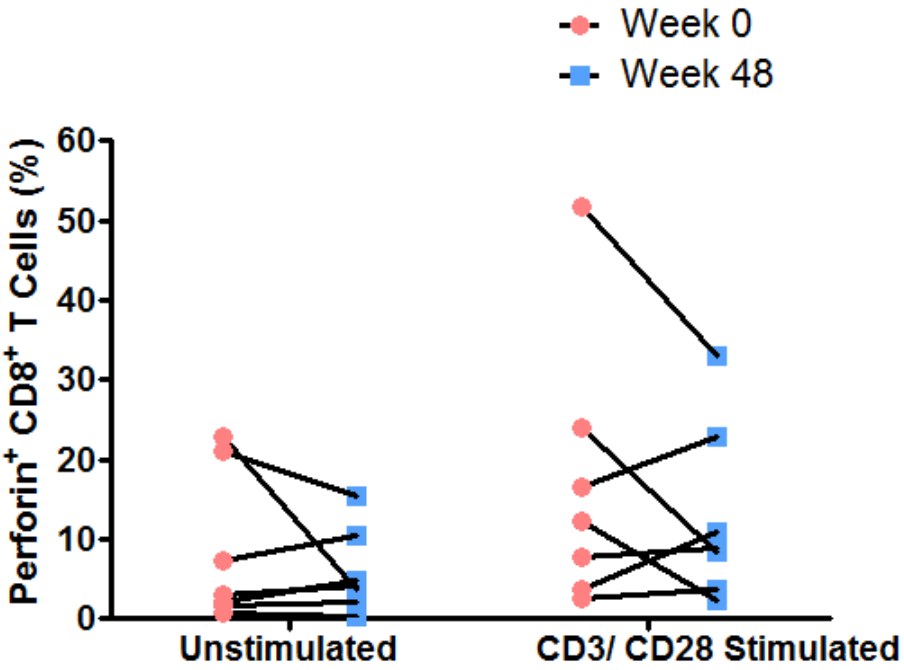

Figure 11: Intracellular perforin expression of bulk $CD8^+$ T cells isolated from HCV^+TX^+ individuals (n = 7) at week 0 and week 48 after 48 hours of anti-CD3/CD28 stimulation measured using flow cytometry.

Chapter 4: Discussion

The data presented in this project reveal the functional abnormalities of bulk $CD8^+$ T cells isolated from individuals with chronic HCV infection. In particular, these findings address the expression of functional $CD8^+$ T cell markers in the context of liver fibrosis induced by chronic HCV infection. Impairment was characterized based on $CD8^+$ T cell subset distribution and anti-CD3/CD28 induced expression of functional markers, including IFN-γ, CD107a, and perforin. Decreasing naïve and increasing late effector memory $CD8^+$ T cell proportions were associated with a greater degree of liver fibrosis in untreated HCV^+ individuals. Intracellular expression of IFN-γ, culture supernatant expression of perforin, and surface expression of CD107a after TCR stimulation of bulk $CD8^+$ T cells was lower for $HCV^{+\text{ Min. Fibrosis.}}$ In contrast, this trend was not observed for intracellular perforin or IFN-γ in culture supernatants. Interestingly, treatment with a 12-week regimen of ABT450r (ombitasvir, dasabuvir ± ribavirin) did not reverse functional impairments in bulk $CD8^+$ T cells from chronic HCV infection.

4.1 Differences in $CD8^+$ T Cell Phenotype in Chronic HCV Infection

The distribution of $CD8^+$ T cell subsets was described for uninfected controls and chronic HCV^+ individuals with either minimal ($HCV^{+\text{ Min. Fibrosis}}$) or advanced ($HCV^{+\text{ Adv. Fibrosis}}$) fibrosis. In this study, $CD8^+$ T cell subsets were distinguished using two methods. The *two-marker* strategy used CD45RA and CCR7 to identify four $CD8^+$ T cell subsets. This gating strategy was previously used in this research group to compare the $CD8^+$ T cell subset distribution in uninfected controls and chronic HCV infection without grouping based on degree of liver damage. The second method used was the *three-marker* strategy which identified eight $CD8^+$ T cell subsets based on expression of CD45RA, CCR7, and CD27. These markers have been used

in several published studies to identify and investigate various aspects of $CD8^+$ T cells (96, 97, 144).

The proportions of blood-derived $CD8^+$ T cell subsets in chronic HCV infection, identified using the *two-marker* strategy, were slightly different than those in uninfected controls. In particular, there were fewer T_N, more T_E, and more T_{EM} cells in chronic HCV infection, and the proportion of $CD8^+$ T cells correlated with increasing liver fibrosis (Figure 4B). Interestingly, the *three-marker* strategy did not identify a significant difference in the proportion of T_E cells between HCV-infected and uninfected controls, but there was a noticeable increasing trend proportional to a greater degree of liver fibrosis. In addition, fewer T_N and more T_{LEM} cells in chronic HCV infection were shown to be associated with increasing liver fibrosis when analyzing using the *three-marker* strategy (Figure 4D). These results indicate an effect of HCV on the phenotype of bulk $CD8^+$ T cells.

The consequences and mechanism of this global effect of HCV have not been elucidated; they require further investigation. As there are few autoimmune and lymphoproliferative disorders associated with chronic HCV infection (166), the effect of HCV on bulk $CD8^+$ T cells may have only modest consequences to the individual. The effect of HCV on the phenotype of bulk $CD8^+$ T cells found in the present study is consistent with previous reports that addressed this relationship in chronic HCV infection (144, 167). The results discovered here and in previous studies are unlikely to be a result of changes in virus-specific $CD8^+$ T cells alone, as virus-specific $CD8^+$ T cells only constitute 0.05-2% of the total bulk $CD8^+$ T cell population (122, 123).

4.2 Relationship Between IFN-γ and Liver Fibrosis in Chronic HCV Infection

Intracellular IFN-γ expression and the concentration of IFN-γ released into culture supernatants was measured for bulk $CD8^+$ T cells isolated from uninfected controls, $HCV^{+\ Min.\ Fibrosis}$, and $HCV^{+\ Adv.\ Fibrosis}$ after 48 hours of anti-CD3/CD28 stimulation. Upon stimulation, there was a significantly lower percentage of IFN-γ^+ $CD8^+$ T cells detected by flow cytometry in $HCV^{+\ Min.\ Fibrosis}$ compared to healthy controls (Figure 3B). In addition, there was a significantly lower concentration of IFN-γ measured in culture supernatants upon stimulation for $HCV^{+\ Min.\ Fibrosis}$ compared to $HCV^{+\ Adv.\ Fibrosis}$ (Figure 3C). Thus, the concentration of IFN-γ in culture supernatants differed from intracellular expression because the IFN-γ concentration after TCR stimulation was not significantly lower for $HCV^{+\ Min.\ Fibrosis}$ compared to uninfected controls. A potential explanation could be a difference in the amount of cytokine released per cell. An increased release of IFN-γ per cell would explain the significantly higher concentration measured in the culture supernatants for $HCV^{+\ Adv.\ Fibrosis}$ compared to $HCV^{+\ Min.\ Fibrosis}$, despite the lack of significance observed for intracellular expression.

Intracellular IFN-γ was also measured for eight $CD8^+$ T cell subsets. There was a significantly higher percentage of IFN-γ^+ T_E, $T_{N\ CD27^-}$, and $T_{CM\ CD27^-}$ in $HCV^{+\ Adv.\ Fibrosis}$ compared to uninfected controls and $HCV^{+\ Min.\ Fibrosis}$. The T_E, $T_{N\ CD27^-}$, and $T_{CM\ CD27^-}$ subsets constitute approximately 12%, 5%, and 13% of the bulk population, respectively. Therefore, the higher percentage of IFN-γ^+ $CD8^+$ T cells observed in these subsets after anti-CD3/CD28 stimulation may not be relevant when considering the overall bulk population or have an impact on the health of the individual. Furthermore, the results showed a significantly higher percentage of IFN-γ^+ T_{LEM} in $HCV^{+\ Adv.\ Fibrosis}$ compared to $HCV^{+\ Min.\ Fibrosis}$. The T_{LEM} subset comprises

approximately 30% of the total bulk population, thus amplifying the implication of a higher percentage of IFN-γ^+ T_{LEM} in $HCV^{+\ Adv.\ Fibrosis}$.

Altogether, these results demonstrate a relationship between $CD8^+$ T cell function and degree of liver fibrosis. In particular, a higher degree of liver fibrosis is associated with a higher percentage of IFN-γ^+ $CD8^+$ T cells within the T_E, $T_{N\ CD27^-}$, $T_{CM\ CD27^-}$, and T_{LEM} subsets. However, the relevance to an individual's health has yet to be determined. The results here are consistent with studies that observed an effect of HCV on bulk $CD8^+$ T cells (167-169).

In chronic HCV infection, the immune response of HCV-specific $CD8^+$ T cells has been characterized by an IFN-γ impairment after stimulation with mitogen or peptides compared to the rest of the $CD8^+$ T cell population in the individuals tested (123, 127, 170). In a previous study, a larger frequency of IFN-γ^+ HCV-specific $CD8^+$ T cells was observed after HCV-peptide stimulation in patients with a minimal stage of fibrosis compared to advanced (107). Thus, a relationship between HCV-specific $CD8^+$ T cell function and liver fibrosis has been demonstrated in the context of chronic HCV infection. To address the capacity of bulk $CD8^+$ T cells to produce IFN-γ in chronic HCV infection, authors of another study stimulated $CD8^+$ T cells isolated from the peripheral blood of human participants with PMA (phorbol 12-myristate 13-acetate) and ionomycin (171). The authors of this study, Murata *et al.*, found an increased frequency of IFN-γ^+ $CD8^+$ T cells after stimulation from HCV^+ individuals compared to uninfected controls. However, Murata *et al.* did not categorize the HCV^+ individuals by liver fibrosis to determine whether the responses were related to hepatic damage. In this project, surface expression markers enabled a more specific characterization of the IFN-γ^+ $CD8^+$ population of cells in the context of HCV-induced liver fibrosis.

4.3 Relationship between CD107a and Liver Fibrosis in Chronic HCV Infection

Expression of CD107a was also measured on bulk $CD8^+$ T cells isolated from uninfected controls, $HCV^{+\text{ Min. Fibrosis}}$, and $HCV^{+\text{ Adv. Fibrosis}}$ after 48 hours of anti-CD3/CD28 stimulation. Ex vivo expression of CD107a on the cell surface is associated with the degranulation capacity of $CD8^+$ T cells (90). Upon stimulation, there was a significantly lower percentage of $CD107a^+$ $CD8^+$ T cells in $HCV^{+\text{ Min. Fibrosis}}$ compared to controls, but this difference was not observed in $HCV^{+\text{ Adv. Fibrosis}}$ (Figure 5A). The trend for CD107a expression is similar to the results found for intracellular IFN-γ expression, indicating a functional impairment associated with minimal fibrosis alone. The consequences of a lowered ability of bulk $CD8^+$ T cells to degranulate upon stimulation have not been determined but could potentially include lowered responses to routine vaccinations, including HBV (172, 173) and influenza (174, 175), as several suggest development of immunological memory may be affected (169).

In a previous study, HCV-specific $CD8^+$ T cells were shown to experience a lower up-regulation of CD107a upon peptide stimulation compared to non-HCV-specific $CD8^+$ T cells from the same individual (176). However, this study did not compare the non-HCV-specific $CD8^+$ T cell responses of chronic HCV^+ individuals with uninfected controls. Another study found a reduced expression of CD107a on intrahepatic bulk $CD8^+$ T cells from HCV^+ individuals after anti-CD3 stimulation compared to those isolated from controls (136). However, this study did not address the relationship with the degree of liver fibrosis, as only four HCV^+ individuals and four controls were used in the experiment. In this thesis, results indicate that chronic HCV^+ individuals have a reduced expression of CD107a for bulk $CD8^+$ T cells upon anti-CD3/CD28 stimulation compared to uninfected controls, and there is no apparent relationship with degree of liver fibrosis. Further studies will need to address the potential mechanism resulting in only

$HCV^{+\ Min.\ Fibrosis}$ having a significantly different expression of CD107a compared to uninfected controls.

CD107a was also measured for eight $CD8^+$ T cell subsets. There was a significantly lower percentage of $CD107a^+$ T_N in $HCV^{+\ Min.\ Fibrosis}$ compared to uninfected controls. Although not significant, there also appeared to be a lower percentage of $CD107a^+$ T_N in $HCV^{+\ Adv.\ Fibrosis}$ compared to uninfected controls. In addition, there was a significantly lower percentage of $CD107a^+$ T_{CM} in $HCV^{+\ Min.\ Fibrosis}$ and $HCV^{+\ Adv.\ Fibrosis}$ compared to uninfected controls. Interestingly, a study performed by Stelekati *et al*. suggests memory development and frequency are negatively impacted by chronic inflammation (177). The present results add to the findings by Stelekati *et al.* through the demonstration of a relationship between anti-CD3/CD28 induced function of memory $CD8^+$ T cells and chronic HCV infection. The observed impairment of CD107a expression in T_N and T_{CM} is a result of chronic HCV infection but may not be associated with liver damage, as either $HCV^{+\ Min.\ Fibrosis}$ alone (T_N^+) or both categories of HCV^+ individuals (T_{CM}) displayed a significantly lower frequency of $CD107a^+$ $CD8^+$ T cells after TCR stimulation. A significantly higher frequency of $CD107a^+$ intrahepatic immune cells was found in HCV compared to individuals with Nonalcoholic Steatohepatitis (NASH) (178). The results from this study, performed by Jouvin-Marche *et al.*, align with results from this thesis by demonstrating a relationship between bulk $CD8^+$ T cell expression of CD107a and HCV infection specifically.

4.4 Relationship between Perforin and Liver Fibrosis in Chronic HCV Infection

Expression of perforin intracellularly and within culture supernatants was measured for bulk $CD8^+$ T cells isolated from uninfected controls, $HCV^{+\ Min.\ Fibrosis}$, and $HCV^{+\ Adv.\ Fibrosis}$ after 48 hours of anti-CD3/CD28 stimulation. Upon stimulation, there was a significantly lower concentration of perforin measured in the culture supernatants for $HCV^{+\ Min.\ Fibrosis}$ compared to

uninfected controls and $HCV^{+\ Adv.\ Fibrosis}$ (Figure 6C). However, no significant differences were observed after stimulation for intracellular expression of perforin between any donor/patient groups. A potential explanation for the difference observed between intracellular and culture supernatant expression of perforin could be that less perforin was released per cell in $HCV^{+\ Min.\ Fibrosis}$ compared to uninfected controls and $HCV^{+\ Adv.\ Fibrosis}$. Conversely, more perforin could have been released per cell in uninfected controls and $HCV^{+\ Adv.\ Fibrosis}$ compared to $HCV^{+\ Min.\ Fibrosis}$. Furthermore, cells analyzed for perforin expression were not treated with a golgi inhibitor. Thus, perforin release from certain $CD8^+$ T cell subsets was possible between stimulation initiation and termination. As the stimulation dose and incubation times were selected based on optimal expression of markers and cytokines for the bulk population, the kinetics of perforin release into culture supernatants for each $CD8^+$ T cell subset was not addressed. Altogether, the results of intracellular and culture supernatant expression of perforin for bulk $CD8^+$ T cells does not indicate a relationship between this particular effector function and degree of liver fibrosis.

Intracellular perforin was also measured for eight $CD8^+$ T cell subsets (Figure 7B and C). Unlike IFN-γ and CD107a, there was a baseline expression of perforin in the unstimulated samples for all donor/patient groups. Importantly, induction of intracellular perforin expression in T_E occurred for both HCV^+ groups of patients but did not occur for uninfected controls. Conversely, no significant induction of intracellular perforin expression in $T_{N,}$ $T_{N\ CD27^-}$, T_{CM}, and $T_{CM\ CD27^-}$ was detected for $HCV^{+\ Adv.\ Fibrosis}$, although it was significantly up-regulated for uninfected controls and $HCV^{+\ Min.\ Fibrosis}$. In addition, induction of perforin expression in T_{EEM} occurred for uninfected controls but did not occur for either HCV^+ groups of patients. Overall, these results indicate a potential relationship between $CD8^+$ T cell effector function in terms of anti-CD3/CD28 induced perforin expression and degree of liver fibrosis.

An increase in the percentage of perforin^{+} $T_{N\ CD27}^{-}$ was observed for $HCV^{+\ Min.\ Fibrosis}$ and $HCV^{+\ Adv.\ Fibrosis}$ compared to uninfected controls. However, the relevance of this observation may be inconsequential, as the $T_{N\ CD27}^{-}$ subset constitutes approximately 5% of the bulk population. Although statistically significant, the presence of outliers and the variation between the perforin expressions in $T_{N\ CD27}^{-}$ for $HCV^{+\ Adv.\ Fibrosis}$ indicate that more replicates would need to be performed to be convinced of the observed trend. Intracellular perforin expression in T_{LEM} was also significantly increased upon stimulation in $HCV^{+\ Min.\ Fibrosis}$ compared to uninfected controls. This suggests an abnormal expression of perforin in $HCV^{+\ Min.\ Fibrosis}$ that may not be related to the degree of liver damage.

Previous studies have demonstrated a lowered expression of granzyme B and perforin in HCV-specific $CD8^{+}$ T cells during chronic HCV infection (179, 180). These studies by Radziewicz *et al.* found that intrahepatic HCV-specific $CD8^{+}$ T cells expressed granzyme B but lacked perforin expression upon stimulation with HCV peptide (NS3 1073-1081). In contrast, circulating HCV-specific $CD8^{+}$ T cells did not express granzyme B or perforin upon stimulation. Consistent with Radziewicz *et al*, another study identified low perforin levels and an impaired ability to up-regulate perforin upon peptide stimulation for circulating HCV-specific $CD8^{+}$ T cells during chronic infection (108). In another study, performed by Nisii *et al.*, no significant difference was observed for perforin expression in liver-residing bulk $CD8^{+}$ T cells after anti-CD3 stimulation, contrasting with IFN-γ expression (136). However, in this study, there was a significantly higher perforin expression in circulating bulk $CD8^{+}$ T cells upon anti-CD3 stimulation compared to liver-infiltrating counterparts. Findings from Nisii *et al.* are consistent with a phenomenon known as T cell tolerance often occurring in the liver (181). Tolerance involves the inactivation of T cells towards harmless antigens (*e.g.*, self-antigens) resulting in

reduced expression of functional markers. Although the importance of perforin$^+$ CD8$^+$ T cells has been established, previous studies have not demonstrated a relationship between effector function of bulk CD8$^+$ T cells and the degree of liver fibrosis of the individual. The results here show a potential relationship between perforin induction in circulating T_N, T_E, T_{CM}, T_{EEM}, $T_{CM\ CD27^-}$, and $T_{N\ CD27^-}$ subsets and the extent of liver fibrosis.

4.5 Effect of HCV Treatment on CD8$^+$ T Cell Phenotype in Chronic HCV Infection

A clinical study enabled the effects of treatment on the function of bulk CD8$^+$ T cells to be observed. In particular, an important question was addressed; are the functions and proportions of CD8$^+$ T cells studied in the untreated chronic HCV$^+$ individuals following successful treatment comparable to those observed in uninfected controls. The cell proportions observed for untreated individuals using the *two-marker* strategy included a significantly larger proportion of T_N and a significantly smaller proportion of T_E and T_{EEM} in uninfected controls compared to HCV$^{+\ Adv.\ Fibrosis}$. The levels observed for untreated individuals using the *three-marker* strategy included a significantly larger proportion of T_N and a significantly smaller proportion of T_{LEM} in uninfected controls compared to HCV$^{+\ Adv.\ Fibrosis}$. However, CD8$^+$ T cell subset distributions at week 48 (24 weeks after SVR) were not significantly different from week 0 (treatment initiation) using the *two-marker* (Figure 8A) or the *three-marker* strategy (Figure 8B).

There are a few potential explanations for the inability of treatment to restore CD8$^+$ T cell subset distributions of chronic HCV$^+$ individuals to those observed for uninfected controls. First, the CD8$^+$ T cell subset distributions observed as a result of chronic HCV infection may be permanent. Caetano *et al.* demonstrated a change in the phenotype of HCV-specific CD8$^+$ T cells

after chronically HCV-infected patients were treated with pegylated alpha interferon and ribavirin (182). In that study, the frequencies of HCV-specific $CD8^+$ T cell subsets (using the *two-marker* gating strategy) were measured at four points in time: before treatment and 1, 3, and 6 months after the start of treatment. Before treatment initiation in sustained-responders, the subset with the highest frequency of cells was T_N. During treatment, the frequency of T_{CM} steadily increased and the frequency of T_{EM} decreased. In addition, the frequency of T_E increased 1 month after treatment initiation, but by the 6-month point, the frequencies were returned to levels observed before treatment. Due to the small percentage of $CD8^+$ T cells specific for HCV in the circulation of chronically infected individuals, it is reasonable that the results found by Caetano *et al.* are not reflected in this project. Bulk $CD8^+$ T cells may require additional time following SVR to re-establish subset distributions similar to those observed in uninfected controls. In addition, Caetano *et al.* studied patients with HCV genotypes 1, 2, and 3 undergoing IFN-based therapy. The HCV genotype and treatment all contribute to the kinetics of viral elimination (183). Thus, the clinical trial included in this project may have a different trend for proportions of HCV-specific $CD8^+$ T cell subsets due to the use of solely HCV genotype 1 and DAA-based therapy. Another difference between the study performed by Caetano *et al.* and the present project include the number of time points addressed. Future studies investigating the effects of successful DAA therapy on the phenotype of bulk $CD8^+$ T cells will need to look at additional time points between treatment initiation and 24 weeks after SVR to further decipher the relationship.

As determined in this study, $CD8^+$ T cell subset distribution in chronic HCV infection is related to the degree of liver damage. Liver damage either does not or is slow to reverse after SVR. Of the eight individuals used from the clinical trial, the degree of liver fibrosis did not

change for three, increased to advanced fibrosis for two, and decreased to minimal fibrosis for two. Unfortunately, the number of individuals in each category (minimal or advanced fibrosis) was not sufficient to determine if liver damage is a contributing factor to the reversal of subset distribution after achieving SVR. However, the contribution of liver damage is another potential explanation for the inability of treatment to restore $CD8^+$ T cell subset distributions of chronic HCV^+ individuals to those observed in uninfected controls.

4.6 Effect of HCV Treatment on Anti-CD3/CD28 Induced Expression of IFN-γ, CD107a, and Perforin in Bulk $CD8^+$ T Cells

The anti-CD3/CD28 induced expressions of IFN-γ, CD107a, and perforin in bulk $CD8^+$ T cells before and after treatment was also investigated for individuals participating in the clinical trial. There was an insufficient number of individuals used from the clinical trial to determine if successful HCV treatment alters bulk $CD8^+$ T cell effector function while reversing the degree of liver fibrosis.

The percentage of IFN-γ^+ bulk $CD8^+$ T cells upon stimulation was not significantly different between week 0 and week 48 of the clinical trial for eight individuals (Figure 9). However, a trend towards a decreased percentage of IFN-γ^+ $CD8^+$ T cells upon stimulation was observed at week 48 of the clinical trial. Of the eight individuals included in this experiment, six experienced a decreased percentage of IFN-γ^+ bulk $CD8^+$ T cells at week 48 compared to week 0.

IFN-γ has immunomodulatory, anti-proliferative, and anti-fibrogenic functions (184, 185). This cytokine has also been shown to play a role in the control of HCV during chronic infection. A significant correlation between IFN-γ mRNA expression levels and stage of liver fibrosis has been demonstrated in chronic HCV infection (186). In addition, elevated levels of

IFN-γ in the serum has been shown to influence the progression of liver disease (187-189). However, in the present thesis, expression of IFN-γ within culture supernatants after TCR stimulation was not measured for the individuals participating in the clinical trial. HCV-specific $CD8^+$ T cell expression of IFN-γ upon peptide stimulation has been characterized by Gruener *et al.* before and after HCV treatment of chronic infection (190). In contrast to the results described in this thesis, Gruener *et al.* identified a lower frequency of circulating HCV-specific $CD8^+$ T cells before treatment and a significant, multi-specific, and sustained $CD8^+$ T cell response after SVR was achieved with IFN-based therapy. Thus, the present results suggest circulating bulk $CD8^+$ T cells experience a trend dissimilar from HCV-specific $CD8^+$ T cells. In particular, bulk $CD8^+$ T cells may have a lowered capacity to induce intracellular IFN-γ expression upon anti-CD3/CD28 stimulation after SVR is achieved.

The percentage of $CD107a^+$ and $perforin^+$ $CD8^+$ T cells upon stimulation was not significantly different between week 0 and week 48 of the clinical trial (Figure 10 and 11). Studies investigating the effects of DAA treatment on $CD8^+$ T cells have not addressed effector function. One study identified increased proliferation of HCV-specific $CD8^+$ T cells after peptide stimulation for most patients approximately four weeks after achieving SVR with faldaprevir and deleobuvir ± ribavirin (155). In contrast to results in the present project, this study suggests that functional changes in HCV-specific $CD8^+$ T cells can be observed as early as six months after achieving SVR. In this thesis, it appears a change in effector function of bulk $CD8^+$ T cells does not occur after achievement of SVR.

4.7 Summary and Relevance

The current study demonstrates that the function of $CD8^+$ T cells is related to the degree of liver fibrosis in chronic HCV infection, independent of antigen specificity. The findings here provide insight into the pathogenesis of HCV infection and may have implications for T cell-based therapies that reverse liver fibrosis caused by chronic HCV infection. $CD8^+$ T cell dysfunction is a challenge that will need to be overcome in order to develop an effective therapeutic vaccine for chronic HCV infection (191, 192).

The mechanism of how HCV alters the proportions of bulk $CD8^+$ T cells has not been established. In addition, the question of whether bulk $CD8^+$ T cell changes observed during chronic HCV infection can cause susceptibility to other pathogens or increase the likelihood of autoimmune complications has not been addressed. Some autoimmune or lymphoproliferative disorders have been reported in the context of HCV (166). Thus, the functional changes of bulk $CD8^+$ T cells during chronic HCV infection are of great interest as they will lead to a better understanding of interactions within the immune system.

HIV/HCV co-infected individuals experience faster progression to liver fibrosis compared to individuals mono-infected with either virus (193). Scientists have hypothesized that $CD8^+$ T cell exhaustion contributes to the rapid progression of HIV-pathogenesis during HIV/HCV co-infection. A higher frequency of bulk $CD8^+$ T cells with exhaustion markers are found in HIV/HCV co-infection compared to HIV mono-infection (194). Thus, the widespread effect of HCV may influence pathogenesis and prevent proper immune responses.

Some studies have discovered additional effects of HCV on bulk $CD8^+$ T cells. The phenotype of CMV-specific $CD8^+$ T cells was previously identified as more phenotypically immature (early or central memory) in chronic HCV infection compared to uninfected controls (more effector memory) (168). These results, obtained by Lucas *et al.*, were contrary to those

found in this thesis as an increased proportion of T_{LEM} and no differences in T_{CM} were observed. However, Lucas *et al.* examined virus-specific cells rather than the entire population of $CD8^+$ T cells, which may account for the differences observed. Another study performed by Murata *et al.* discovered that an increased proportion of bulk $CD8^+$ T cells in HCV infection exhibit a memory phenotype ($CD45RA^-CD28^+CD8^+$) (171). In this project, an increasing proportion of late effector memory $CD8^+$ T cells was associated with advancing liver fibrosis. Importantly, T_{LEM} were defined based on expression of three markers not used by Murata *et al.* including CD45RA, CCR7, and CD27.

The results in the present study uncovered a trend not previously observed in published work about HCV-specific $CD8^+$ T cells. In particular, the capacity to induce IFN-γ, CD107a, and perforin did not lower with increasing liver fibrosis. The $HCV^{+\ \text{Min. Fibrosis}}$ individuals had a significantly lower percentage of IFN-γ^+ and $CD107^+$ $CD8^+$ T cells upon stimulation compared to uninfected controls. However, $HCV^{+\ \text{Adv. Fibrosis}}$ individuals did not have a significantly different percentage of IFN-γ^+ and $CD107^+$ $CD8^+$ T cells upon stimulation compared to uninfected controls. Furthermore, the distinct relationship between liver fibrosis and certain $CD8^+$ T cell subsets will need further investigation. Another important concept that will need to be addressed in future studies is the ability of perforin to aid in the destruction of target cells. A killing assay, such as the chromium release assay, will be able to answer this question.

Many questions remain regarding the relationship between bulk $CD8^+$ T cells and liver fibrosis in the context of chronic HCV infection. A clinical trial with an increased number of individuals could be used to discern whether successful DAA treatment affects the function of bulk $CD8^+$ T cells while reversing liver fibrosis. Moreover, the effects of SVR on effector function of bulk $CD8^+$ T cells will need to be addressed with a time point farther from SVR.

Additional observations and trends may be uncovered if expression of IFN-γ and perforin within culture supernatants are measured for bulk $CD8^+$ T cells of individuals part of the clinical trial. Furthermore, investigation of other cytokines known to play a significant role in chronic HCV infection, such as IL-10, may yield additional insights. In conclusion, although several questions remain, it is apparent from the results in this project that some aspects of bulk $CD8^+$ T cell function are related to the degree of liver fibrosis. Future studies will need to more closely define and characterize this relationship.

References

1. Mohd Hanafiah, K., J. Groeger, A. D. Flaxman, and S. T. Wiersma. 2013. Global epidemiology of hepatitis C virus infection: New estimates of age-specific antibody to HCV seroprevalence. *Hepatology* 57: 1333–1342.

2. Macdonald, A., K. Saksela, M. Harris, J. Mankouri, A. Kazlauskas, and Z. Igloi. 2015. Hepatitis C virus NS5A protein blocks epidermal growth factor receptor degradation via a proline motif- dependent interaction. *J. Gen. Virol.* 96: 2133–2144.

3. Martinello, M., and G. V. Matthews. 2015. Enhancing the detection and management of acute hepatitis C virus infection. *Int. J. Drug Policy* 26: 899–910.

4. Nouroz, F., S. Shaheen, G. Mujtaba, and S. Noreen. 2015. An overview on hepatitis C virus genotypes and its control. *Egyptian Journal of Medical Human Genetics* 16: 291–298.

5. Heim, M. H. 2013. 25 years of interferon-based treatment of chronic hepatitis C: an epoch coming to an end. *Nat Rev Immunol* 13: 535–542.

6. Bansal, S. 2015. Impact of all oral anti-hepatitis C virus therapy: A meta-analysis. *World Journal of Hepatology* 7: 806.

7. Veldt, B. J. 2007. Sustained Virologic Response and Clinical Outcomes in Patients with Chronic Hepatitis C and Advanced Fibrosis. *Ann Intern Med* 147: 677.

8. Ehsaan Akhtar, V. M., and S. Saab. Cirrhosis regression in hepatitis C patients with sustained virologicalresponse after antiviral therapy: a meta-analysis. *Liver International* 35: 30–36.

9. Lu, M., J. Li, T. Zhang, L. B. Rupp, S. Trudeau, S. D. Holmberg, A. C. Moorman, P. R. Spradling, E. H. Teshale, F. Xu, J. A. Boscarino, and C. H. C. S. Investigators. Serum Biomarkers Indicate Long-term Reduction in Liver Fibrosis in Patients With Sustained Virological Response to Treatment for HCV Infection. *Clinical Gastroenterology and Hepatology* 14: 1044–1055.

10. Barrett, L., N. Trehanpati, N. Trehanpati, S. Poonia, S. Poonia, L. Daigh, L. Daigh, S. K. Sarin, S. K. Sarin, H. Masur, H. Masur, and S. Kottilil. 2014. Hepatic compartmentalization of exhausted and regulatory cells in HIV/HCV-coinfected patients. *J Viral Hepat* 22: 281–288.

11. Sharma, S., M. Carballo, J. J. Feld, and H. L. A. Janssen. 2015. Immigration and viral hepatitis. *Journal of Hepatology* 63: 515–522.

12. Nayak, A., N. Pattabiraman, N. Fadra, R. Goldman, S. L. Kosakovsky Pond, and R. Mazumder. 2015. Structure-function analysis of hepatitis C virus envelope glycoproteins E1 and E2. *J. Biomol. Struct. Dyn.* 33: 1682–1694.

13. Gerold, G., and T. Pietschmann. 2014. The HCV life cycle: in vitro tissue culture systems and therapeutic targets. *Dig Dis* 32: 525–537.

14. Li, Q., C. Sodroski, B. Lowey, C. J. Schweitzer, H. Cha, F. Zhang, and T. J. Liang. 2016. Hepatitis C virus depends on E-cadherin as an entry factor and regulates its expression in epithelial-to-mesenchymal transition. *Proc. Natl. Acad. Sci. U.S.A.* 113: 7620–7625.

15. Wahid, A., F. Helle, V. Descamps, G. Duverlie, F. Penin, and J. Dubuisson. 2013. Disulfide bonds in hepatitis C virus glycoprotein E1 control the assembly and entry functions of E2 glycoprotein. *Journal of Virology* 87: 1605–1617.

16. Blanchard, E., S. Belouzard, L. Goueslain, T. Wakita, J. Dubuisson, C. Wychowski, and Y. Rouillé. 2006. Hepatitis C virus entry depends on clathrin-mediated endocytosis. *Journal of Virology* 80: 6964–6972.

17. Kim, C. W., and K.-M. Chang. 2013. Hepatitis C virus: virology and life cycle. *Clinical and Molecular Hepatology* 19: 17–25.

18. Niepmann, M. 2013. Hepatitis C Virus RNA Translation. In *Hepatitis C Virus: From Molecular Virology to Antiviral Therapy*. Current Topics in Microbiology and Immunology vol. 369. Springer Berlin Heidelberg, Berlin, Heidelberg. 143–166.

19. Dubuisson, J., H. H. Hsu, R. C. Cheung, H. B. Greenberg, D. G. Russell, and C. M. Rice. 1994. Formation and intracellular localization of hepatitis C virus envelope glycoprotein complexes expressed by recombinant vaccinia and Sindbis viruses. *Journal of Virology* 68: 6147–6160.

20. Oh, J. W., T. Ito, and M. M. Lai. 1999. A recombinant hepatitis C virus RNA-dependent RNA polymerase capable of copying the full-length viral RNA. *Journal of Virology* 73: 7694–7702.

21. Gosert, R., D. Egger, V. Lohmann, R. Bartenschlager, H. E. Blum, K. Bienz, and D. Moradpour. 2003. Identification of the hepatitis C virus RNA replication complex in Huh-7 cells harboring subgenomic replicons. *Journal of Virology* 77: 5487–5492.

22. Gentzsch, J., C. Brohm, E. Steinmann, M. Friesland, N. Menzel, G. Vieyres, P. M. Perin, A. Frentzen, L. Kaderali, and T. Pietschmann. 2013. hepatitis c Virus p7 is critical for capsid assembly and envelopment. *PLoS Pathog* 9: e1003355.

23. Lindenbach, B. D., and C. M. Rice. 2013. The ins and outs of hepatitis C virus entry and assembly. *Nat. Rev. Microbiol.* 11: 688–700.

24. Triyatni, M., E. A. Berger, and B. Saunier. 2016. Assembly and release of infectious hepatitis C virus involving unusual organization of the secretory pathway. *World Journal of Hepatology* 8: 796.

25. Lavanchy, D. 2009. The global burden of hepatitis C. *Liver Int.* 29: 74–81.

26. Tong, M. J., K. R. Reddy, W. M. Lee, P. J. Pockros, J. C. Hoefs, E. B. Keeffe, F. B. Hollinger, E. J. Hathcote, H. White, R. T. Foust, D. M. Jensen, E. L. Krawitt, H. Fromm, M. Black, L. M. Blatt, M. Klein, and J. Lubina. 1997. Treatment of chronic hepatitis C

with consensus interferon: A multicenter, randomized, controlled trial. *Hepatology* 26: 747–754.

27. Di, A. B., P. Martin, C. Kassianides, M. Lisker-Melman, L. Murray, J. Waggoner, Z. Goodman, S. M. Banks, and J. H. Hoofnagle. 1989. Recombinant interferon alfa therapy for chronic hepatitis C. A randomized, double-blind, placebo-controlled trial. *N Engl J Med* 321: 1506–1510.

28. Poynard, T., V. Leroy, M. Cohard, T. Thevenot, P. Mathurin, P. Opolon, and J. P. Zarski. 1996. Meta-analysis of interferon randomized trials in the treatment of viral hepatitis C: Effects of dose and duration. *Hepatology* 24: 778–789.

29. Manns, M. P., H. Wedemeyer, and M. Cornberg. 2006. Treating viral hepatitis C: efficacy, side effects, and complications. *Gut* 55: 1350–1359.

30. Rockstroh, J. K., J. J. Feld, S. Chevaliez, K. Cheng, H. Wedemeyer, C. Sarrazin, B. Maasoumy, C. Herman, J. Hackett Jr., D. E. Cohen, G. J. Dawson, G. Cloherty, and J.-M. Pawlotsky. 2017. HCV core antigen as an alternate test to HCV RNA for assessment of virologic responses to all-oral, interferon-free treatment in HCV genotype 1 infected patients. *Journal of Virological Methods* 245: 14–18.

31. Dore, G. J., and J. J. Feld. 2015. Hepatitis C virus therapeutic development: in pursuit of "perfectovir." *Clinical Infectious Diseases* 60: 1829–1836.

32. Poordad, F., C. Hezode, R. Trinh, K. V. Kowdley, S. Zeuzem, K. Agarwal, M. L. Shiffman, H. Wedemeyer, T. Berg, E. M. Yoshida, X. Forns, S. S. Lovell, B. Da Silva-Tillmann, C. A. Collins, A. L. Campbell, T. Podsadecki, and B. Bernstein. 2014. ABT-450/r–Ombitasvir and Dasabuvir with Ribavirin for Hepatitis C with Cirrhosis. *The New England Journal of Medicine* 370: 1973–1982.

33. Afdhal, N., S. Zeuzem, P. Kwo, M. Chojkier, N. Gitlin, M. Puoti, M. Romero-Gomez, J.-P. Zarski, K. Agarwal, P. Buggisch, G. R. Foster, N. Bräu, M. Buti, I. M. Jacobson, G. M. Subramanian, X. Ding, H. Mo, J. C. Yang, P. S. Pang, W. T. Symonds, J. G. McHutchison, A. J. Muir, A. Mangia, and P. Marcellin. 2014. Ledipasvir and Sofosbuvir for Untreated HCV Genotype 1 Infection. *The New England Journal of Medicine* 370: 1889–1898.

34. Chaudhary, R. K., M. Tepper, S. Eisaadany, and P. R. Gully. 1999. Distribution of Hepatitis C Virus Genotypes in Canada: Results from the LCDC Sentinel Health Unit Surveillance System. *Canadian Journal of Infectious Diseases and Medical Microbiology* 10: 53–56.

35. Martin, N. K., G. R. Foster, J. Vilar, S. Ryder, M. E. Cramp, F. Gordon, J. F. Dillon, N. Craine, H. Busse, A. Clements, S. J. Hutchinson, A. Ustianowski, M. Ramsay, D. J. Goldberg, W. Irving, V. Hope, D. De Angelis, M. Lyons, P. Vickerman, and M. Hickman. 2015. HCV treatment rates and sustained viral response among people who inject drugs in seven UK sites: real world results and modelling of treatment impact. *J Viral Hepat* 22: 399–408.

36. Leidner, A. J., H. W. Chesson, F. Xu, J. W. Ward, P. R. Spradling, and S. D. Holmberg. 2015. Cost-effectiveness of hepatitis C treatment for patients in early stages of liver disease. *Hepatology* 61: 1860–1869.

37. Linas, B. P., D. M. Barter, J. A. Leff, S. A. Assoumou, J. A. Salomon, M. C. Weinstein, A. Y. Kim, and B. R. Schackman. 2014. The Hepatitis C Cascade of Care: Identifying Priorities to Improve Clinical Outcomes. *PLoS ONE* 9: e97317.

38. Nelson, P., B. Mathers, B. Cowie, H. Hagan, D. Des Jarlais, D. Horyniak, and L. Degenhardt. 2011. The epidemiology of viral hepatitis among people who inject drugs: Results of global systematic reviews. *Lancet* 378: 571–583.

39. Jenne, C. N., and P. Kubes. 2013. Immune surveillance by the liver. *Nat Immunol* 14: 996–1006.

40. Jacobs, F., E. Wisse, and B. De Geest. 2010. The role of liver sinusoidal cells in hepatocyte-directed gene transfer. *Am. J. Pathol.* 176: 14–21.

41. Møller, S. 2014. Extrahepatic complications to cirrhosis and portal hypertension: Haemodynamic and homeostatic aspects. *World Journal of Gastroenterology* 20: 15499.

42. Zheng, Z.-Y. 2009. Signal molecule-mediated hepatic cell communication during liver regeneration. *World Journal of Gastroenterology* 15: 5776.

43. Sirica, A. E. 1992. The Role of Cell Types in Hepatocarcinogenesis.

44. McCaughan, G. W. 2004. Fibrosis progression in chronic hepatitis C virus infection. *Gut* 53: 318–321.

45. Wynn, T. A. 2008. Cellular and molecular mechanisms of fibrosis. *The Journal of Pathology* 214: 199–210.

46. Lurie, Y. 2015. Non-invasive diagnosis of liver fibrosis and cirrhosis. *World Journal of Gastroenterology* 21: 11567.

47. Wynn, T. A., and T. R. Ramalingam. 2012. Mechanisms of fibrosis: therapeutic translation for fibrotic disease. *Nat. Med.* 18: 1028–1040.

48. Zhou, W.-C. 2014. Pathogenesis of liver cirrhosis. *World Journal of Gastroenterology* 20: 7312.

49. Akira, S., and H. Hemmi. 2003. Recognition of pathogen-associated molecular patterns by TLR family. *Immunology Letters* 85: 85–95.

50. Buonaguro, L., A. Petrizzo, M. L. Tornesello, and F. M. Buonaguro. 2012. Innate immunity and hepatitis C virus infection: a microarray's view. *Infectious Agents and Cancer* 7:1–12.

51. Saito, T., R. Hirai, Y.-M. Loo, D. Owen, C. L. Johnson, S. C. Sinha, S. Akira, T. Fujita, and M. Gale. 2007. Regulation of innate antiviral defenses through a shared repressor domain in RIG-I and LGP2. *Proc. Natl. Acad. Sci. U.S.A.* 104: 582–587.

52. Loo, Y.-M., D. M. Owen, K. Li, A. K. Erickson, C. L. Johnson, P. M. Fish, D. S. Carney, T. Wang, H. Ishida, M. Yoneyama, T. Fujita, T. Saito, W. M. Lee, C. H. Hagedorn, D. T. Y. Lau, S. A. Weinman, S. M. Lemon, and M. Gale. 2006. Viral and therapeutic control of IFN-beta promoter stimulator 1 during hepatitis C virus infection. *Proc. Natl. Acad. Sci. U.S.A.* 103: 6001–6006.

53. Li, X.-D., L. Sun, R. B. Seth, G. Pineda, and Z. J. Chen. 2005. Hepatitis C virus protease NS3/4A cleaves mitochondrial antiviral signaling protein off the mitochondria to evade innate immunity. *Proc. Natl. Acad. Sci. U.S.A.* 102: 17717–17722.

54. Li, K., N. L. Li, D. Wei, S. R. Pfeffer, M. Fan, and L. M. Pfeffer. 2012. Activation of chemokine and inflammatory cytokine response in hepatitis C virus–infected hepatocytes depends on toll-like receptor 3 sensing of hepatitis C virus double-stranded RNA intermediates. *Hepatology* 55: 666–675.

55. Li, K., E. Foy, J. C. Ferreon, M. Nakamura, A. C. M. Ferreon, M. Ikeda, S. C. Ray, M. Gale, and S. M. Lemon. 2005. Immune evasion by hepatitis C virus NS3/4A protease-mediated cleavage of the Toll-like receptor 3 adaptor protein TRIF. *Proc. Natl. Acad. Sci. U.S.A.* 102: 2992–2997.

56. Franchi, L., C. McDonald, T.-D. Kanneganti, A. Amer, and G. Núñez. 2006. Nucleotide-Binding Oligomerization Domain-Like Receptors: Intracellular Pattern Recognition Molecules for Pathogen Detection and Host Defense. *The Journal of Immunology* 177: 3507–3513.

57. Shin, E.-C., S.-H. Park, M. DeMino, M. Nascimbeni, K. Mihalik, M. Major, N. S. Veerapu, T. Heller, S. M. Feinstone, C. M. Rice, and B. Rehermann. 2011. Delayed Induction, Not Impaired Recruitment, of Specific CD8+ T Cells Causes the Late Onset of Acute Hepatitis C. *Gastroenterology* 141: 686–695.

58. Hiroishi, K., T. Ito, and M. Imawari. 2008. Immune responses in hepatitis C virus infection and mechanisms of hepatitis C virus persistence. *Journal of Gastroenterology and Hepatology* 23: 1473–1482.

59. Banchereau, J., and R. M. Steinman. 1998. Dendritic cells and the control of immunity. *Nature* 392: 245–252.

60. Siegal, F. P., N. Kadowaki, M. Shodell, P. A. Fitzgerald-Bocarsly, K. Shah, S. Ho, S. Antonenko, and Y. J. Liu. 1999. The nature of the principal type 1 interferon-producing cells in human blood. *Science* 284: 1835–1837.

61. Matsui, T., J. E. Connolly, M. Michnevitz, D. Chaussabel, C.-I. Yu, C. Glaser, S. Tindle, M. Pypaert, H. Freitas, B. Piqueras, J. Banchereau, and A. K. Palucka. 2009. CD2 distinguishes two subsets of human plasmacytoid dendritic cells with distinct phenotype and functions. *J. Immunol.* 182: 6815–6823.

62. Kanto, T., M. Inoue, H. Miyatake, A. Sato, M. Sakakibara, T. Yakushijin, C. Oki, I. Itose, N.

Hiramatsu, T. Takehara, A. Kasahara, and N. Hayashi. 2004. Reduced Numbers and Impaired Ability of Myeloid and Plasmacytoid Dendritic Cells to Polarize T Helper Cells in Chronic Hepatitis C Virus Infection. *J. Infect. Dis.* 190: 1919–1926.

63. Kadowaki, N., S. Ho, S. Antonenko, R. de Waal Malefyt, R. A. Kastelein, F. Bazan, and Y.-J. Liu. 2001. Subsets of Human Dendritic Cell Precursors Express Different Toll-like Receptors and Respond to Different Microbial Antigens. *J Exp Med* 194: 863–870.

64. Heufler, C., F. Koch, U. Stanzl, G. Topar, M. Wysocka, G. Trinchieri, A. Enk, R. M. Steinman, N. Romani, and G. Schuler. 1996. Interleukin-12 is produced by dendritic cells and mediates T helper 1 development as well as interferon-gamma production by T helper 1 cells. *Eur. J. Immunol.* 26: 659–668.

65. Wertheimer, A. M., A. Bakke, and H. R. Rosen. 2004. Direct enumeration and functional assessment of circulating dendritic cells in patients with liver disease. *Hepatology* 40: 335–345.

66. Collins, A. S., S. Ahmed, S. Napoletano, M. Schroeder, J. A. Johnston, J. E. Hegarty, C. O'Farrelly, and N. J. Stevenson. 2014. Hepatitis C virus (HCV)-induced suppressor of cytokine signaling (SOCS) 3 regulates proinflammatory TNF-α responses. *J Leukoc Biol* 96: 255–263.

67. Sagnelli, E., N. Coppola, C. Marrocco, G. Coviello, M. Battaglia, V. Messina, G. Rossi, C. Sagnelli, C. Scolastico, and P. Filippini. 2005. Diagnosis of hepatitis C virus related acute hepatitis by serial determination of IgM anti-HCV titres. *Journal of Hepatology* 42: 646–651.

68. Edwards, V. C., A. W. Tarr, R. A. Urbanowicz, and J. K. Ball. 2012. The role of neutralizing antibodies in hepatitis C virus infection. *J. Gen. Virol.* 93: 1–19.

69. Giang, E., M. Dorner, J. C. Prentoe, M. Dreux, M. J. Evans, J. Bukh, C. M. Rice, A. Ploss, D. R. Burton, and M. Law. 2012. Human broadly neutralizing antibodies to the envelope glycoprotein complex of hepatitis C virus. *Proc. Natl. Acad. Sci. U.S.A.* 109: 6205–6210.

70. Zhang, P., C. G. Wu, K. Mihalik, M. L. Virata-Theimer, M.-Y. W. Yu, H. J. Alter, and S. M. Feinstone. 2007. Hepatitis C virus epitope-specific neutralizing antibodies in Igs prepared from human plasma. *PNAS* 104: 8449–8454.

71. Keck, Z.-Y., A. Saha, J. Xia, Y. Wang, P. Lau, T. Krey, F. A. Rey, and S. K. H. Foung. 2011. Mapping a region of hepatitis C virus E2 that is responsible for escape from neutralizing antibodies and a core CD81-binding region that does not tolerate neutralization escape mutations. *Journal of Virology* 85: 10451–10463.

72. Pileri, P. 1998. Binding of Hepatitis C Virus to CD81. *Science* 282: 938–941.

73. Cashman, S. B., B. D. Marsden, and L. B. Dustin. 2014. The Humoral Immune Response to HCV: Understanding is Key to Vaccine Development. *Front. Immunol.* 5: 550.

74. Osburn, W. O., A. E. Snider, B. L. Wells, R. Latanich, J. R. Bailey, D. L. Thomas, A. L. Cox, and S. C. Ray. 2014. Clearance of hepatitis C infection is associated with the early appearance of broad neutralizing antibody responses. *Hepatology* 59: 2140–2151.

75. Osburn, W. O., B. E. Fisher, K. A. Dowd, G. Urban, L. Liu, S. C. Ray, D. L. Thomas, and A. L. Cox. 2010. Spontaneous Control of Primary Hepatitis C Virus Infection and Immunity Against Persistent Reinfection. *Gastroenterology* 138: 315–324.

76. Pestka, J. M., M. B. Zeisel, E. Bläser, P. Schürmann, B. Bartosch, F.-L. Cosset, A. H. Patel, H. Meisel, J. Baumert, S. Viazov, K. Rispeter, H. E. Blum, M. Roggendorf, and T. F. Baumert. 2007. Rapid induction of virus-neutralizing antibodies and viral clearance in a single-source outbreak of hepatitis C. *PNAS* 104: 6025–6030.

77. Bjoro, K., S. S. Froland, Z. Yun, H. H. Samdal, and T. Haaland. 2010. Hepatitis C Infection in Patients with Primary Hypogammaglobulinemia after Treatment with Contaminated Immune Globulin. *The New England Journal of Medicine* 331: 1607–1611.

78. Neumann, A. U., N. P. Lam, H. Dahari, D. R. Gretch, T. E. Wiley, T. J. Layden, and A. S. Perelson. 1998. Hepatitis C Viral Dynamics in Vivo and the Antiviral Efficacy of Interferon-α Therapy. *Science* 282: 103–107.

79. Bankwitz, D., E. Steinmann, J. Bitzegeio, S. Ciesek, M. Friesland, E. Herrmann, M. B. Zeisel, T. F. Baumert, Z.-Y. Keck, S. K. H. Foung, E.-I. Pécheur, and T. Pietschmann. 2010. Hepatitis C virus hypervariable region 1 modulates receptor interactions, conceals the CD81 binding site, and protects conserved neutralizing epitopes. *Journal of Virology* 84: 5751–5763.

80. Helle, F., A. Goffard, V. Morel, G. Duverlie, J. McKeating, Z.-Y. Keck, S. Foung, F. Penin, J. Dubuisson, and C. Voisset. 2007. The neutralizing activity of anti-hepatitis C virus antibodies is modulated by specific glycans on the E2 envelope protein. *Journal of Virology* 81: 8101–8111.

81. Grove, J., S. Nielsen, J. Zhong, M. F. Bassendine, H. E. Drummer, P. Balfe, and J. A. McKeating. 2008. Identification of a residue in hepatitis C virus E2 glycoprotein that determines scavenger receptor BI and CD81 receptor dependency and sensitivity to neutralizing antibodies. *Journal of Virology* 82: 12020–12029.

82. Brimacombe, C. L., J. Grove, L. W. Meredith, K. Hu, A. J. Syder, M. V. Flores, J. M. Timpe, S. E. Krieger, T. F. Baumert, T. L. Tellinghuisen, F. Wong-Staal, P. Balfe, and J. A. McKeating. 2011. Neutralizing antibody-resistant hepatitis C virus cell-to-cell transmission. *Journal of Virology* 85: 596–605.

83. Rehermann, B. 2013. Pathogenesis of chronic viral hepatitis: differential roles of T cells and NK cells. *Nat. Med.* 19: 859–868.

84. Larrubia, J.-R., E. Moreno-Cubero, M.-U. Lokhande, S. García-Garzón, A. Lázaro, J. Miquel, C. Perna, and E. Sanz-de-Villalobos. 2014. Adaptive immune response during

hepatitis C virus infection. *World Journal of Gastroenterology* 20: 3418–3430.

85. Choudhuri, K., A. Kearney, T. R. Bakker, and P. A. van der Merwe. 2005. Immunology: How Do T Cells Recognize Antigen? *Current Biology* 15: R382–R385.

86. Larrubia, J. R., and S. Benito-Martínez. 2009. Cytokines-their pathogenic and therapeutic role in chronic viral hepatitis. *Rev Esp Enferm Dig* 101: 343–351.

87. Xie, A., X. Zheng, M. Khattar, P. Schroder, S. Stepkowski, J. Xia, and W. Chen. 2015. TCR stimulation without co-stimulatory signals induces expression of "tolerogenic" genes in memory CD4 T cells but does not compromise cell proliferation. *Molecular Immunology* 63: 406–411.

88. Petrovic, D., E. Dempsey, D. G. Doherty, D. Kelleher, and A. Long. 2012. Hepatitis C virus – T-cell responses and viral escape mutations. *Eur. J. Immunol.* 42: 17–26.

89. Sugimoto, K., F. Ikeda, J. Stadanlick, F. A. Nunes, H. J. Alter, and K.-M. Chang. 2003. Suppression of HCV-specific T cells without differential hierarchy demonstrated ex vivo in persistent HCV infection. *Hepatology* 38: 1437–1448.

90. Penna, A., M. Pilli, A. Zerbini, A. Orlandini, S. Mezzadri, L. Sacchelli, G. Missale, and C. Ferrari. 2007. Dysfunction and functional restoration of HCV-specific CD8 responses in chronic hepatitis C virus infection. *Hepatology* 45: 588–601.

91. Zehner, M., A. L. Marschall, E. Bos, J.-G. Schloetel, C. Kreer, D. Fehrenschild, A. Limmer, F. Ossendorp, T. Lang, A. J. Koster, S. Dübel, and S. Burgdorf. 2015. The Translocon Protein Sec61 Mediates Antigen Transport from Endosomes in the Cytosol for Cross-Presentation to CD8+ T Cells. *Immunity* 42: 850–863.

92. Barbier, L., S. S. Tay, C. McGuffog, J. A. Triccas, G. W. McCaughan, D. G. Bowen, and P. Bertolino. 2012. Two lymph nodes draining the mouse liver are the preferential site of DC migration and T cell activation. *Journal of Hepatology* 57: 352–358.

93. Neve-Oz, Y., Y. Razvag, J. Sajman, and E. Sherman. 2015. Mechanisms of localized activation of the T cell antigen receptor inside clusters. *Biochim. Biophys. Acta* 1853: 810–821.

94. Kang, W., P. S. Sung, S.-H. Park, S. Yoon, D.-Y. Chang, S. Kim, K. H. Han, J. K. Kim, B. Rehermann, Y.-J. Chwae, and E.-C. Shin. 2014. Hepatitis C Virus Attenuates Interferon-Induced Major Histocompatibility Complex Class I Expression and Decreases CD8+ T Cell Effector Functions. *Gastroenterology* 146: 1351–1360.

95. Chen, L., and D. B. Flies. 2013. Molecular Mechanisms of T cell Co-stimulation and Co-inhibition. *Nature Reviews* 13: 227–242.

96. Rufer, N. 2003. Ex vivo characterization of human CD8+ T subsets with distinct replicative history and partial effector functions. *Blood* 102: 1779–1787.

97. Kurth, I., Romero, P., Zippelius, A., Romero, P., A. Zippelius, I. Kurth, M. J. Pittet, J. Mikaël, C. Touvrey, C. Touvrey, E. M. Iancu, E. M. Iancu, P. Corthesy, E. Devevre, D. E. Speiser, E. Devevre, D. E. Speiser, E.-M. C. D. T. Lymphocytes, N. Rufer, J. Pittet, E. M. Iancu, P. Corthesy, E. Devevre, D. E. Speiser, and N. Rufer. 2007. Four Functionally Distinct Populations of Human Effector-Memory CD8+ T Lymphocytes. *The Journal of Immunology* 178: 4112–4119.

98. Koch, S., A. Larbi, E. Derhovanessian, D. Özcelik, E. Naumova, and G. Pawelec. 2008. Multiparameter flow cytometric analysis of CD4 and CD8 T cell subsets in young and old people. *Immun Ageing* 5: 6–12.

99. Sallusto, F., D. Lenig, R. Forster, and M. L. A. Lanzavecchia. 1999. Two subsets of memory T lymphocytes with distinct homing potentials and effector functions. *Immunology Letters to Nature* 401: 708–712.

100. Hintzen, R. Q., R. de Jong, S. M. Lens, M. Brouwer, P. Baars, and R. A. van Lier. 1993. Regulation of CD27 expression on subsets of mature T-lymphocytes. *The Journal of Immunology* 151: 2426–2435.

101. Hendriks, J., L. A. Gravestein, K. Tesselaar, and R. A. van Lier. 2000. CD27 is required for generation and long-term maintenance of T cell immunity. *Nat Immunol* 1: 433–440.

102. Campbell, J. J., K. E. Murphy, E. J. Kunkel, C. E. Brightling, D. Soler, Z. Shen, J. Boisvert, H. B. Greenberg, M. A. Vierra, S. B. Goodman, M. C. Genovese, A. J. Wardlaw, E. C. Butcher, and L. Wu. 2001. CCR7 Expression and Memory T Cell Diversity in Humans. *The Journal of Immunology* 166: 877–884.

103. Takata, H., and M. Takiguchi. 2006. Three Memory Subsets of Human CD8+ T Cells Differently Expressing Three Cytolytic Effector Molecules. *The Journal of Immunology* 177: 4330–4340.

104. Ahmed, R., Barber, D. L., and Wherry, E. J. 2003. Cutting Edge: Rapid In Vivo Killing by Memory CD8 T Cells. *The Journal of Immunology* 171: 27–31.

105. Whitmire, J. K., J. T. Tan, and J. L. Whitton. 2005. Interferon-gamma acts directly on CD8+ T cells to increase their abundance during virus infection. *J Exp Med* 201: 1053–1059.

106. Feau, S., R. Arens, S. Togher, and S. P. Schoenberger. 2012. Autocrine IL-2 is required for secondary population expansion of CD8+ memory T cells. *Nat Immunol* 12: 908–913.

107. Bonilla, N., N. Barget, M. Andrieu, D. Roulot, P. Letoumelin, V. Grando, J. C. Trinchet, N. Ganne-Carrié, M. Beaugrand, P. Deny, J. Choppin, J. Guillet, and M. Ziol. 2006. Interferon gamma-secreting HCV-specific CD8+ T cells in the liver of patients with chronic C hepatitis: relation to liver fibrosis--ANRS HC EP07 study. *J Viral Hepat* 13: 474–481.

108. Jo, J., B. Bengsch, B. Seigel, S. J. Rau, J. Schmidt, E. Bisse, P. Aichele, U. Aichele, L.

Joeckel, C. Royer, K. Sá Ferreira, C. Borner, T. F. Baumert, H. E. Blum, V. Lohmann, R. Fischer, and R. Thimme. 2012. Low perforin expression of early differentiated HCV-specific CD8+ T cells limits their hepatotoxic potential. *Journal of Hepatology* 57: 9–16.

109. Bach, E. A., M. Aguet, and R. D. Schreiber. 1997. THE IFN-γ RECEPTOR: A Paradigm for Cytokine Receptor Signaling. *Annual Review of Immunology* 15: 563–591.

110. U Boehm, T Klamp, A. M Groot, and J. C. Howard. 2003. CELLULAR RESPONSES TO INTERFERON-γ. *http://dx.doi.org/10.1146/annurev.immunol.15.1.749* 15: 749–795.

111. Guidotti, L. G., P. Borrow, A. Brown, H. McClary, R. Koch, and F. V. Chisari. 1999. Noncytopathic Clearance of Lymphocytic Choriomeningitis Virus from the Hepatocyte. *J Exp Med* 189: 1555–1564.

112. Trapani, J. A., and M. J. Smyth. 2002. Functional significance of the perforin/granzyme cell death pathway. *Nat Rev Immunol* 2: 735–747.

113. Osińska, I., K. Popko, and U. Demkow. 2014. Perforin: an important player in immune response. *Central-European Journal of Immunology* 39: 109–115.

114. Voskoboinik, I., and J. C. Whisstock. 2015. Perforin and granzymes: function, dysfunction and human pathology. *Nature Reviews* 15: 388–400.

115. Peters, P. J., J. Borst, V. Oorschot, M. Fukuda, O. Krähenbühl, J. Tschopp, J. W. Slot, and H. J. Geuze. 1991. Cytotoxic T lymphocyte granules are secretory lysosomes, containing both perforin and granzymes. *J Exp Med* 173: 1099–1109.

116. Chan, K. S., and A. Kaur. 2007. Flow cytometric detection of degranulation reveals phenotypic heterogeneity of degranulating CMV-specific CD8+ T lymphocytes in rhesus macaques. *Journal of Immunological Methods* 325: 20–34.

117. Betts, M. R., J. M. Brenchley, D. A. Price, and S. C. De Rosa. 2003. Sensitive and viable identification of antigen-specific CD8+ T cells by a flow cytometric assay for degranulation. *Journal of Immunological Methods* 281: 65–78.

118. Kaech, S. M., S. Hemby, E. Kersh, and R. Ahmed. 2002. Molecular and Functional Profiling of Memory CD8 T Cell Differentiation. *Cell* 111: 837–851.

119. Glimcher, L. H., and M. J. Townsend. 2004. Recent developments in the transcriptional regulation of cytolytic effector cells. *Nature Reviews* 4: 900–11.

120. Penix, L. A., M. T. Sweetser, W. M. Weaver, J. P. Hoeffler, T. K. Kerppola, and C. B. Wilson. 1996. The proximal regulatory element of the interferon-gamma promoter mediates selective expression in T cells. *J. Biol. Chem.* 271: 31964–31972.

121. Ritter, A. T., K. L. Angus, and G. M. Griffiths. 2013. The role of the cytoskeleton at the immunological synapse. *Immunological Reviews* 256: 107–117.

122. Abel, M., D. Sène, S. Pol, M. Bourlière, T. Poynard, F. Charlotte, P. Cacoub, and S. Caillat-

Zucman. 2006. Intrahepatic virus-specific IL-10-producing CD8 T cells prevent liver damage during chronic hepatitis C virus infection. *Hepatology* 44: 1607–1616.

123. Wedemeyer, H., X. S. He, M. Nascimbeni, A. R. Davis, H. B. Greenberg, J. H. Hoofnagle, T. J. Liang, H. Alter, and B. Rehermann. 2002. Impaired Effector Function of Hepatitis C Virus-Specific CD8+ T Cells in Chronic Hepatitis C Virus Infection. *The Journal of Immunology* 169: 3447–3458.

124. Zajac, A. J., J. N. Blattman, K. Murali-Krishna, D. J. D. Sourdive, M. Suresh, J. D. Altman, and R. Ahmed. 1998. Viral Immune Evasion Due to Persistence of Activated T Cells Without Effector Function. *J Exp Med* 188: 2205–2213.

125. Blackburn, S. D., H. Shin, W. N. Haining, T. Zou, C. J. Workman, A. Polley, M. R. Betts, G. J. Freeman, D. A. A. Vignali, and E. J. Wherry. 2009. Coregulation of CD8+ T cell exhaustion by multiple inhibitory receptors during chronic viral infection. *Nat Immunol* 10: 29–37.

126. Radziewicz, H., C. C. Ibegbu, M. L. Fernandez, K. A. Workowski, K. Obideen, M. Wehbi, H. L. Hanson, J. P. Steinberg, D. Masopust, E. J. Wherry, J. D. Altman, B. T. Rouse, G. J. Freeman, R. Ahmed, and A. Grakoui. 2007. Liver-infiltrating lymphocytes in chronic human hepatitis C virus infection display an exhausted phenotype with high levels of PD-1 and low levels of CD127 expression. *Journal of Virology* 81: 2545–2553.

127. Gruener, N. H., F. Lechner, M. C. Jung, H. Diepolder, T. Gerlach, G. Lauer, B. Walker, J. Sullivan, R. Phillips, G. R. Pape, and P. Klenerman. 2001. Sustained dysfunction of antiviral CD8+ T lymphocytes after infection with hepatitis C virus. *Journal of Virology* 75: 5550–5558.

128. Urbani, S., B. Amadei, D. Tola, M. Massari, S. Schivazappa, G. Missale, and C. Ferrari. 2006. PD-1 expression in acute hepatitis C virus (HCV) infection is associated with HCV-specific CD8 exhaustion. *Journal of Virology* 80: 11398–11403.

129. Wherry, E. J., J. N. Blattman, K. Murali-Krishna, R. van der Most, and R. Ahmed. 2003. Viral persistence alters CD8 T-cell immunodominance and tissue distribution and results in distinct stages of functional impairment. *Journal of Virology* 77: 4911–4927.

130. Kao, C., K. J. Oestreich, M. A. Paley, A. Crawford, J. M. Angelosanto, M.-A. A. Ali, A. M. Intlekofer, J. M. Boss, S. L. Reiner, A. S. Weinmann, and E. J. Wherry. 2011. Transcription factor T-bet represses expression of the inhibitory receptor PD-1 and sustains virus-specific CD8+ T cell responses during chronic infection. *Nat Immunol* 12: 663–671.

131. Guidotti, L. G., and F. V. Chisari. 2006. Immunobiology and pathogenesis of viral hepatitis. *Annu Rev Pathol Mech Dis* 1: 23–16.

132. Lee, W. Y., and P. Kubes. 2008. Leukocyte adhesion in the liver: distinct adhesion paradigm from other organs. *Journal of Hepatology* 48: 504–512.

133. Wang, J., T. H. Holmes, R. Cheung, H. B. Greenberg, and X.-S. He. 2004. Expression of Chemokine Receptors on Intrahepatic and Peripheral Lymphocytes in Chronic Hepatitis C Infection: Its Relationship to Liver Inflammation. *J. Infect. Dis.* 190: 989–997.

134. Crispe, I. N., T. Dao, K. Klugewitz, W. Z. Mehal, and D. P. Metz. 2000. The liver as a site of T-cell apoptosis: graveyard, or killing field? *Immunological Reviews* 174: 47–62.

135. Wang, J., T. H. Holmes, and L. L. Guevara. 2006. Phenotypic and functional status of intrahepatic T cells in chronic hepatitis C. *The Journal of Infectious Diseases* 194:1068–1077.

136. Nisii, C., M. Tempestilli, C. Agrati, F. Poccia, G. Tocci, M. A. Longo, G. D'Offizi, R. Tersigni, O. Lo Iacono, G. Antonucci, and A. Oliva. 2006. Accumulation of dysfunctional effector CD8+ T cells in the liver of patients with chronic HCV infection. *Journal of Hepatology* 44: 475–483.

137. Spangenberg, H. C., S. Viazov, N. Kersting, C. Neumann-Haefelin, D. McKinney, M. Roggendorf, F. von Weizsäcker, H. E. Blum, and R. Thimme. 2005. Intrahepatic CD8+ T-cell failure during chronic hepatitis C virus infection. *Hepatology* 42: 828–837.

138. Curtsinger, J. M., D. C. Lins, C. M. Johnson, and M. F. Mescher. 2005. Signal 3 Tolerant CD8 T Cells Degranulate in Response to Antigen but Lack Granzyme B to Mediate Cytolysis. *The Journal of Immunology* 175: 4392–4399.

139. Hahn, C. S., Y. G. Cho, B.-S. Kang, I. M. Lester, and Y. S. Hahn. 2000. The HCV Core Protein Acts as a Positive Regulator of Fas-Mediated Apoptosis in a Human Lymphoblastoid T Cell Line. *Virology* 276: 127–137.

140. Nuti, S., D. Rosa, N. M. Valiante, and G. Saletti. 1998. Dynamics of intra-hepatic lymphocytes in chronic hepatitis C: enrichment for Va24+ T cells and rapid elimination of effector cells by apoptosis. *European Journal of Immunology* 28: 3448–3455.

141. Golden-Mason, L., B. E. Palmer, N. Kassam, L. Townshend-Bulson, S. Livingston, B. J. McMahon, N. Castelblanco, V. Kuchroo, D. R. Gretch, and H. R. Rosen. 2009. Negative immune regulator Tim-3 is overexpressed on T cells in hepatitis C virus infection and its blockade rescues dysfunctional CD4+ and CD8+ T cells. *Journal of Virology* 83: 9122–9130.

142. Lucas, M., Lucas, M., Lauer, G. M., Klenerman, P., Walker, B. D., A. L. Vargas-cuero, A. L. Vargas-Cuero, G. M. Lauer, E. Barnes, E. Barnes, C. B. Willberg, C. B. Willberg, N. Semmo, N. Semmo, B. D. Walker, R. Phillips, R. Phillips, P. Klenerman, M. Lucas, A. L. Vargas-cuero, E. Barnes, C. B. Willberg, N. Semmo, and R. Phillips. 2004. Pervasive Influence of Hepatitis C Virus on the Phenotype of Antiviral CD8+ T Cells. *The Journal of Immunology* 172: 1744–1753.

143. Zhao, B.-B., S.-J. Zheng, L.-L. Gong, Y. Wang, C.-F. Chen, W.-J. Jin, D. Zhang, X.-H. Yuan, J. Guo, Z.-P. Duan, and Y.-W. He. 2013. T lymphocytes from chronic HCV-infected

patients are primed for activation-induced apoptosis and express unique pro-apoptotic gene signature. *PLoS ONE* 8: e77008–13.

144. Burke Schinkel, S. C., L. Carrasco-Medina, C. L. Cooper, and A. M. Crawley. 2016. Generalized Liver- and Blood-Derived CD8+ T-Cell Impairment in Response to Cytokines in Chronic Hepatitis C Virus Infection. *PLoS ONE* 11: e0157055.

145. Hoare, M., A. Shankar, M. Shah, S. Rushbrook, W. Gelson, S. Davies, A. Akbar, and G. J. M. Alexander. 2013. γ-H2AX+CD8+ T lymphocytes cannot respond to IFN-α, IL-2 or IL-6 in chronic hepatitis C virus infection. *Journal of Hepatology* 58: 868–874.

146. Tripathi, P., S. Kurtulus, S. Wojciechowski, A. Sholl, K. Hoebe, S. C. Morris, F. D. Finkelman, H. L. Grimes, and D. A. Hildeman. 2010. STAT5 Is Critical To Maintain Effector CD8+ T Cell Responses. *The Journal of Immunology* 185: 2116–2124.

147. Woo, S.-R., M. E. Turnis, M. V. Goldberg, J. Bankoti, M. Selby, C. J. Nirschl, M. L. Bettini, D. M. Gravano, P. Vogel, C. L. Liu, S. Tangsombatvisit, J. F. Grosso, G. Netto, M. P. Smeltzer, A. Chaux, P. J. Utz, C. J. Workman, D. M. Pardoll, A. J. Korman, C. G. Drake, and D. A. A. Vignali. 2012. Immune Inhibitory Molecules LAG-3 and PD-1 Synergistically Regulate T-cell Function to Promote Tumoral Immune Escape. *Cancer Res* 72: 917–927.

148. Okazaki, T., I.-M. Okazaki, J. Wang, D. Sugiura, F. Nakaki, T. Yoshida, Y. Kato, S. Fagarasan, M. Muramatsu, T. Eto, K. Hioki, and T. Honjo. 2011. PD-1 and LAG-3 inhibitory co-receptors act synergistically to prevent autoimmunity in mice. *J Exp Med* 208: 1–13.

149. Nakamoto, N., H. Cho, A. Shaked, K. Olthoff, M. E. Valiga, M. Kaminski, E. Gostick, D. A. Price, G. J. Freeman, E. J. Wherry, and K.-M. Chang. 2009. Synergistic Reversal of Intrahepatic HCV-Specific CD8 T Cell Exhaustion by Combined PD-1/CTLA-4 Blockade. *PLoS Pathog* 5: e1000313.

150. Barber, D. L., E. J. Wherry, D. Masopust, B. Zhu, and J. P. Allison. 2006. Restoring function in exhausted CD8 T cells during chronic viral infection. *Nature* 439: 682–687.

151. Missale, G., M. Pilli, A. Zerbini, A. Penna, L. Ravanetti, V. Barili, A. Orlandini, A. Molinari, M. Fasano, T. Santantonio, and C. Ferrari. 2012. Lack of full CD8 functional restoration after antiviral treatment for acute and chronic hepatitis C virus infection. *Gut* 61: 1076–1084.

152. Abdel-Hakeem, M. S., N. Bédard, G. Badr, M. Ostrowski, R. P. Sékaly, J. Bruneau, B. Willems, E. J. Heathcote, and N. H. Shoukry. 2010. Comparison of immune restoration in early versus late alpha interferon therapy against hepatitis C virus. *Journal of Virology* 84: 10429–10435.

153. Badr, G., N. Bédard, M. S. Abdel-Hakeem, L. Trautmann, B. Willems, J.-P. Villeneuve, E. K. Haddad, R. P. Sékaly, J. Bruneau, and N. H. Shoukry. 2008. Early interferon therapy for

hepatitis C virus infection rescues polyfunctional, long-lived CD8+ memory T cells. *Journal of Virology* 82: 10017–10031.

154. Seigel, B., B. Bengsch, V. Lohmann, R. Bartenschlager, H. E. Blum, and R. Thimme. 2013. Factors that determine the antiviral efficacy of HCV-specific CD8(+) T cells ex vivo. *Gastroenterology* 144: 426–436.

155. Martin, B., N. Hennecke, V. Lohmann, A. Kayser, C. Neumann-Haefelin, G. Kukolj, W. O. Böcher, and R. Thimme. 2014. Restoration of HCV-specific CD8+ T cell function by interferon-free therapy. *Journal of Hepatology* 61: 538–543.

156. Shoukry, N. H., A. Grakoui, M. Houghton, D. Y. Chien, J. Ghrayeb, K. A. Reimann, and C. M. Walker. 2003. Memory CD8+ T cells are required for protection from persistent hepatitis C virus infection. *J Exp Med* 197: 1645–1655.

157. Li, Y., X. Wang, S. D. Douglas, D. S. Metzger, G. Woody, T. Zhang, L. Song, and W. Z. Ho. 2005. CD8+ T cell depletion amplifies hepatitis C virus replication in peripheral blood mononuclear cells. *J. Infect. Dis.* 192: 1093–1101.

158. Jo, J., U. Aichele, N. Kersting, R. Klein, P. Aichele, E. Bisse, A. K. Sewell, H. E. Blum, R. Bartenschlager, V. Lohmann, and R. Thimme. 2009. Analysis of CD8+ T-Cell–Mediated Inhibition of Hepatitis C Virus Replication Using a Novel Immunological Model. *Gastroenterology* 136: 1391–1401.

159. Abdel-Hakeem, M. S., N. Bédard, D. Murphy, J. Bruneau, and N. H. Shoukry. 2014. Signatures of protective memory immune responses during hepatitis C virus reinfection. *Gastroenterology* 147: 870–881.

160. Shin, H., and E. J. Wherry. 2007. CD8 T cell dysfunction during chronic viral infection. *Current Opinion in Immunology* 19: 408–415.

161. Das, A., M. Hoare, N. Davies, A. R. Lopes, C. Dunn, P. T. F. Kennedy, G. Alexander, H. Finney, A. Lawson, F. J. Plunkett, A. Bertoletti, A. N. Akbar, and M. K. Maini. 2008. Functional skewing of the global CD8 T cell population in chronic hepatitis B virus infection. *J Exp Med* 205: 2111–2124.

162. Weinberg, A., L. Y. Song, C. Wilkening, A. Sevin, B. Blais, R. Louzao, D. Stein, P. Defechereux, D. Durand, E. Riedel, N. Raftery, R. Jesser, B. Brown, M. F. Keller, R. Dickover, E. McFarland, T. Fenton, for the Pediatric ACTG Cryopreservation Working Group. 2009. Optimization and Limitations of Use of Cryopreserved Peripheral Blood Mononuclear Cells for Functional and Phenotypic T-Cell Characterization. *Clinical and Vaccine Immunology* 16: 1176–1186.

163. O'Connor, A. M., A. M. Crawley, and J. B. Angel. 2010. Interleukin-7 enhances memory CD8(+) T-cell recall responses in health but its activity is impaired in human immunodeficiency virus infection. *Immunology* 131: 525–536.

164. Tomiyama, H., and T. Matsuda. 2002. Differentiation of human CD8+ T cells from a memory to memory/effector phenotype. *The Journal of Immunology* 168: 5538–5550.

165. Hamann, D., P. A. Baars, M. H. G. Rep, B. Hooibrink, S. R. Kerkhof-Garde, M. R. Klein, and R. A. W. V. Lier. 1997. Phenotypic and Functional Separation of Memory and Effector Human CD8+ T Cells. *J Exp Med* 186: 1407–1418.

166. Cacoub, P., L. Gragnani, C. Comarmond, and A. L. Zignego. 2014. Extrahepatic manifestations of chronic hepatitis C virus infection. *Digestive and Liver Disease* 46: S165–S173.

167. Alanio, C., F. Nicoli, P. Sultanik, T. Flecken, B. Perot, D. Duffy, E. Bianchi, A. Lim, E. Clave, M. M. van Buuren, A. Schnuriger, K. Johnsson, J. Boussier, A. Garbarg-Chenon, L. Bousquet, E. Mottez, T. N. Schumacher, A. Toubert, V. Appay, F. Heshmati, R. Thimme, S. Pol, V. Mallet, and M. L. Albert. 2015. Bystander hyperactivation of preimmune CD8+ T cells in chronic HCV patients. *Elife* 4: e07916.

168. Lucas, M., A. L. Vargas-cuero, G. M. Lauer, E. Barnes, C. B. Willberg, N. Semmo, B. D. Walker, R. Phillips, and P. Klenerman. 2004. Pervasive influence of hepatitis C virus on the phenotype of antiviral CD8+ T cells. *The Journal of Immunology* 172: 1744–1753.

169. Stelekati, E., and E. J. Wherry. 2012. Chronic bystander infections and immunity to unrelated antigens. *Cell Host Microbe* 12: 458–469.

170. Seigel, B., B. Bengsch, V. Lohmann, R. Bartenschlager, H. E. Blum, and R. Thimme. 2013. Factors That Determine the Antiviral Efficacy of HCV-Specific CD8+ T Cells Ex Vivo. *Gastroenterology* 144: 426–436.

171. Murata, M., S. Nabeshima, N. Maeda, H. Nakashima, S. Kashiwagi, and J. Hayashi. 2002. Increased frequency of IFN-gamma-producing peripheral CD8+ T cells with memory-phenotype in patients with chronic hepatitis C. *Journal of Medical Virology* 67: 162–170.

172. Moorman, J. P., C. L. Zhang, L. Ni, C. J. Ma, Y. Zhang, X. Y. Wu, P. Thayer, T. M. Islam, T. Borthwick, and Z. Q. Yao. 2011. Impaired hepatitis B vaccine responses during chronic hepatitis C infection: involvement of the PD-1 pathway in regulating CD4(+) T cell responses. *Vaccine* 29: 3169–3176.

173. Wiedmann, M., U. G. Liebert, U. Oesen, H. Porst, M. Wiese, S. Schroeder, U. Halm, J. Mössner, and F. Berr. 2000. Decreased immunogenicity of recombinant hepatitis B vaccine in chronic hepatitis C. *Hepatology* 31: 230–234.

174. Greenbaum, E., R. Nir-Paz, D. M. Linton, T. Ben-Hur, A. Meirovitz, and Z. Zakay-Rones. 2004. Severe influenza infection in a chronic hepatitis C carrier: failure of protective serum HI antibodies after IM vaccination. *Journal of Clinical Virology* 29: 23–26.

175. Gaeta, G. B., G. Stornaiuolo, D. F. Precone, A. Amendola, and A. R. Zanetti. 2002. Immunogenicity and safety of an adjuvanted influenza vaccine in patients with

decompensated cirrhosis. *Vaccine* 20: B33–B35.

176. Penna, A., M. Pilli, A. Zerbini, A. Orlandini, S. Mezzadri, L. Sacchelli, G. Missale, and C. Ferrari. 2007. Dysfunction and functional restoration of HCV-specific CD8 responses in chronic hepatitis C virus infection. *Hepatology* 45: 588–601.

177. Stelekati, E., H. Shin, T. A. Doering, D. V. Dolfi, C. G. Ziegler, D. P. Beiting, L. Dawson, J. Liboon, D. Wolski, M.-A. A. Ali, P. D. Katsikis, H. Shen, D. S. Roos, W. N. Haining, G. M. Lauer, and E. J. Wherry. 2014. Bystander chronic infection negatively impacts development of CD8(+) T cell memory. *Immunity* 40: 801–813.

178. Jouvin-Marche, E., and Z. M. Jílková. 2014. Lymphocytes degranulation in liver in hepatitis C virus carriers is associated with IFNL4 polymorphisms and ALT levels. *The Journal of Infection Diseases* 209: 1907–1915.

179. Radziewicz, H., C. C. Ibegbu, H. Hon, M. K. Osborn, K. Obideen, M. Wehbi, G. J. Freeman, J. L. Lennox, K. A. Workowski, H. L. Hanson, and A. Grakoui. 2008. Impaired hepatitis C virus (HCV)-specific effector CD8+ T cells undergo massive apoptosis in the peripheral blood during acute HCV infection and in the liver during the chronic phase of infection. *Journal of Virology* 82: 9808–9822.

180. Radziewicz, H., C. C. Ibegbu, M. L. Fernandez, K. A. Workowski, K. Obideen, M. Wehbi, H. L. Hanson, J. P. Steinberg, D. Masopust, E. J. Wherry, J. D. Altman, B. T. Rouse, G. J. Freeman, R. Ahmed, and A. Grakoui. 2007. Liver-infiltrating lymphocytes in chronic human hepatitis C virus infection display an exhausted phenotype with high levels of PD-1 and low levels of CD127 expression. *Journal of Virology* 81: 2545–2553.

181. Calne, R. Y., R. A. Sells, J. R. Pena, D. R. Davis, and P. R. Millard. 1969. Induction of immunological tolerance by porcine liver allografts. *Nature* 223: 472–476.

182. Caetano, J., A. Martinho, A. Paiva, B. Pais, C. Valente, and C. Luxo. 2008. Differences in Hepatitis C Virus (HCV)-Specific CD8 T-Cell Phenotype during Pegylated Alpha Interferon and Ribavirin Treatment Are Related to Response to Antiviral Therapy in Patients Chronically Infected with HCV. *Journal of Virology* 82: 7567–7577.

183. Diepolder, H. M. 2004. Interferon-α for hepatitis C: antiviral or immunotherapy? *Journal of Hepatology* 40: 1030-1031.

184. Kano, A., Y. Watanabe, N. Takeda, S.-I. Aizawa, and T. Akaike. 1997. Analysis of IFN-γ-Induced Cell Cycle Arrest and Cell Death in Hepatocytes. *J Biochem (Tokyo)* 121: 677–683.

185. Baroni, G. S., L. D'Ambrosio, P. Curto, A. Casini, R. Mancini, A. M. Jezequel, and A. Benedetti. 1996. Interferon gamma decreases hepatic stellate cell activation and extracellular matrix deposition in rat liver fibrosis. *Hepatology* 23: 1189–1199.

186. Gigi, E., M. R. Gigi, and A. Kalogeridis. 2008. Cytokine mRNA expression in hepatitis C

virus infection: TH1 predominance in patients with chronic hepatitis C and TH1–TH2 cytokine profile in subjects with self-limited disease. *Journal of viral hepatitis* 15: 145-154.

187. Sobue, S., T. Nomura, T. Ishikawa, S. Ito, and K. Saso. 2001. Th1/Th2 cytokine profiles and their relationship to clinical features in patients with chronic hepatitis C virus infection. *Journal of Gastroenterology* 36: 544- 551.

188. Falasca, K., C. Ucciferri, M. Dalessandro, P. Zingariello, P. Mancino, C. Petrarca, E. Pizzigallo, P. Conti, and J. Vecchiet. 2006. Cytokine patterns correlate with liver damage in patients with chronic hepatitis B and C. *Ann Clin Lab Sci* 36: 144–150.

189. Attallah, A. M., M. El-Far, F. Zahran, G. E. Shiha, K. Farid, M. M. Omran, M. A. Abdelrazek, A. A. Attallah, A. A. El-Beh, R. M. El-Hosiny, and A. M. El-Waseef. 2016. Interferon-gamma is associated with hepatic dysfunction in fibrosis, cirrhosis, and hepatocellular carcinoma. *J Immunoassay Immunochem* 37: 597–610.

190. Gruener, N. H., M.-C. Jung, A. Ulsenheimer, J. T. Gerlach, R. Zachoval, H. M. Diepolder, G. Baretton, R. Schauer, G. R. Pape, and C. A. Schirren. 2004. Analysis of a successful HCV-specific CD8+ T cell response in patients with recurrent HCV-infection after orthotopic liver transplantation. *Liver Transplantation* 10: 1487–1496.

191. Houghton, M. 2011. Prospects for prophylactic and therapeutic vaccines against the hepatitis C viruses. *Immunological Reviews* 239: 99–108.

192. Stoll-Keller, F., H. Barth, S. Fafi-Kremer, M. B. Zeisel, and T. F. Baumert. 2014. Development of hepatitis C virus vaccines: challenges and progress. *Expert Review of Vaccines* 8: 333–345.

193. Martinez-Sierra, C., A. Arizcorreta, F. Diaz, R. Roldan, L. Martin-Herrera, E. Perez-Guzman, and J. A. Giron-Gonzalez. 2003. Progression of Chronic Hepatitis C to Liver Fibrosis and Cirrhosis in Patients Coinfected with Hepatitis C Virus and Human Immunodeficiency Virus. *Clinical Infectious Diseases* 36: 491–498.

194. Rallón, N., M. García, J. García-Samaniego, N. Rodríguez, A. Cabello, C. Restrepo, B. Álvarez, R. García, M. Górgolas, and J. M. Benito. 2017. HCV coinfection contributes to HIV pathogenesis by increasing immune exhaustion in CD8 T-cells. *PLoS ONE* 12: e0173943.

Supplemental Figures

A

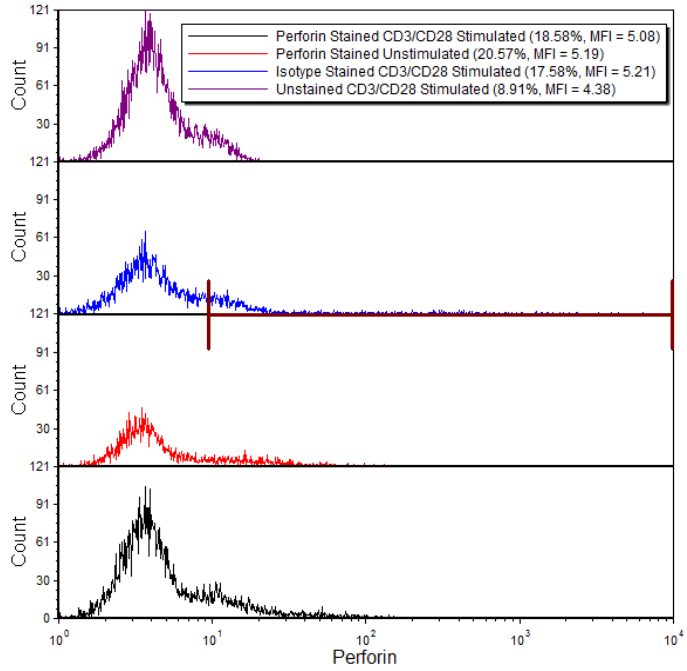

B

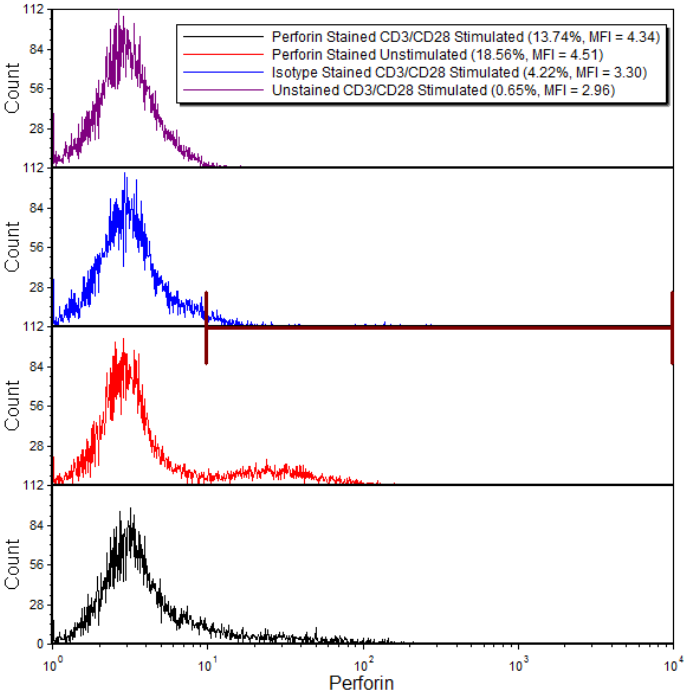

Supplemental Figure S1: Reducing non-specific binding for perforin with 10% human AB serum during intracellular staining step. A) Absence of human AB serum. **B)** Presence of human AB serum.

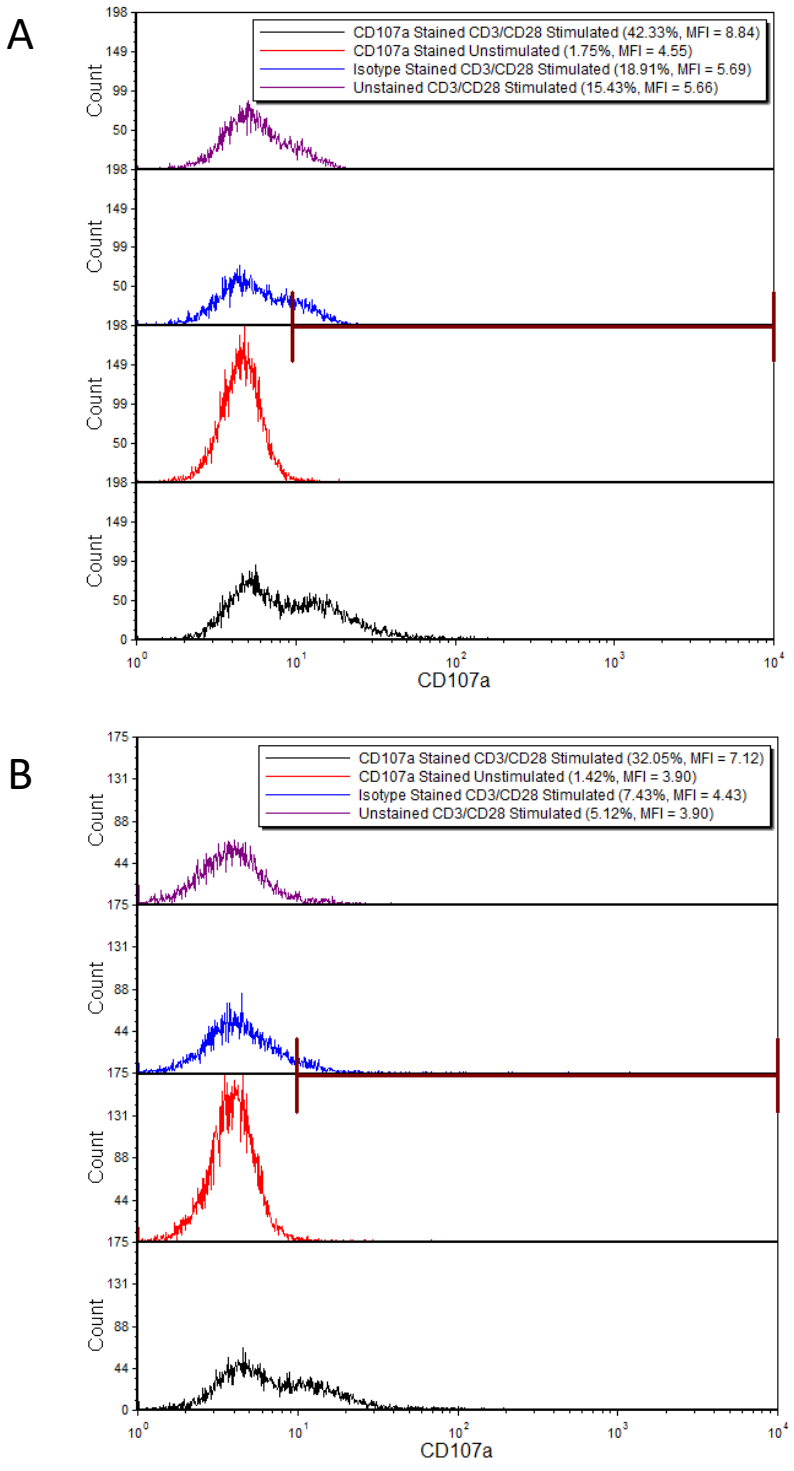

Supplemental Figure S2: Reducing non-specific binding for CD107a with 10% human AB serum during intracellular staining step. A) Absence of human AB serum. **B)** Presence of human AB serum.

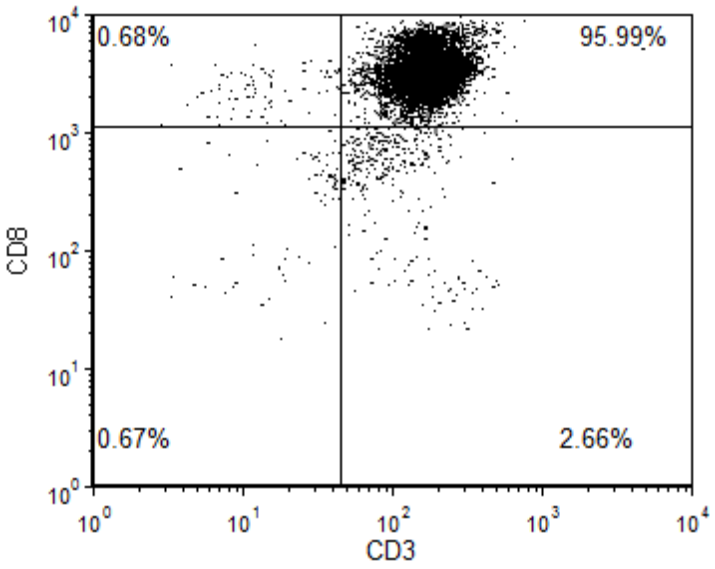

Supplemental Figure S3: Representative dot plot depicting percentage of $CD8^+CD3^+$ T cells after sorting for $CD8^+$ T cells using EasySep™ Human CD8 Positive Selection Kit 2 in an uninfected control.

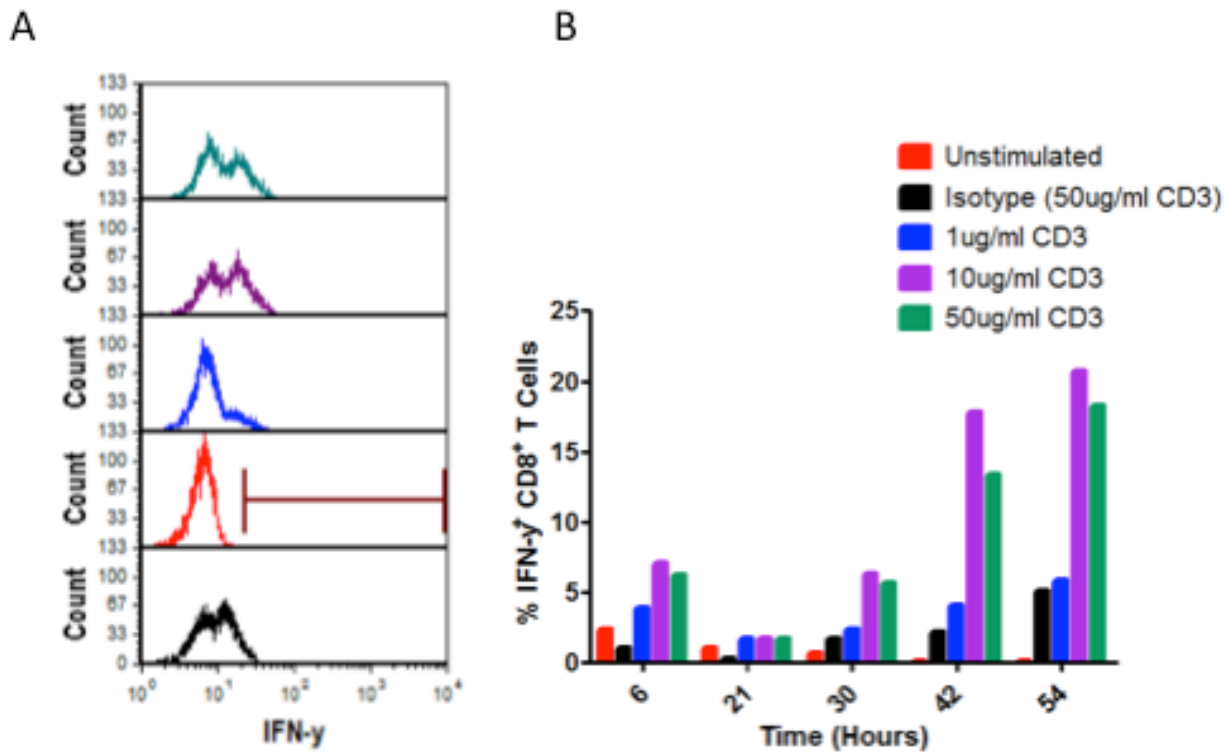

Supplemental Figure S4: Anti-CD3/CD28 stimulation time course for measuring intracellular IFN-γ expression of CD8$^+$ T cells using flow cytometry. A) Histogram depicting intracellular IFN-γ expression for five conditions after 54 hours: unstimulated (red), isotype stained 50µg/ml anti-CD3 stimulated (black), IFN-γ stained 1µg/ml anti-CD3 stimulated (blue), IFN-γ stained 10µg/ml anti-CD3 stimulated (purple), and IFN-γ stained 50µg/ml anti-CD3 stimulated (green). All stimulated conditions were also treated with anti-CD28 (5µg/ml in the well). **B)** Time course for intracellular IFN-γ expression measured using flow cytometry after 6, 21, 30, 42, and 54 hours. Brefeldin A (5µg/ml in the well) was added during the previous time point.

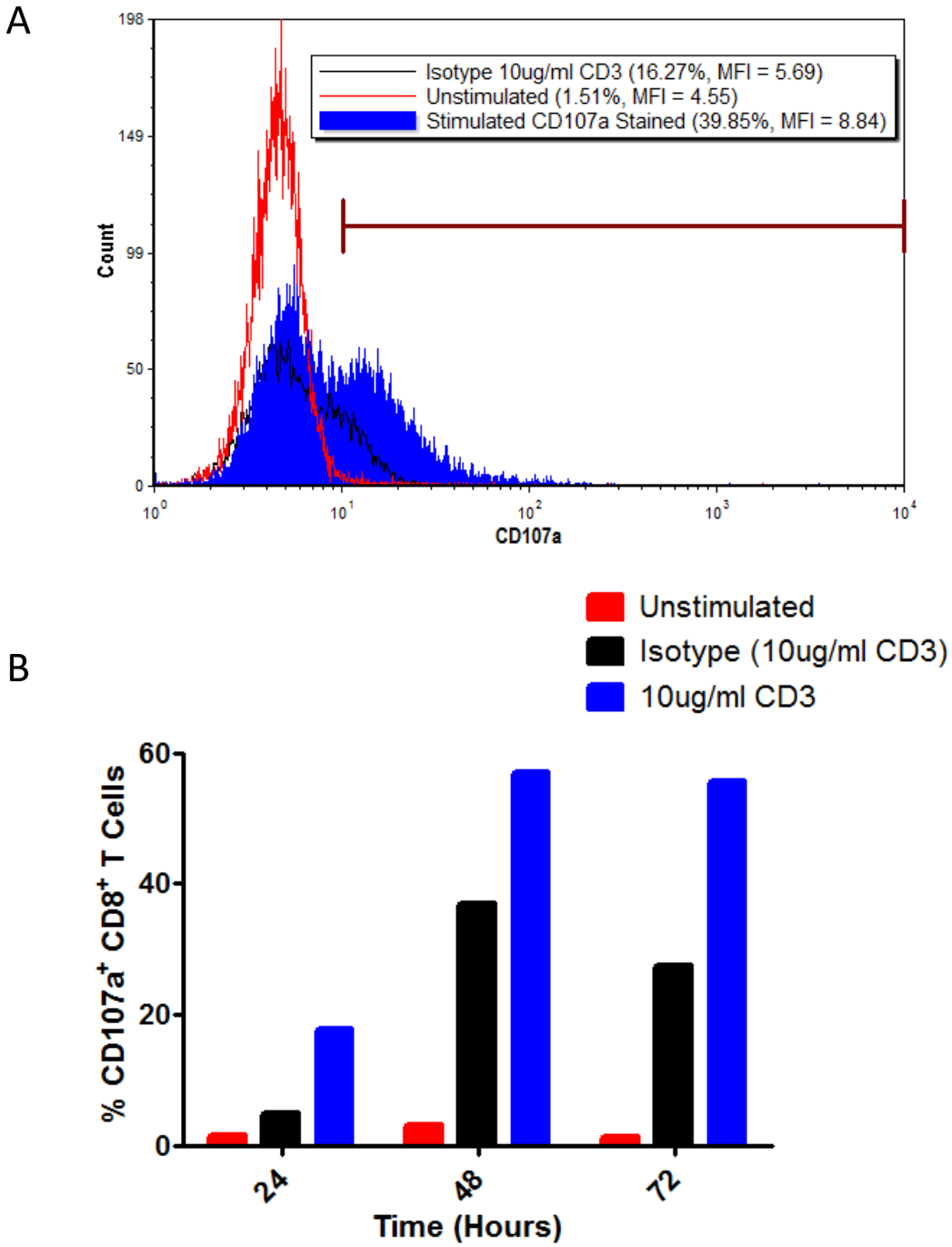

Supplemental Figure S5: Anti-CD3/CD28 stimulation time course for measuring CD107a expression of CD8$^+$ T cells using flow cytometry. A) Histogram depicting CD107a expression for three conditions after 48 hours: unstimulated (red), isotype stained 10µg/ml anti-CD3 stimulated (black), and CD107a stained 10ug/ml anti-CD3 stimulated (solid blue). All stimulated conditions were also treated with anti-CD28 (5µg/ml in the well). **B)** Time course for CD107a expression measured using flow cytometry after 24, 48, and 72 hours. Monensin (8µM) was added six hours before the end of the incubation.

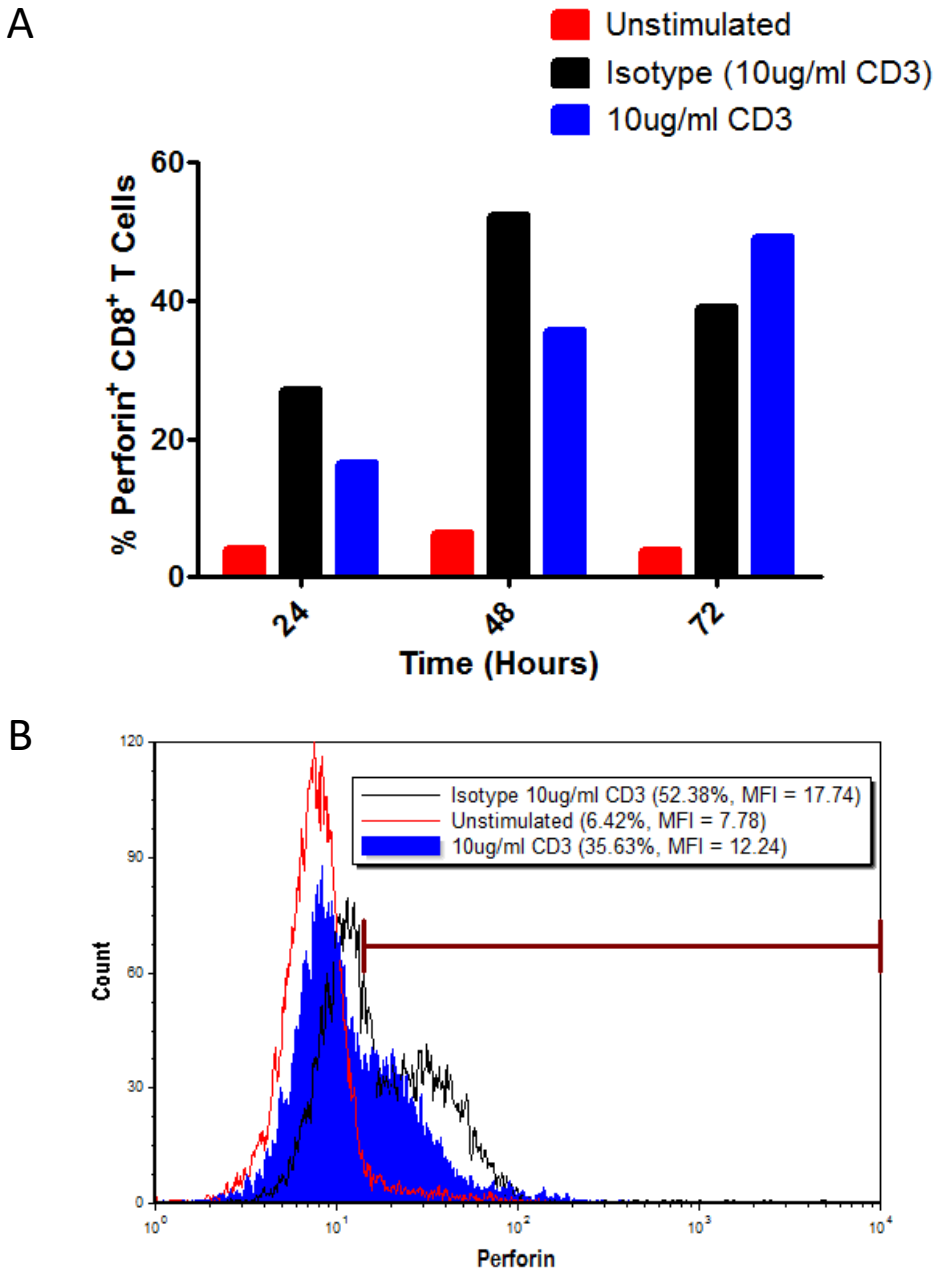

Supplemental Figure S6: Anti-CD3/CD28 stimulation time course for measuring intracellular perforin expression of $CD8^+$ T cells using flow cytometry. A) Histogram depicting intracellular perforin expression for three conditions after 48 hours: unstimulated (red), isotype stained 10µg/ml anti-CD3 stimulated (black), and perforin stained 10ug/ml anti-CD3 stimulated (solid blue). All stimulated conditions were also treated with anti-CD28 (5µg/ml in the well). **B)** Time course for perforin expression measured using flow cytometry after 24, 48, and 72 hours.